

Addendum to
"Bays Eutrophication Model (BEM):
modeling analysis for the period of
1992-1994"

Massachusetts Water Resources Authority

Environmental Quality Department
Report 2001-13



Citation:

HydroQual. 2001. **Addendum to "Bays Eutrophication Model (BEM): modeling analysis for the period of 1992-1994"**. Boston: Massachusetts Water Resources Authority. Report ENQUAD 2001-13. 60 p.

TABLE OF CONTENTS

<u>Section</u>		<u>Page</u>
1	INTRODUCTION	1-1
1.1	HISTORY AND RATIONALE FOR ADDENDUM	1-1
1.2	ADDENDUM CONTENT	1-2
2	BOUNDARY CONDITIONS	2-1
2.1	RATIONALE FOR BOUNDARY CONDITION MODIFICATION	2-1
2.2	BOUNDARY CONDITION COMPARISON FOR 1992	2-2
2.3	1992-1994 BOUNDARY CONDITIONS	2-21
3	MODEL COEFFICIENTS	3-1
3.1	WATER QUALITY MODEL COEFFICIENTS	3-1
	3.1.1 Rationale for Modifying Model Coefficients	3-1
	3.1.2 Final Model Coefficients	3-2
3.2	SEDIMENT MODEL COEFFICIENTS	3-22
4	GRID AGGREGATION	4-1
4.1	INTRODUCTION	4-1
4.2	METHODOLOGY	4-3
4.3	SUMMARY	4-16
5	REFERENCES	5-1

FIGURES

<u>Figure</u>	<u>Page</u>
2-1. Standard Level 1 Boundary Condition Comparison Between Original and Revised 1992 Calibration for Salinity, DO, Phytoplankton and Inorganic Nutrients	2-13
2-2. Standard Level 1 Boundary Condition Comparison Between Original and Revised 1992 Calibration for Organic Nutrients and Organic Carbon	2-14
2-3. Standard Level 2 Boundary Condition Comparison Between Original and Revised 1992 Calibration for Salinity, DO, Phytoplankton and Inorganic Nutrients	2-15
2-4. Standard Level 2 Boundary Condition Comparison Between Original and Revised 1992 Calibration for Organic Nutrients and Organic Carbon	2-16
2-5. Standard Level 3 Boundary Condition Comparison Between Original and Revised 1992 Calibration for Organic Nutrients and Organic Carbon	2-17
2-6. Standard Level 3 Boundary Condition Comparison Between Original and Revised 1992 Calibration for Organic Nutrients and Organic Carbon	2-18
2-7. Standard Level 4 Boundary Condition Comparison Between Original and Revised 1992 Calibration for Salinity, DO, Phytoplankton and Inorganic Nutrients	2-19
2-8. Standard Level 4 Boundary Condition Comparison Between Original and Revised 1992 Calibration for Organic Nutrients and Organic Carbon	2-20
2-9. 1992-1994 Winter Diatom Boundary Conditions	2-22
2-10. 1992-1994 Summer Assemblage Boundary Conditions	2-23
2-11. 1992-1994 Refractory Particulate Organic Phosphorus Boundary Conditions	2-24
2-12. 1992-1994 Labile Particulate Organic Phosphorus Boundary Conditions	2-25
2-13. 1992-1994 Refractory Dissolved Organic Phosphorus Boundary Conditions	2-26
2-14. 1992-1994 Labile Dissolved Organic Phosphorus Boundary Conditions	2-27
2-15. 1992-1994 Dissolved Inorganic Phosphorus Boundary Conditions	2-28
2-16. 1992-1994 Refractory Particulate Organic Nitrogen Boundary Conditions	2-29
2-17. 1992-1994 Labile Particulate Organic Nitrogen Boundary Conditions	2-30
2-18. 1992-1994 Refractory Dissolved Organic Nitrogen Boundary Conditions	2-31
2-19. 1992-1994 Labile Dissolved Organic Nitrogen Boundary Conditions	2-32
2-20. 1992-1994 Ammonium-Nitrogen Boundary Conditions	2-33
2-21. 1992-1994 Nitrite + Nitrate-Nitrogen Boundary Conditions	2-34
2-22. 1992-1994 Biogenic Silica Boundary Conditions	2-35
2-23. 1992-1994 Dissolved Silica Boundary Conditions	2-36
2-24. 1992-1994 Refractory Particulate Organic Carbon Boundary Conditions	2-37
2-25. 1992-1994 Labile Particulate Organic Carbon Boundary Conditions	2-38
2-26. 1992-1994 Refractory Dissolved Organic Carbon Boundary Conditions	2-39
2-27. 1992-1994 Labile Dissolved Organic Carbon Boundary Conditions	2-40
2-28. 1992-1994 Dissolved Oxygen Boundary Conditions	2-41
2-29. 1992-1994 Particulate Organic Carbon Boundary Conditions	2-42
2-30. 1992-1994 Particulate Organic Nitrogen Boundary Conditions	2-43
2-31. 1992-1994 Dissolved Organic Carbon Boundary Conditions	2-44

FIGURES (Continued)

<u>Figure</u>	<u>Page</u>
2-32. 1992-1994 Total Dissolved Nitrogen Boundary Conditions	2-45
2-33. 1992-1994 Total Dissolved Phosphorus Boundary Conditions	2-46
4-1. Hydrodynamic Model Grid and Aggregated Water Quality Model Grid	4-2
4-2. Comparison of Salinity Results from the Hydrodynamic Model and the Aggregated Water Quality Model	4-4
4-3. Aggregated and Unaggregated Water Quality Model Grids	4-5
4-4. Volume Weighted Average	4-6
4-5. Comparison of Surface and Bottom Salinity Results Between the Aggregated and Unaggregated Water Quality Model Grids	4-8
4-6. Comparison of Surface and Bottom Chlorophyll-a Results Between the Aggregated and Unaggregated Water Quality Model Grids	4-9
4-7. Comparison of Surface and Bottom Particulate Organic Carbon Results Between the Aggregated and Unaggregated Water Quality Model Grids	4-10
4-8. Comparison of Surface and Bottom Dissolved Oxygen Results Between the Aggregated and Unaggregated Water Quality Model Grids	4-11
4-9. Comparison of Surface and Bottom NO ₂ + NO ₃ Results Between the Aggregated and Unaggregated Water Quality Model Grids	4-12
4-10. NO ₂ + NO ₃ Concentrations at the Boundary for the Aggregated and Unaggregated Water Quality Model Grids	4-14
4-11. Comparison of Surface and Bottom Tracer Concentration Results Between the Aggregated and Unaggregated Water Quality Model Grids	4-15
4-12. Comparison of Bottom NO ₂ + NO ₃ Results from the Aggregated and Unaggregated Water Quality Model Grids at Day 162.	4-17
4-13. Comparison of Surface Average Chl-a Concentration Results from the Aggregated and Unaggregated Water Quality Model Grids at Day 82	4-18
4-14. Comparison of Bottom Minimum DO Concentration Results from the Aggregated and Unaggregated Water Quality Model Grids at Day 292.	4-19

TABLES

<u>Table</u>	<u>Page</u>
2-1. Boundary Conditions	2-3
2-2. Boundary Conditions	2-4
2-3. Boundary Conditions	2-5
2-4. Boundary Conditions	2-6
2-5. Boundary Conditions	2-7
2-6. Boundary Conditions	2-8
2-7. Boundary Conditions	2-9
2-8. Boundary Conditions	2-10
2-9. Boundary Conditions	2-12
3-1. State System Variables Utilized by the Kinetic Framework	3-3
3-2. Phytoplankton Net Growth Equations	3-4
3-3. Phosphorus Reaction Equations	3-8
3-4. Nitrogen Reaction Equations	3-11
3-5. Silica Reaction Equations	3-15
3-6. Organic Carbon Reaction Equations	3-17
3-7. Dissolved Oxygen and Oxygen Reaction Rates	3-20
3-8. Constants Varied Between 1989-1992 Calibration and 1992-1994 Calibration	3-22
3-9. Sediment Model Coefficients	3-22

SECTION 1

INTRODUCTION

1.1 HISTORY AND RATIONALE FOR ADDENDUM

In 1991, the Massachusetts Water Resources Authority (MWRA) funded the development of a coupled hydrodynamic/water quality model of Massachusetts and Cape Cod Bays as part of their Harbor and Outfall Monitoring Program (HOM). This model, the Bays Eutrophication Model (BEM), was developed to assess the potential impact of relocating the discharge of primary treated effluent of the Nut and Deer Island wastewater treatment plants from Boston Harbor into Massachusetts Bay. The initial calibration of the model was completed in 1995 and was conducted for the periods of October 1989 to May 1991 and the calendar year 1992. The Model Evaluation Group (MEG), assembled to provide a peer-review for the BEM, recommended, among other things, that additional validation of the model be conducted for the years 1993 and 1994. Events occurred in 1993 (a fall diatom bloom) and 1994 (a low dissolved oxygen event) that were considered by the MEG to be good tests for the model's predictive capability.

In September 1999, HydroQual released its report "Bays Eutrophication Model (BEM): Modeling Analysis for the Period of 1992-1994" to present the results of the additional model validation for MEG review. In June of 2000, the MEG presented their conclusions and recommendations concerning the modeling study to the Outfall Monitoring Science Advisory Panel (OMSAP, <http://www.epa.gov/region01/omsap/meg1299.html>). While the MEG was pleased that the additional modeling that they requested had been completed they also believed that further analysis should be conducted. Recommendations for further analysis included the addition of a third algal group to the model kinetics; running the water quality model on the same spatial grid as the circulation model; sensitivity analysis of the upstream boundary conditions; as well as additional documentation for the model. This addendum, which is a companion document to the 1999 report (which was finalized as "HydroQual, 2000. Bays Eutrophication Model (BEM): Modeling analysis for the period 1992-1994: Massachusetts Water Resources Authority. Report ENQUAD 2000-02 158p.), addresses some of the issues raised by the MEG.

1.2 ADDENDUM CONTENT

This addendum follows the recommendations made by the MEG for the report addendum. Section 2 documents the boundary conditions used in the 1992 simulation as well as differences between the boundary conditions used for the original 1992 calibration and the revised 1992 calibration. It also provides documentation, in the form of figures, of the boundary conditions used for the calibration period of 1992 through 1994. Section 3 includes documentation of the water quality kinetics and model parameters used in the 1992-1994 simulation. An additional table notes the changes made to model parameters between the 1990/1992 calibration and the 1992 calibration. Section 4 discusses the effects of grid aggregation on model results.

To address additional MEG comments, two separate reports have been completed. One report (HydroQual, 2001a) presents a sensitivity of the concentrations assigned as boundary conditions to BEM. The other report (HydroQual, 2001b) presents an analysis of the addition of a third algae group to the BEM kinetics.

SECTION 2

BOUNDARY CONDITIONS

2.1 RATIONALE FOR BOUNDARY CONDITION MODIFICATION

During the course of modeling the Massachusetts/Cape Cod Bays system it has become apparent that the Gulf of Maine plays a major role in the circulation and water quality conditions within Massachusetts and Cape Cod Bays. Consequently, assigning boundary conditions to the model has a major impact on the results of the water quality model. In 1992, the original HOM sampling included 21 near field and 25 far field water quality monitoring stations. Five of these stations (F4, F8, F12, F21 and F22) were used to infer the boundary concentrations for the model. However, these stations were within the model domain itself, 15 to 20 km from the model boundary. HydroQual, as well as the MEG, recommended that additional monitoring stations be added to the HOM program closer to the boundary, so that more accurate boundary conditions could be assigned. In 1994, MWRA responded by modifying the locations of the water quality monitoring stations including two new stations (F26 and F27) close to the northern boundary of the model where the largest influences of the Gulf of Maine are observed.

In 1997, HydroQual was funded to model the years 1993 and 1994. HydroQual decided to recalibrate the year 1992 as part of this work. Two major factors were involved in the decision to recalibrate 1992 as part of this effort. First, the water quality model is highly dependent on the results of the hydrodynamic model that provides transport, temperature and salinity information. Dr. Richard Signell (USGS), who provided the initial hydrodynamic results, added a new flux correcting advection scheme (Smolarkiewicz scheme) to the hydrodynamic model to prevent overshoots and undershoots in the salinity that were occurring around the new outfall, and recalibrated the model. It was this recalibrated 1992 hydrodynamic model that was used to provide initial conditions for the 1993-1994 model runs that were used to provide the transport for the water quality model. The updated 1992 hydrodynamic model computations changed the results of the water quality model for 1992. Second, the new water quality monitoring stations implemented in 1994, while not providing new data for 1992, provided data that provided better insight as to the water quality that was entering the bays from the Gulf of Maine. The additional data from 1994 were used to improve the 1992 calibration. The next section of this addendum documents the modifications made to the 1992 boundary conditions.

2.2 BOUNDARY CONDITION COMPARISON FOR 1992

Tables 2-1 through 2-9 present the concentrations used for the two calibration efforts for 1992. The first calibration effort is referred to in the tables as the “Original 1992” and the second calibration is referred to in the tables as the “Revised 1992.” Boundary conditions are assigned for each of the state-variables in the model. Tables are not included for salinity, which is obtained directly from the hydrodynamic model, nor are tables included for reactive dissolved organic carbon, algal exudate, and aqueous sediment oxygen demand which were assigned as zero at the boundary. Due to the sparseness of the data, boundary conditions were assigned to be horizontally constant. Vertically, boundary conditions were specified at four standard levels (0 m, 25 m, 60 m, and 140 m). The water quality model then interpolates the appropriate sigma layer boundary concentration from the standard level concentrations based on the local water column depth at each boundary segment. Standard levels were used so that the assigned boundary concentrations would remain consistent with depth. To assign boundary conditions to sigma layers directly would have been more difficult because of the changing bathymetry at the model’s open boundary. The depths of the standard levels were changed in the revised 1992 calibration (0 m, 20 m, 60 m, 110 m) based on the vertical structure of the data collected in 1994. The 0-20 m range represents the surface mixed layer and comprises most of the euphotic zone. The 20-60 m depth is a transition zone, and the 60-110 m depth represents the bottom waters. There are no segments in the water quality model that are deeper than 110 m. Temporally, boundary conditions were assigned every 15 to 31 days based on the available data both near the boundary and within the model domain.

When possible the boundary conditions assigned were based on data. The parameters for which the most data were available were dissolved inorganic phosphorus (PO_4), ammonia (NH_3), nitrite + nitrate ($\text{NO}_2 + \text{NO}_3$), silica (Si), and dissolved oxygen (DO). While particulate organic phosphorus (POP), total dissolved phosphorus (TDP), particulate organic nitrogen (PON), total dissolved nitrogen (TDN), particulate organic carbon (POC), and dissolved organic carbon (DOC) were measured, the particulate and dissolved organic carbon, nitrogen and phosphorus state-variables were more difficult to assign because data were collected at fewer stations and less often than the inorganic nutrients. Since some of the model’s state-variables were not measured directly, these constituents had to be determined by difference, (e.g., organic phosphorus was determined as the difference between TDP and PO_4) which on occasion resulted in negative concentrations. Additionally, labile and refractory fractions had to be assigned for the organic pools. All of these factors required the specification of boundary conditions to be based on assumption, approximation, previous experience, and calibration. Figures 2-1 through 2-8 present comparisons between the original and revised boundary conditions for fifteen state-variables at each of the four standard levels. The remaining nine state-variables are not included because the boundary conditions were the same for both calibrations. Most of the changes to the inorganic

**TABLE 2-1
BOUNDARY CONDITIONS**

Original 1992						Revised 1992				
Standard Level Depths (m)	0	25	60	140		0	20	60	110	
<u>Winter Phytoplankton</u> (mg C/L)										
	Day	1	2	3	4	Day	1	2	3	4
January	0	0.020	0.015	0.010	0.005	0	0.020	0.015	0.010	0.005
February	31	0.040	0.030	0.010	0.007	31	0.030	0.020	0.010	0.007
						45	0.040	0.030	0.015	0.007
March	60	0.050	0.040	0.015	0.007	59	0.050	0.040	0.015	0.007
						75	0.060	0.050	0.015	0.007
April	91	0.050	0.040	0.015	0.007	90	0.050	0.040	0.015	0.007
						105	0.040	0.025	0.015	0.010
May	121	0.025	0.020	0.015	0.010	120	0.025	0.020	0.010	0.007
						135	0.020	0.015	0.007	0.005
June	152	0.010	0.010	0.005	0.005	151	0.010	0.005	0.002	0.002
July	182	0.010	0.010	0.005	0.005	181	0.005	0.005	0.002	0.002
August	213	0.010	0.010	0.005	0.005	212	0.005	0.005	0.002	0.002
September	244	0.010	0.010	0.005	0.005	243	0.020	0.015	0.005	0.005
October	274	0.015	0.010	0.005	0.005	273	0.030	0.020	0.007	0.005
November	305	0.015	0.010	0.007	0.005	304	0.020	0.020	0.010	0.007
December	335	0.020	0.015	0.010	0.007	335	0.020	0.015	0.012	0.007
						370	0.020	0.015	0.012	0.007

**TABLE 2-2
BOUNDARY CONDITIONS**

Original 1992						Revised 1992				
Standard Level Depths (m)	0	25	60	140		0	20	60	110	
<u>Summer Phytoplankton</u> (mg C/L)	Layer					Layer				
	Day	1	2	3	4	Day	1	2	3	4
January	0	0.005	0.005	0.002	0.002	0	0.005	0.005	0.002	0.002
February	31	0.005	0.005	0.002	0.002	31	0.005	0.005	0.002	0.002
						45	0.005	0.005	0.002	0.002
March	60	0.005	0.005	0.002	0.002	59	0.005	0.005	0.002	0.002
						75	0.005	0.005	0.002	0.002
April	91	0.005	0.005	0.002	0.002	90	0.005	0.005	0.002	0.002
						105	0.005	0.005	0.002	0.002
May	121	0.021	0.015	0.010	0.002	120	0.010	0.007	0.005	0.004
						135	0.021	0.015	0.010	0.007
June	152	0.043	0.031	0.020	0.010	151	0.043	0.031	0.020	0.010
July	182	0.063	0.041	0.020	0.010	181	0.063	0.041	0.020	0.010
August	213	0.053	0.031	0.015	0.010	212	0.053	0.031	0.015	0.005
September	244	0.043	0.021	0.010	0.005	243	0.040	0.020	0.010	0.002
October	274	0.021	0.010	0.002	0.002	273	0.015	0.010	0.002	0.002
November	305	0.010	0.005	0.002	0.002	304	0.005	0.005	0.002	0.002
December	335	0.005	0.005	0.002	0.002	335	0.005	0.005	0.002	0.002
						370	0.005	0.005	0.002	0.002

**TABLE 2-3
BOUNDARY CONDITIONS**

Original 1992					Revised 1992					
Units = mg P/L	RPOP	LPOP	RDOP	LDOP		RPOP	LPOP	RDOP	LDOP	
Layer					Layer					
	Day	1-4	1-4	1-4	1-4	Day	1-4	1-4	1-4	1-4
January	0	0.00075	0.001	0.004	0.003	0	0.0075	0.001	0.004	0.003
February	31	0.00075	0.001	0.004	0.003	31	0.0075	0.001	0.004	0.003
						45	0.0075	0.001	0.004	0.003
March	60	0.00075	0.001	0.004	0.003	59	0.0075	0.001	0.004	0.003
						75	0.0075	0.001	0.004	0.003
April	91	0.00075	0.001	0.004	0.003	90	0.0075	0.001	0.004	0.003
						105	0.0075	0.001	0.003	0.002
May	121	0.00075	0.001	0.003	0.002	120	0.0075	0.001	0.003	0.001
						135	0.0075	0.001	0.003	0.001
June	152	0.00075	0.001	0.003	0.001	151	0.0075	0.001	0.003	0.002
July	182	0.00075	0.001	0.003	0.001	181	0.0075	0.001	0.004	0.003
August	213	0.00075	0.001	0.003	0.002	212	0.0075	0.001	0.004	0.003
September	244	0.00075	0.001	0.004	0.003	243	0.0075	0.001	0.004	0.003
October	274	0.00075	0.001	0.004	0.003	273	0.0075	0.001	0.004	0.003
November	305	0.00075	0.001	0.004	0.003	304	0.0075	0.001	0.004	0.003
December	335	0.00075	0.001	0.004	0.003	335	0.0075	0.001	0.004	0.003
						370	0.0075	0.001	0.004	0.003

TABLE 2-4
BOUNDARY CONDITIONS

Original 1992						Revised 1992				
PO₄ (mg P/L)										
Layer						Layer				
	Day	1	2	3	4	Day	1	2	3	4
January	0	0.023	0.024	0.030	0.030	0	0.023	0.024	0.026	0.027
February	31	0.009	0.013	0.018	0.018	31	0.019	0.021	0.024	0.025
						45	0.015	0.018	0.023	0.024
March	60	0.016	0.016	0.018	0.018	59	0.012	0.014	0.022	0.023
						75	0.009	0.011	0.022	0.023
April	91	0.007	0.011	0.018	0.020	90	0.003	0.006	0.018	0.020
						105	0.012	0.014	0.021	0.023
May	121	0.005	0.013	0.019	0.023	120	0.007	0.011	0.022	0.024
						135	0.004	0.008	0.024	0.026
June	152	0.001	0.015	0.021	0.026	151	0.004	0.008	0.026	0.028
July	182	0.002	0.013	0.021	0.025	181	0.004	0.007	0.028	0.030
August	213	0.003	0.013	0.021	0.024	212	0.004	0.007	0.029	0.031
September	244	0.006	0.012	0.021	0.025	243	0.004	0.006	0.031	0.032
October	274	0.009	0.011	0.021	0.027	273	0.010	0.012	0.031	0.033
November	305	0.014	0.014	0.030	0.030	304	0.015	0.016	0.017	0.018
December	335	0.016	0.017	0.030	0.030	335	0.019	0.020	0.022	0.023
						370	0.022	0.022	0.023	0.026

**TABLE 2-5
BOUNDARY CONDITIONS**

Original 1992								Revised 1992							
Units = mg N/L	RPON	LPON			RDON		LDON		RPON	LPON			RDON		LDON
Layer								Layer							
	Day	1-4	1-2	3-4	1-2	3-4	1-4	Day	1-4	1-2	3-4	1-2	3-4	1-4	
January	0	0.008	0.003	0.002	0.100	0.100	0.035	0	0.008	0.003	0.002	0.100	0.100	0.035	
February	31	0.008	0.003	0.002	0.100	0.100	0.035	31	0.008	0.003	0.002	0.100	0.100	0.035	
								45	0.008	0.003	0.002	0.100	0.100	0.035	
March	60	0.008	0.003	0.002	0.100	0.100	0.035	59	0.008	0.003	0.002	0.100	0.100	0.035	
								75	0.008	0.003	0.002	0.100	0.100	0.035	
April	91	0.008	0.004	0.003	0.100	0.100	0.035	90	0.008	0.004	0.003	0.100	0.100	0.035	
								105	0.008	0.004	0.003	0.090	0.090	0.035	
May	121	0.008	0.005	0.003	0.070	0.080	0.035	120	0.008	0.005	0.003	0.070	0.080	0.030	
								135	0.008	0.006	0.003	0.050	0.070	0.030	
June	152	0.008	0.006	0.003	0.050	0.070	0.030	151	0.008	0.006	0.003	0.080	0.070	0.025	
July	182	0.008	0.006	0.003	0.050	0.070	0.025	181	0.008	0.006	0.003	0.050	0.070	0.025	
August	213	0.008	0.006	0.003	0.050	0.070	0.025	212	0.008	0.005	0.003	0.080	0.080	0.030	
September	244	0.008	0.005	0.003	0.080	0.080	0.030	243	0.008	0.005	0.003	0.100	0.100	0.035	
October	274	0.008	0.005	0.003	0.100	0.100	0.035	273	0.008	0.004	0.002	0.100	0.100	0.035	
November	305	0.008	0.004	0.002	0.100	0.100	0.035	304	0.008	0.003	0.002	0.100	0.100	0.035	
December	335	0.008	0.003	0.002	0.100	0.100	0.035	335	0.008	0.003	0.002	0.100	0.100	0.035	
								370	0.008	0.003	0.002	0.100	0.100	0.035	

**TABLE 2-6
BOUNDARY CONDITIONS**

Original 1992										Revised 1992								
Units = mg N/L		<u>NH₃</u>				<u>NO₂ + NO₃</u>					<u>NH₃</u>				<u>NO₂ + NO₃</u>			
		Layer				Layer					Layer				Layer			
	Day	1	2	3	4	1	2	3	4	Day	1	2	3	4	1	2	3	4
January	0	0.006	0.007	0.008	0.009	0.110	0.100	0.130	0.150	0	0.009	0.009	0.010	0.010	0.120	0.130	0.140	0.150
February	31	0.002	0.004	0.008	0.012	0.070	0.082	0.115	0.135	31	0.007	0.008	0.011	0.012	0.110	0.120	0.130	0.150
										45	0.005	0.006	0.012	0.015	0.090	0.100	0.130	0.140
March	60	0.001	0.002	0.012	0.018	0.040	0.050	0.100	0.120	59	0.004	0.006	0.014	0.018	0.030	0.070	0.110	0.125
										75	0.003	0.005	0.016	0.021	0.010	0.020	0.100	0.120
April	91	0.001	0.001	0.011	0.022	0.010	0.010	0.100	0.120	90	0.003	0.005	0.020	0.025	0.006	0.010	0.090	0.120
										105	0.005	0.008	0.025	0.029	0.020	0.040	0.105	0.125
May	121	0.001	0.003	0.016	0.032	0.010	0.021	0.100	0.120	120	0.007	0.011	0.030	0.033	0.010	0.020	0.120	0.130
										135	0.005	0.008	0.031	0.035	0.007	0.016	0.125	0.135
June	152	0.001	0.007	0.032	0.044	0.017	0.028	0.110	0.130	151	0.005	0.008	0.032	0.035	0.004	0.013	0.130	0.140
July	182	0.001	0.005	0.022	0.027	0.010	0.024	0.120	0.140	181	0.005	0.008	0.025	0.029	0.003	0.010	0.140	0.150
August	213	0.001	0.003	0.007	0.011	0.002	0.019	0.130	0.150	212	0.005	0.008	0.017	0.020	0.002	0.007	0.160	0.170
September	244	0.001	0.007	0.009	0.011	0.006	0.028	0.130	0.150	243	0.005	0.008	0.010	0.011	0.005	0.010	0.170	0.180
October	274	0.003	0.007	0.009	0.010	0.011	0.037	0.120	0.140	273	0.006	0.007	0.008	0.009	0.007	0.012	0.170	0.180
November	305	0.007	0.007	0.009	0.009	0.070	0.070	0.100	0.130	304	0.006	0.007	0.008	0.009	0.045	0.060	0.070	0.080
December	335	0.006	0.007	0.008	0.008	0.110	0.100	0.100	0.150	335	0.008	0.009	0.010	0.010	0.080	0.090	0.100	0.110
										370	0.010	0.010	0.011	0.012	0.110	0.120	0.140	0.150

**TABLE 2-7
BOUNDARY CONDITIONS**

Original 1992							Revised 1992					
Units = mg Si/L		BSi	Si					BSi	Si			
		Layer	Layer					Layer	Layer			
	Day	1-4	1	2	3	4	Day	1-4	1	2	3	4
January	0	0.100	0.291	0.283	0.296	0.298	0	0.100	0.230	0.240	0.250	0.260
February	31	0.100	0.125	0.097	0.173	0.177	31	0.100	0.190	0.200	0.230	0.240
							45	0.100	0.140	0.160	0.180	0.200
March	60	0.100	0.089	0.093	0.114	0.117	59	0.100	0.090	0.110	0.120	0.125
	75	0.100	0.289	0.333	0.383	0.387	75	0.100	0.200	0.250	0.220	0.270
April	91	0.100	0.287	0.331	0.383	0.387	90	0.100	0.230	0.280	0.310	0.330
							105	0.100	0.210	0.250	0.300	0.330
May	121	0.100	0.049	0.138	0.181	0.189	120	0.100	0.130	0.170	0.240	0.250
							135	0.100	0.085	0.130	0.210	0.225
June	152	0.100	0.032	0.102	0.187	0.189	151	0.100	0.065	0.120	0.220	0.235
July	182	0.100	0.033	0.102	0.196	0.197	181	0.100	0.065	0.110	0.230	0.250
August	213	0.100	0.050	0.103	0.227	0.227	212	0.100	0.060	0.100	0.250	0.270
September	244	0.100	0.062	0.101	0.237	0.238	243	0.100	0.060	0.100	0.260	0.280
October	274	0.100	0.071	0.097	0.258	0.258	273	0.100	0.060	0.100	0.260	0.280
November	305	0.100	0.128	0.130	0.297	0.298	304	0.100	0.120	0.130	0.145	0.160
December	335	0.100	0.166	0.168	0.296	0.297	335	0.100	0.170	0.180	0.190	0.200
							370	0.100	0.230	0.235	0.250	0.250

**TABLE 2-8
BOUNDARY CONDITIONS**

Original 1992						Revised 1992				
		LPOC (mg C/L)					LPOC (mg C/L)			
		Layer					Layer			
	Day	1	2	3	4	Day	1	2	3	4
January	0	0.016	0.012	0.006	0.005	0	0.016	0.012	0.006	0.005
February	31	0.015	0.011	0.005	0.005	31	0.015	0.011	0.005	0.005
						45	0.018	0.013	0.005	0.005
March	60	0.018	0.013	0.005	0.005	59	0.018	0.013	0.005	0.005
						75	0.022	0.020	0.007	0.007
April	91	0.022	0.016	0.010	0.010	90	0.024	0.022	0.010	0.010
						105	0.026	0.016	0.010	0.010
May	121	0.028	0.021	0.012	0.012	120	0.028	0.021	0.012	0.012
						135	0.030	0.024	0.012	0.012
June	152	0.030	0.024	0.012	0.012	151	0.030	0.024	0.012	0.012
July	182	0.030	0.024	0.012	0.012	181	0.030	0.024	0.012	0.012
August	213	0.030	0.024	0.012	0.012	212	0.028	0.022	0.011	0.011
September	244	0.028	0.022	0.011	0.011	243	0.025	0.019	0.009	0.008
October	274	0.025	0.019	0.009	0.008	273	0.022	0.015	0.006	0.005
November	305	0.022	0.015	0.005	0.005	304	0.019	0.013	0.005	0.005
December	335	0.019	0.013	0.005	0.005	335	0.016	0.011	0.005	0.005
						370	0.015	0.010	0.005	0.005

**TABLE 2-8 (continued)
BOUNDARY CONDITIONS**

Original 1992				Revised 1992				
Units = mg C/L	RPOC	RDOC	LDOC		RPOC	RDOC	LDOC	
		Layer			Layer			
	Day	1-4	1-4	1-4	Day	1-4	1-4	1-4
January	0	0.040	1.300	0.200	0	0.040	1.200	0.200
February	31	0.040	1.300	0.200	31	0.040	1.200	0.200
					45	0.040	1.200	0.200
March	60	0.040	1.300	0.200	59	0.040	1.200	0.200
					75	0.040	1.200	0.200
April	91	0.040	1.300	0.200	90	0.040	1.200	0.200
					105	0.040	1.200	0.200
May	121	0.040	1.300	0.200	120	0.040	1.200	0.200
					135	0.040	1.200	0.200
June	152	0.040	1.300	0.200	151	0.040	1.200	0.200
July	182	0.040	1.300	0.200	181	0.040	1.200	0.200
August	213	0.040	1.300	0.200	212	0.040	1.200	0.200
September	244	0.040	1.300	0.200	243	0.040	1.200	0.200
October	274	0.040	1.300	0.200	273	0.040	1.200	0.200
November	305	0.040	1.300	0.200	304	0.040	1.200	0.200
December	335	0.040	1.300	0.200	335	0.040	1.200	0.200
					370	0.040	1.200	0.200

ReDOC, ExDOC, 02EQ = 0

**TABLE 2-9
BOUNDARY CONDITIONS**

Original 1992						Revised 1992				
DO (mg O ₂ /L)						DO (mg O ₂ /L)				
Layer						Layer				
	Day	1	2	3	4	Day	1	2	3	4
January	0	10.0	9.8	9.8	9.7	0	10.0	10.0	9.9	9.8
February	31	12.7	12.5	12.2	12.0	31	10.7	10.6	10.5	10.4
						45	11.2	11.1	11.0	10.9
March	60	12.0	11.9	11.5	11.5	59	11.6	11.5	11.1	11.0
	75	11.5	11.4	11.2	11.2	75	11.3	11.0	10.8	10.5
April	91	11.0	10.9	10.6	10.6	90	10.6	10.3	10.1	9.9
						105	9.9	9.7	9.5	9.3
May	121	10.5	10.3	10.0	10.0	120	9.5	9.4	9.2	9.0
						135	9.8	9.7	9.4	9.2
June	152	10.0	9.8	9.5	9.4	151	9.9	9.9	9.8	9.7
July	182	9.75	9.5	9.3	9.2	181	9.75	9.8	9.7	9.5
August	213	9.0	9.1	9.2	9.1	212	9.4	9.2	9.2	9.1
September	244	9.0	8.9	8.9	8.7	243	9.0	8.9	8.8	8.6
October	274	9.0	8.9	8.5	8.4	273	9.0	8.9	8.5	8.2
November	305	9.2	9.2	8.8	8.8	304	9.2	9.1	9.0	8.9
December	335	9.7	9.7	9.5	9.5	335	9.5	9.4	9.4	9.3
						370	10.2	10.0	9.9	9.7

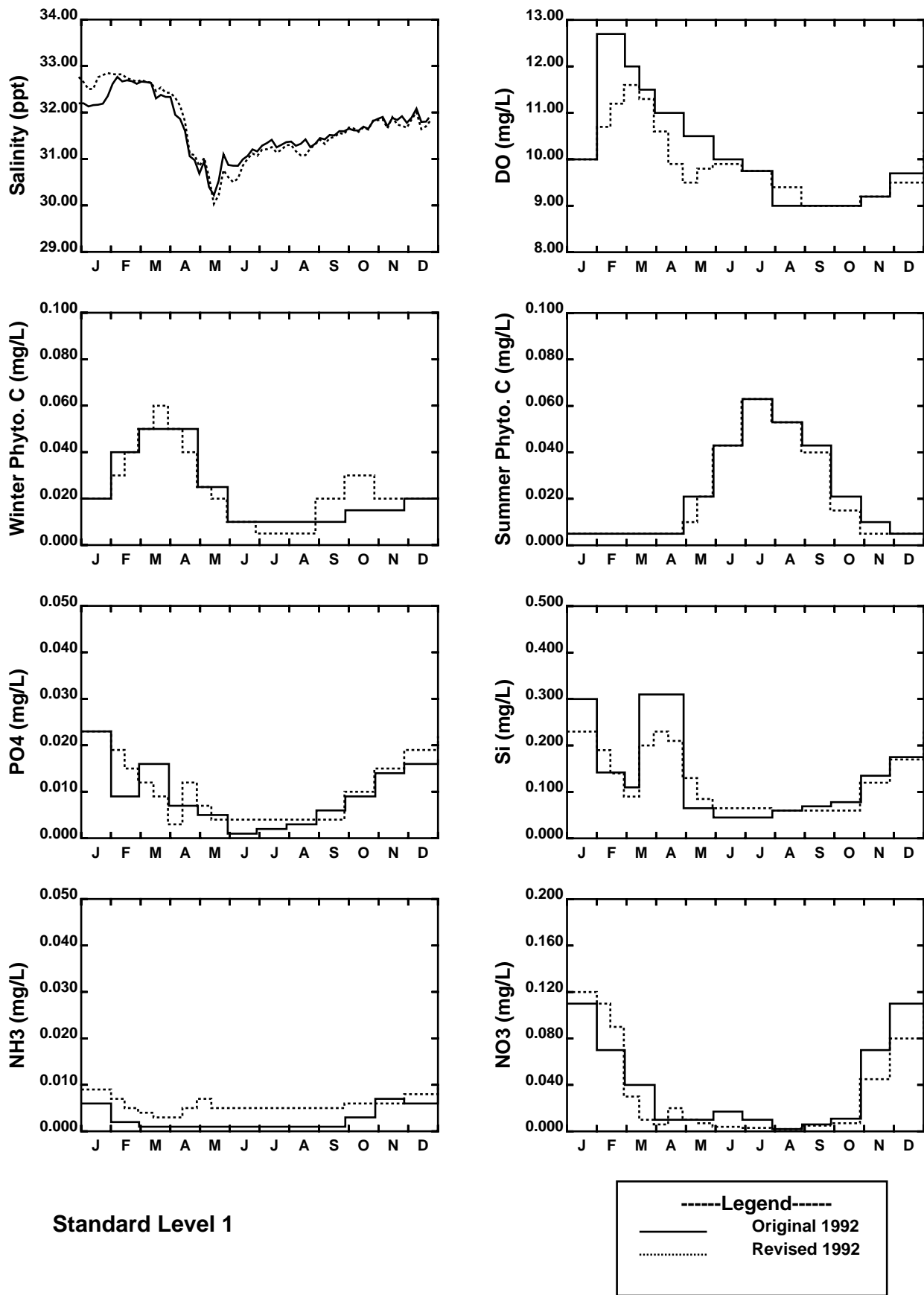
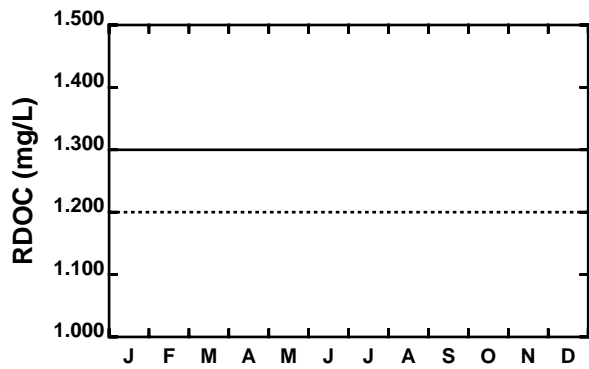
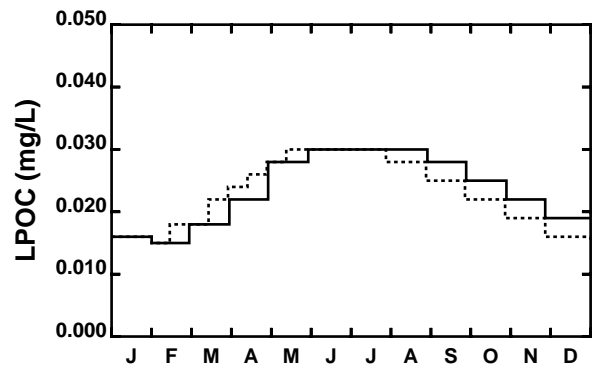
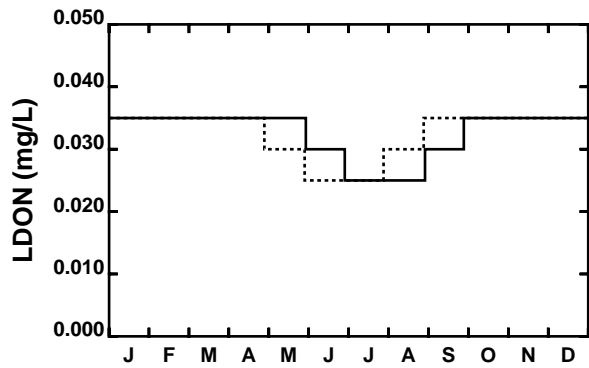
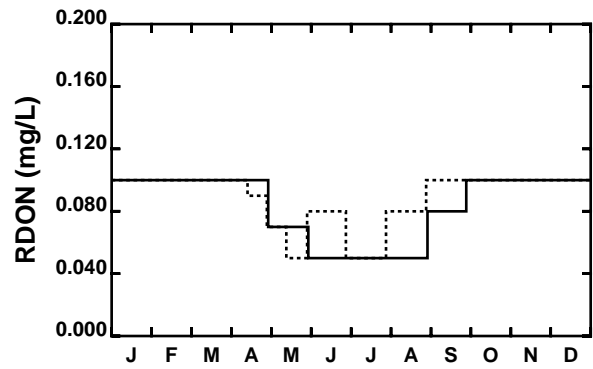
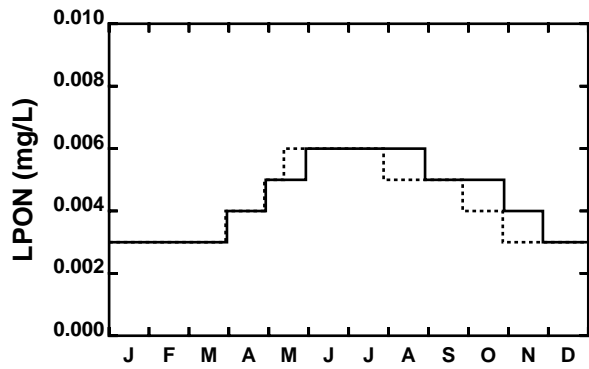
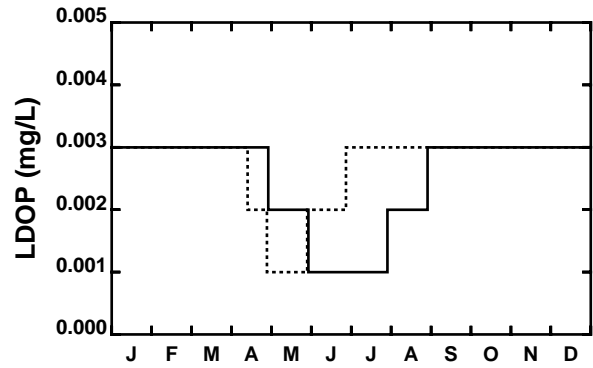
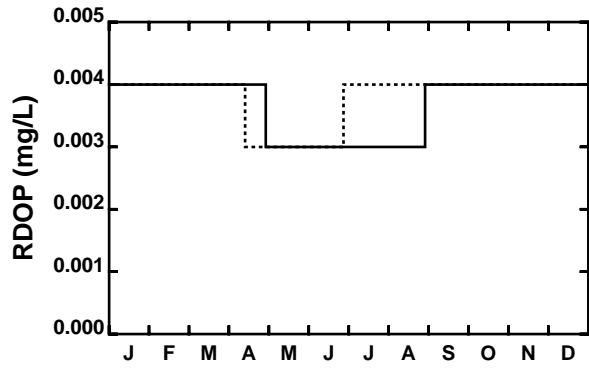


Figure 2-1. Standard Level 1 Boundary Condition Comparison Between Original and Revised 1992 Calibration for Salinity, DO, Phytoplankton and Inorganic Nutrients



Standard Level 1

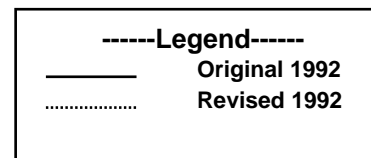


Figure 2-2. Standard Level 1 Boundary Condition Comparison Between Original and Revised 1992 Calibration for Organic Nutrients and Organic Carbon

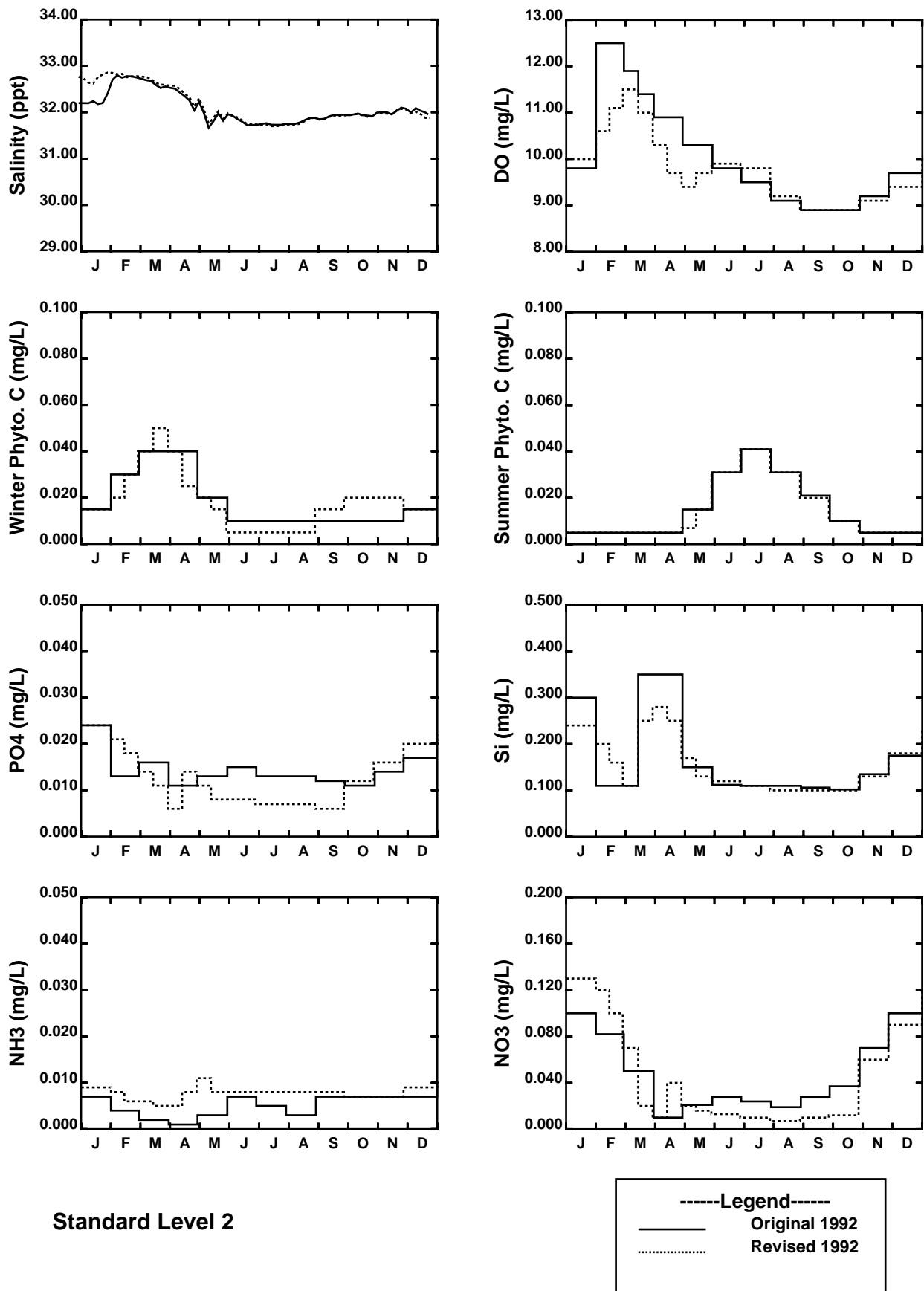
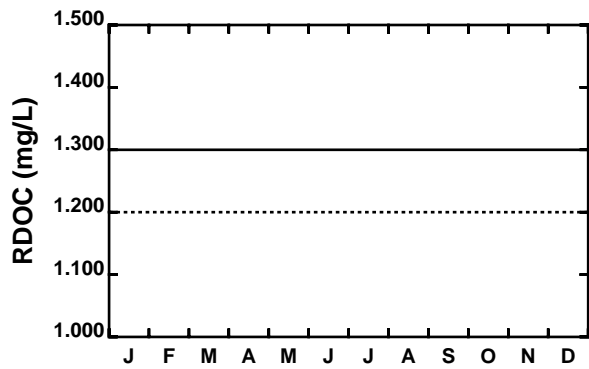
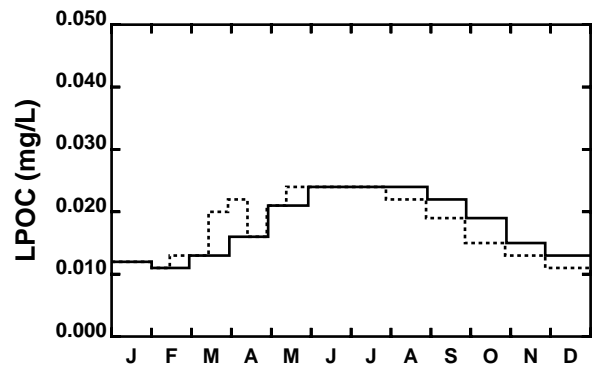
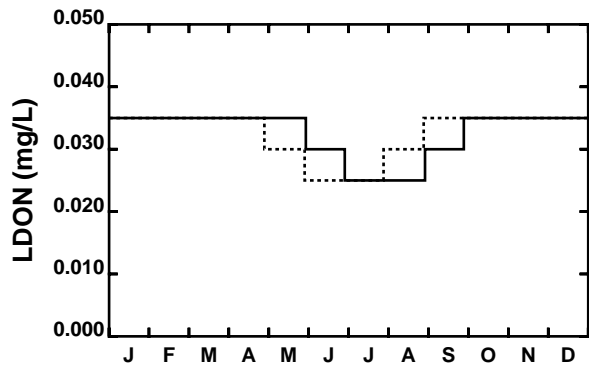
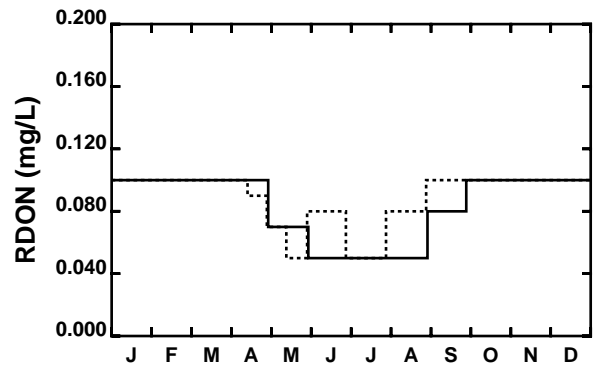
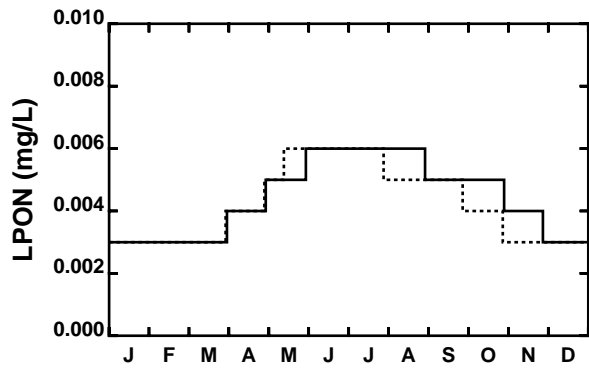
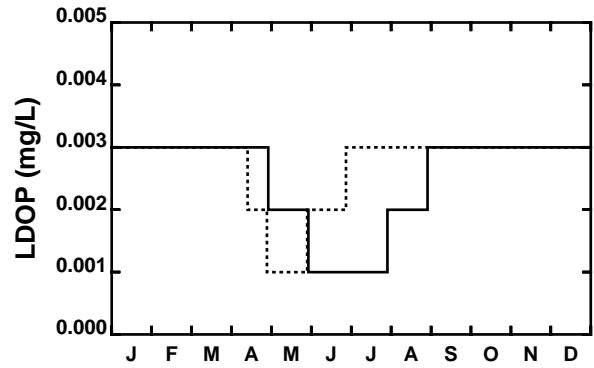
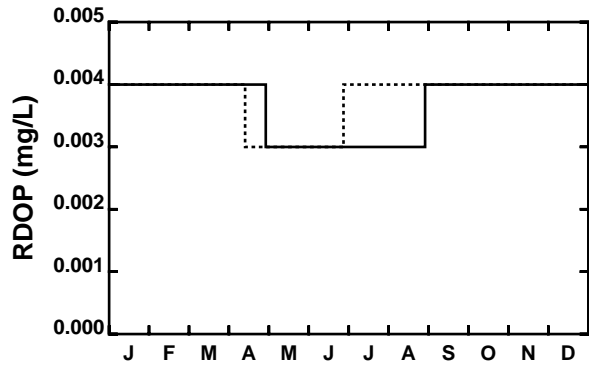


Figure 2-3. Standard Level 2 Boundary Condition Comparison Between Original and Revised 1992 Calibration for Salinity, DO, Phytoplankton and Inorganic Nutrients



Standard Level 2

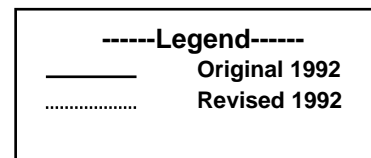


Figure 2-4. Standard Level 2 Boundary Condition Comparison Between Original and Revised 1992 Calibration for Organic Nutrients and Organic Carbon

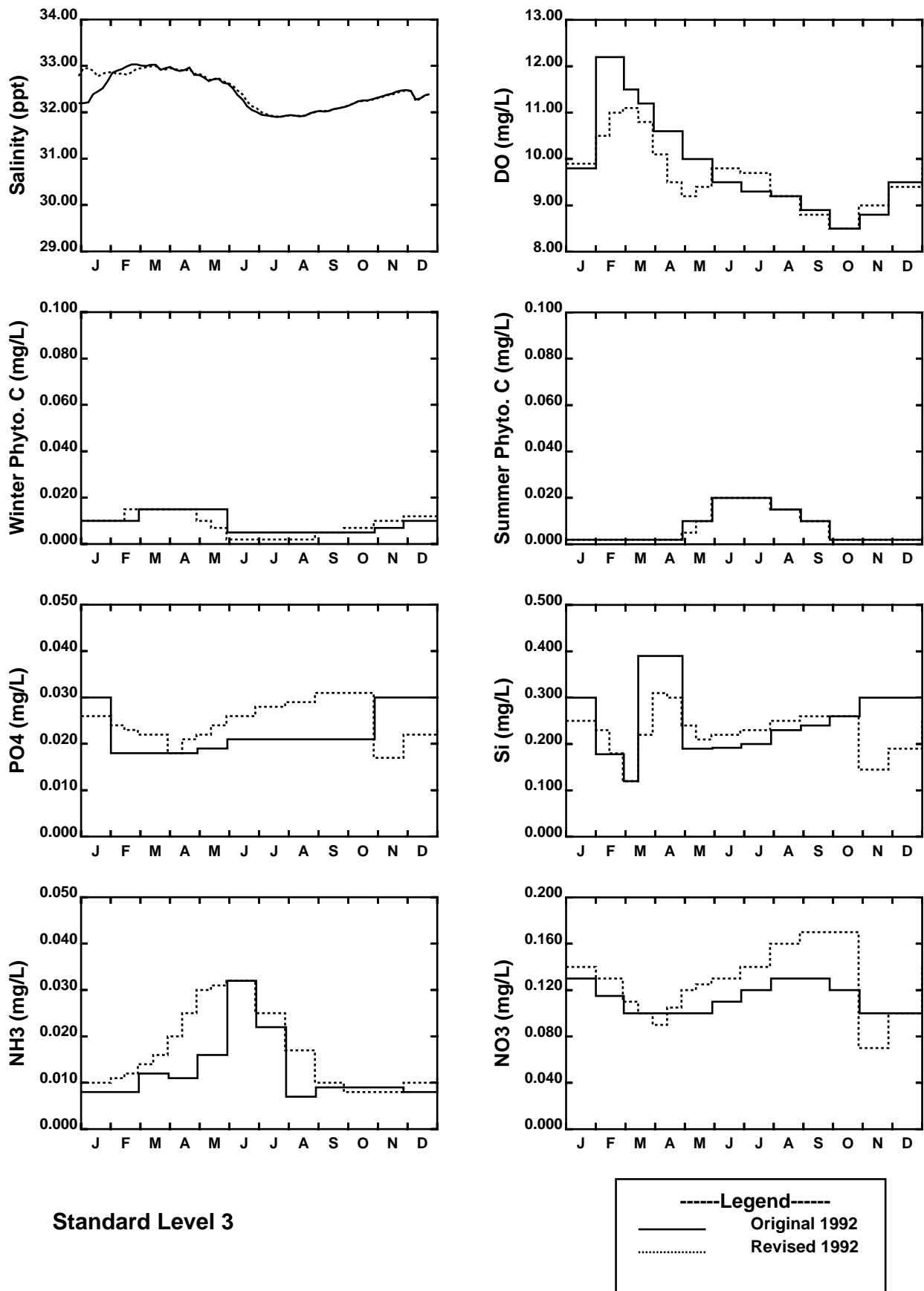
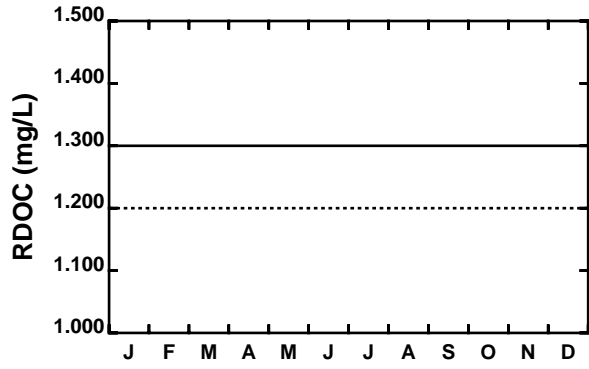
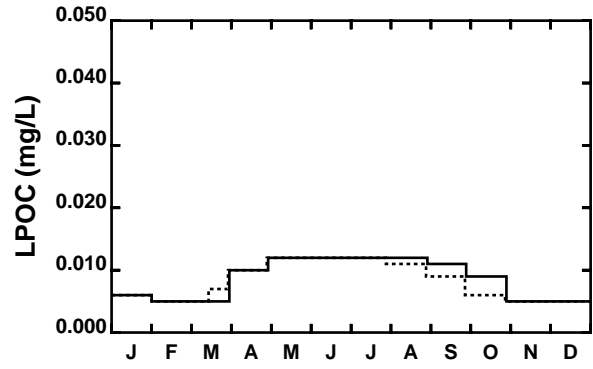
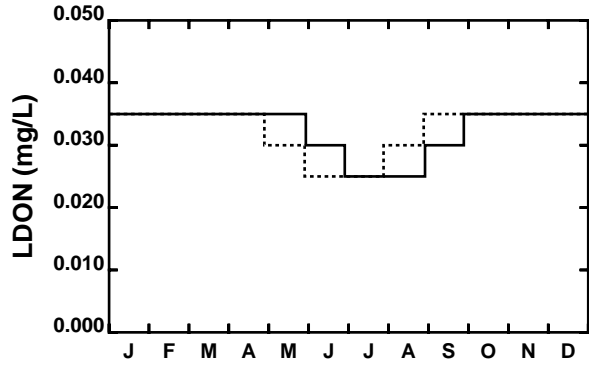
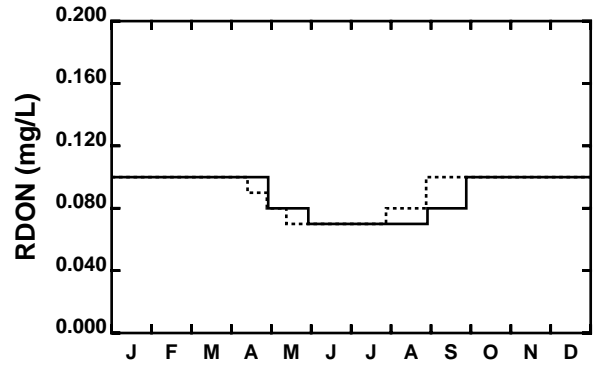
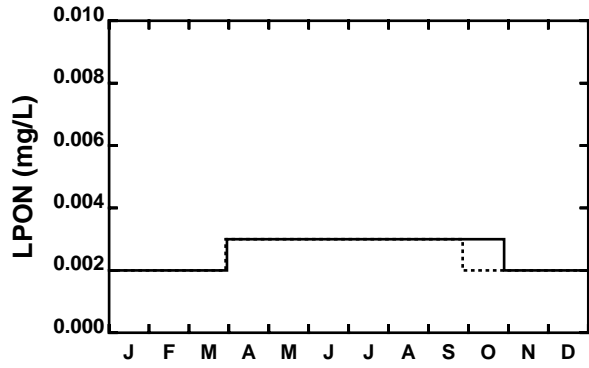
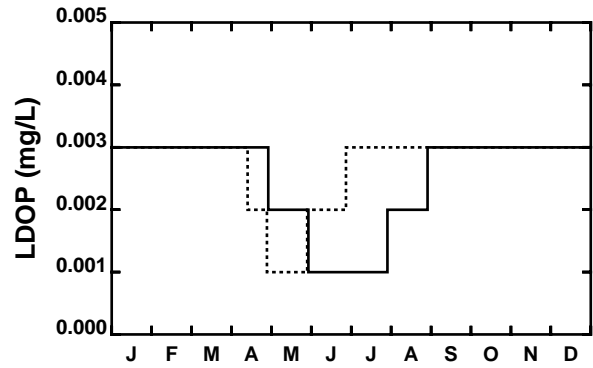
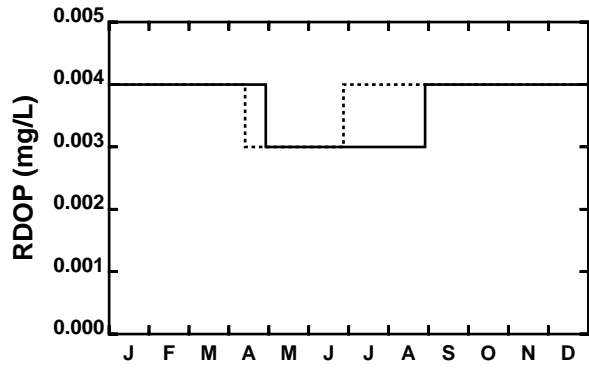


Figure 2-5. Standard Level 3 Boundary Condition Comparison Between Original and Revised 1992 Calibration for Organic Nutrients and Organic Carbon



Standard Level 3

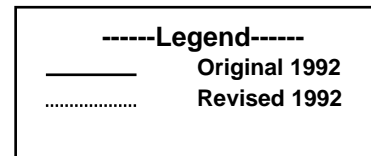


Figure 2-6. Standard Level 3 Boundary Condition Comparison Between Original and Revised 1992 Calibration for Organic Nutrients and Organic Carbon

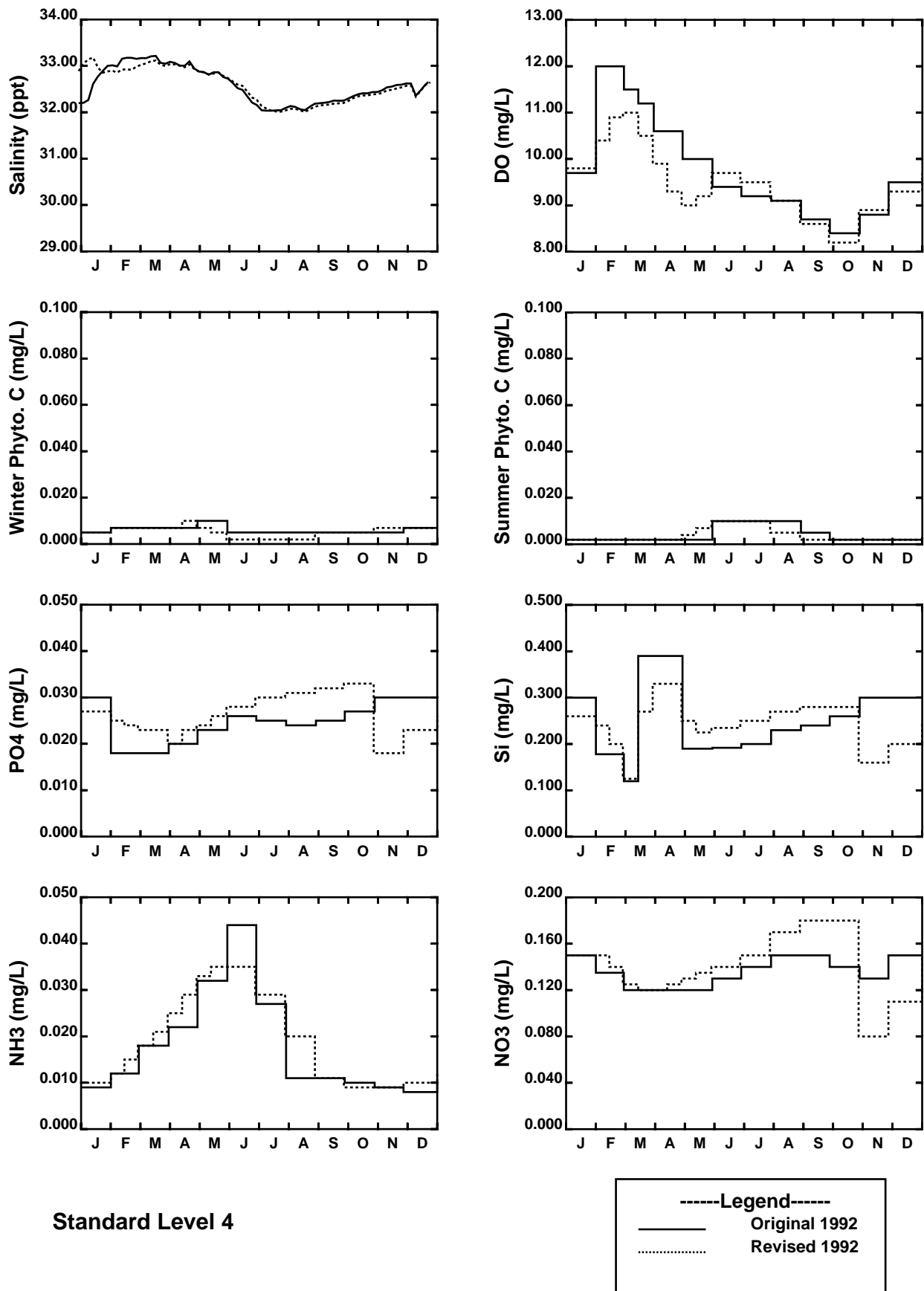
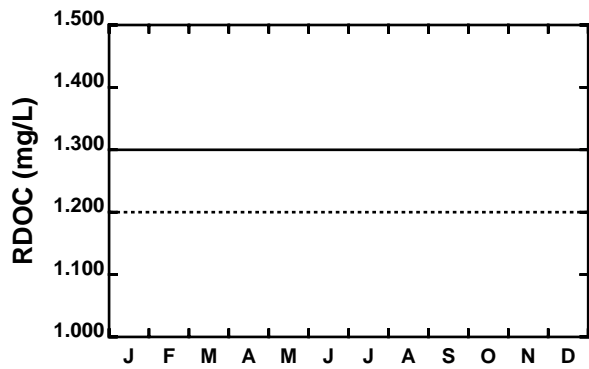
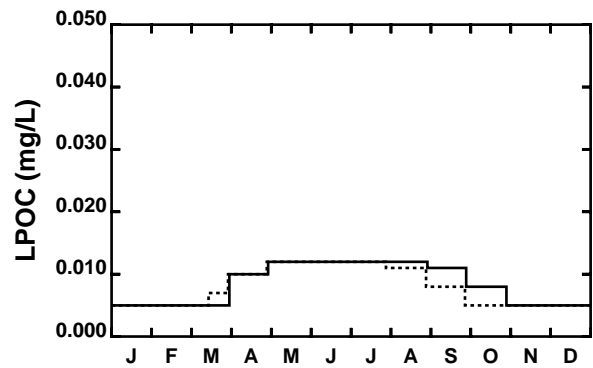
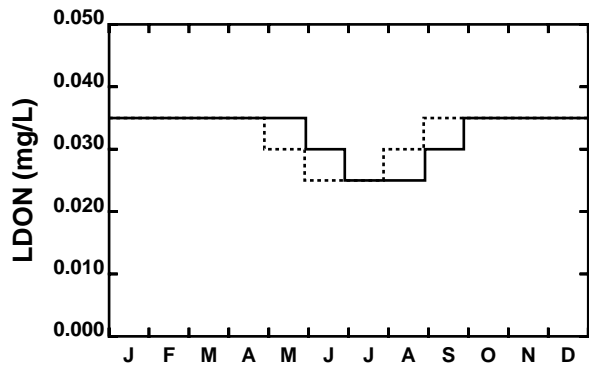
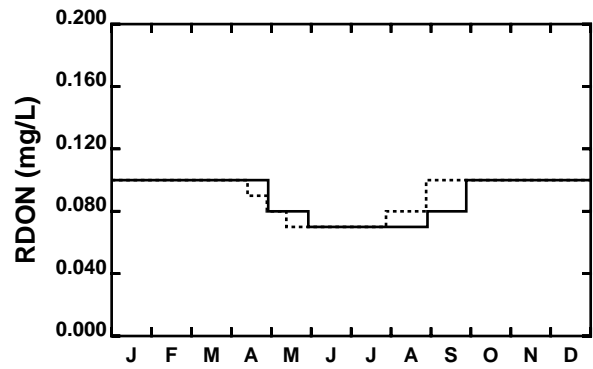
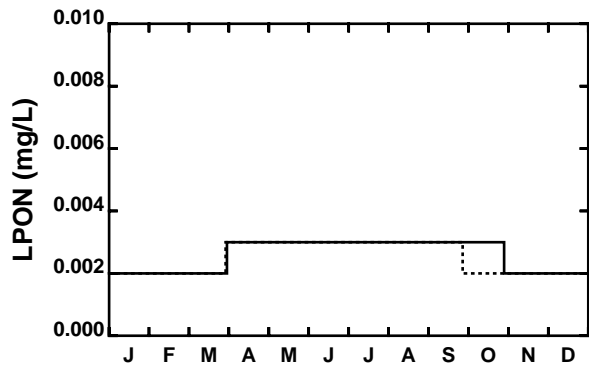
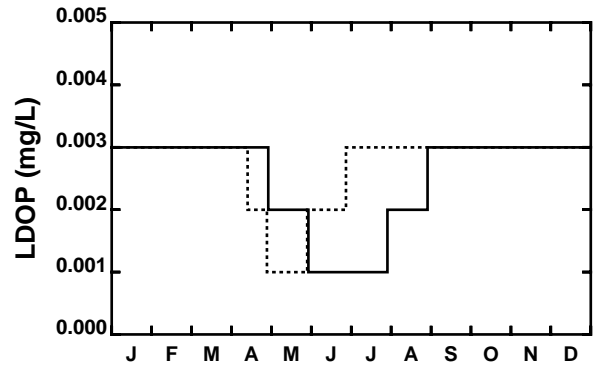
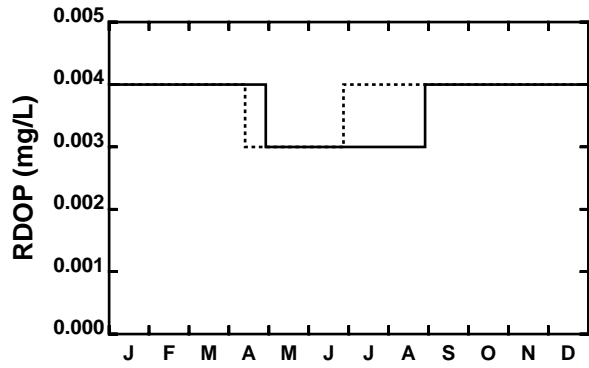


Figure 2-7. Standard Level 4 Boundary Condition Comparison Between Original and Revised 1992 Calibraton for Salinity, DO, Phytoplankton and Inorganic Nutrients



Standard Level 4

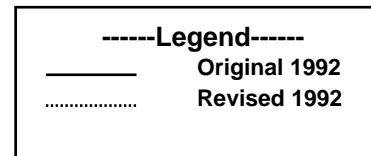


Figure 2-8. Standard Level 4 Boundary Condition Comparison Between Original and Revised 1992 Calibration for Organic Nutrients and Organic Carbon

nutrients and dissolved oxygen were based on data. Most of the changes to the organic constituents involved shifting the timing of the concentration changes based on the additional interior data and a better understanding of how boundary concentrations affect the internal water quality concentrations.

2.3 1992-1994 BOUNDARY CONDITIONS

Figures 2-9 through 2-28 present the boundary conditions assigned to the water quality model for the period of 1992 through 1994. For PO_4 , NH_3 , NO_2+NO_3 , Si, and DO the 1994 data from stations F26 and F27 are plotted along with the 1994 boundary conditions (there were no boundary data in 1992 or 1993). The dissolved oxygen figure (2-28) also includes data on the DO concentration at 100 percent saturation as computed from temperature and salinity data. Those state-variables that are not included in these figures were assigned a zero concentration at the boundary. Figures 2-29 to 2-33 present the assigned boundary conditions compared with measured data for POC, PON, DOC, TDN, and TDP. These data provided starting points for the assignment of boundary conditions.

The majority of the dissolved and particulate organic boundary condition concentrations were assigned to be identical for each year (with the lone exception being LPOC). This was done primarily because only six measurements taken at station F27 in 1994, were available to guide the assignment of the boundary conditions for these state variables. Using the same boundary conditions for each of the three years produced reasonable results, so they were not modified on a year-to-year basis. LPOC, however, was modified year-to-year to take into account the variability of phytoplankton and, hence, detrital organic carbon at the boundary. For the remaining systems, including the two phytoplankton groups, the inorganic nutrients, and DO, data were available at the near-field stations generally at least once a month for all three years. These data provided insight as to what was happening at the boundary and led to time-varying boundary conditions for each year. Essentially, the near-field data were used to infer boundary condition concentrations. These boundary condition concentrations were used to help calibrate the model. If simple boundary conditions were adequate to calibrate the model, simple boundary conditions were used. When more time-varying boundary conditions were required to improve the model's calibration to data, more time-varying boundary conditions were used. Based on the comparison of boundary condition concentrations to measured data, the assigned boundary conditions appear reasonable.

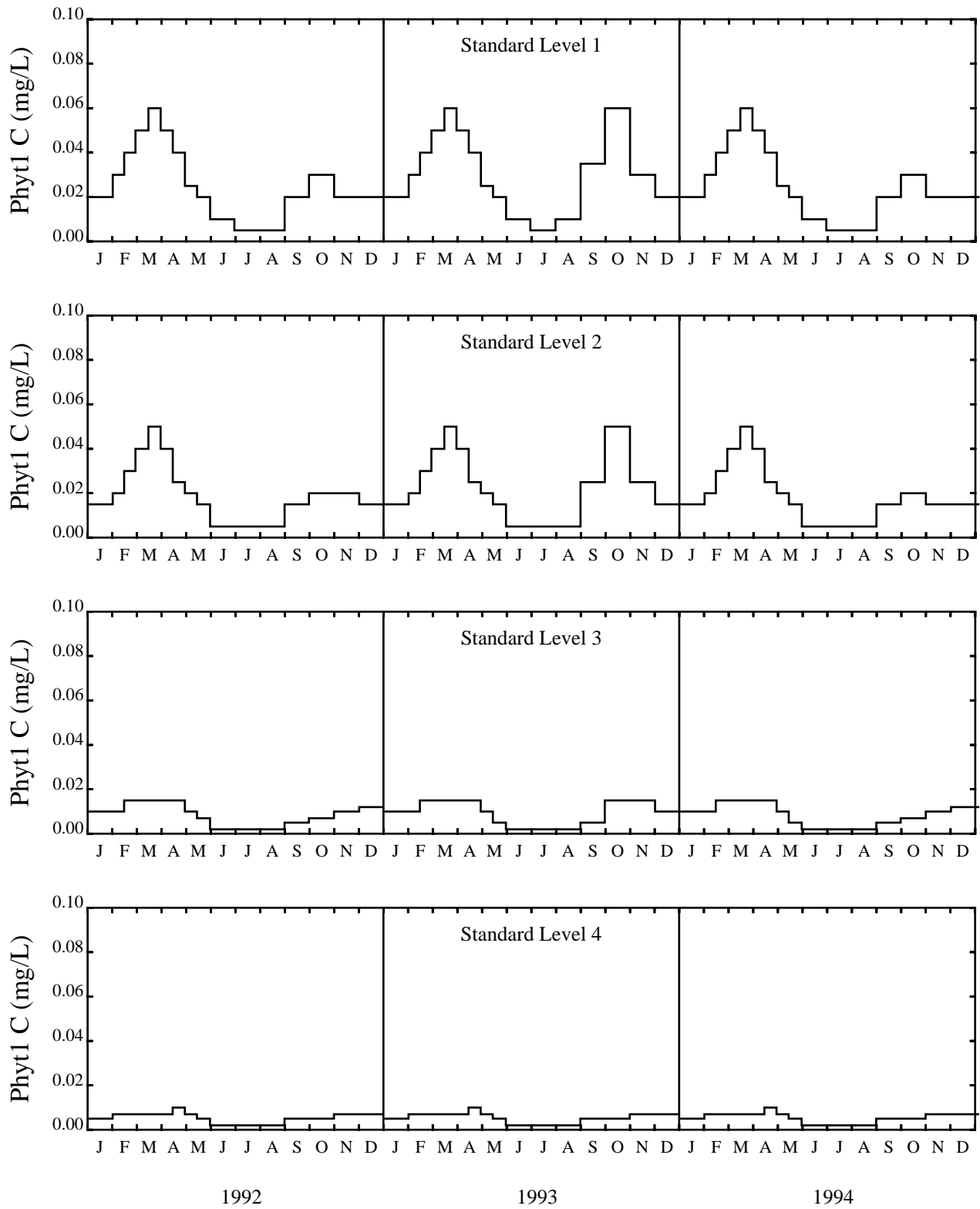


Figure 2-9. 1992-1994 Winter Diatom Boundary Conditions

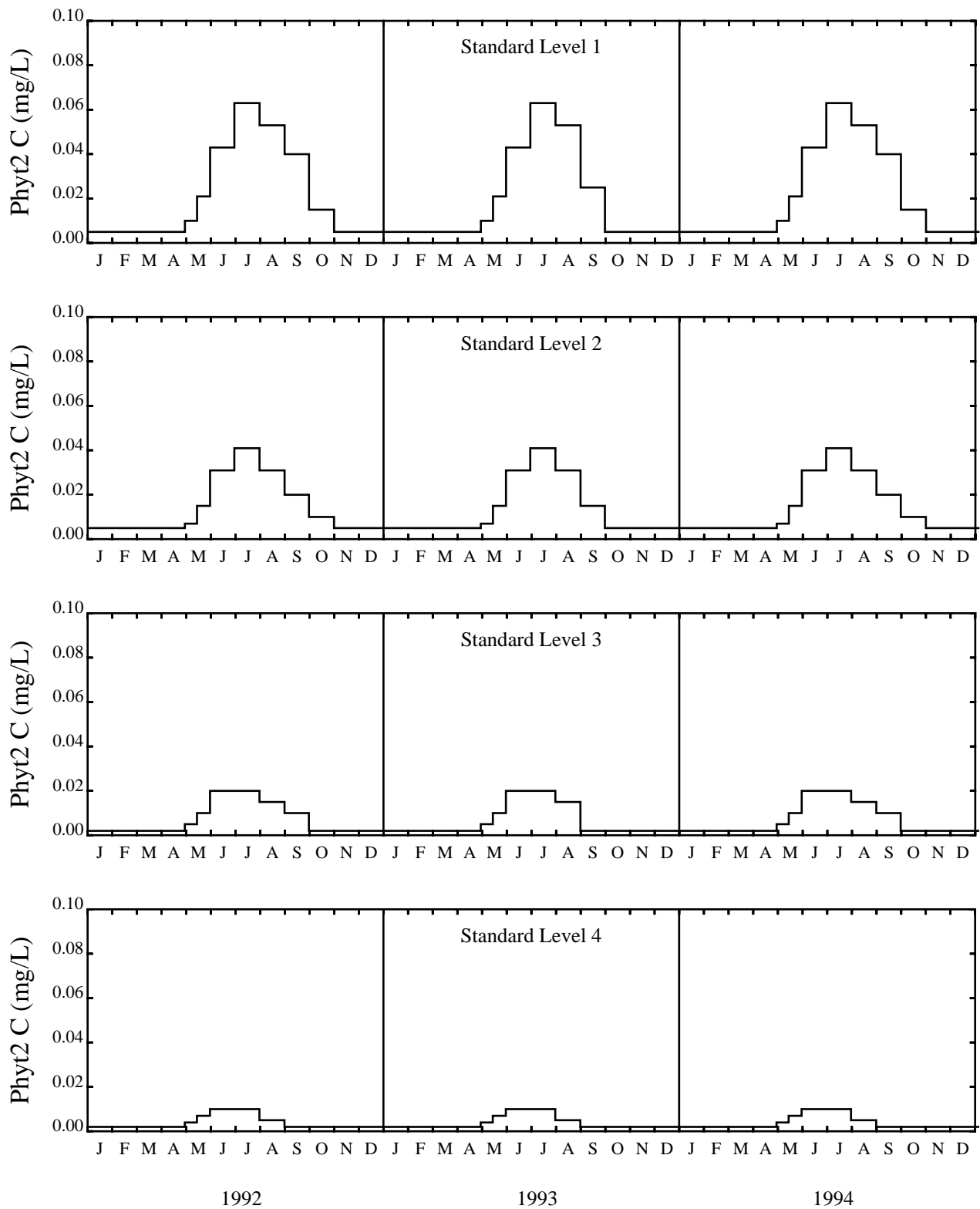


Figure 2-10. 1992-1994 Summer Assemblage Boundary Conditions

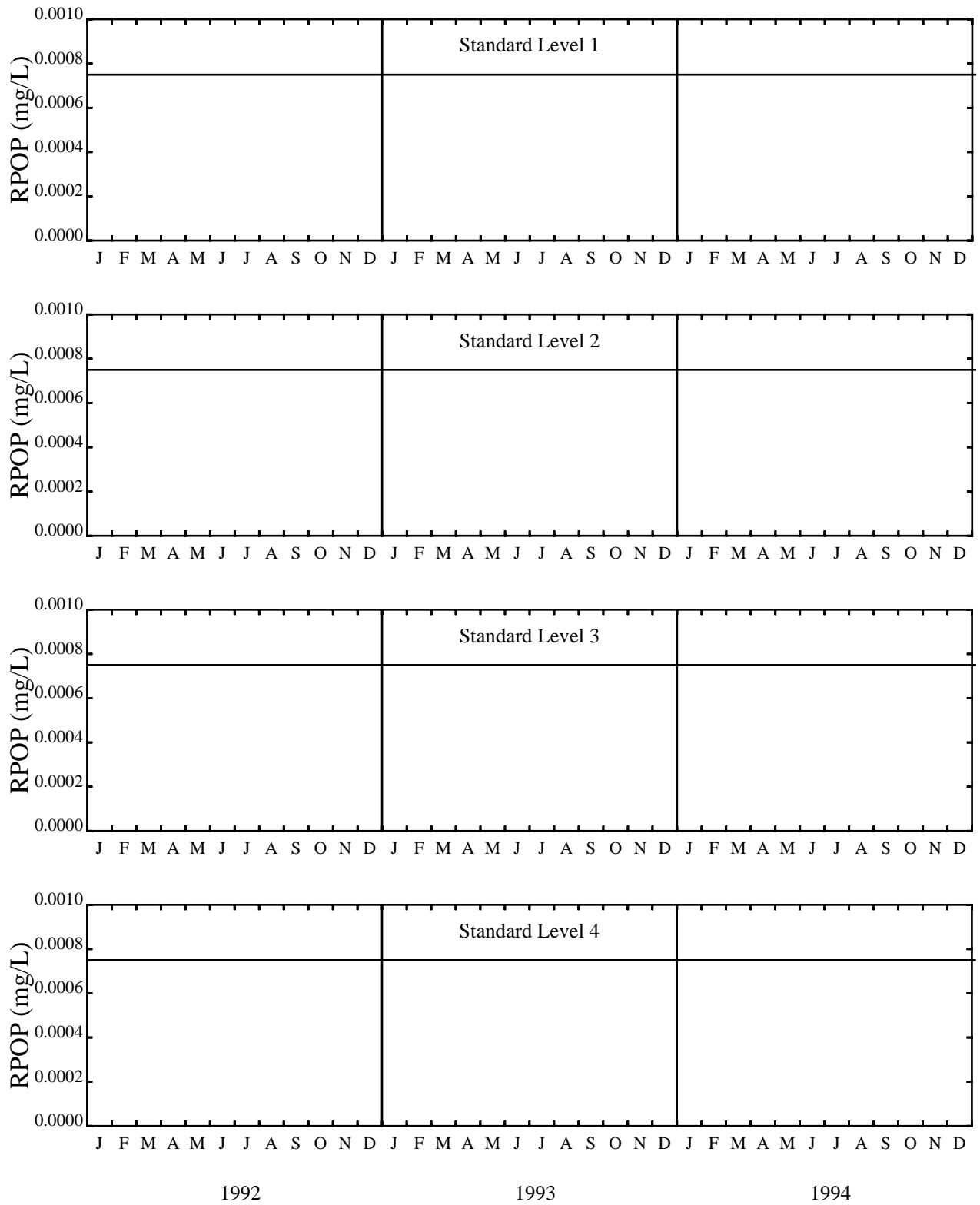


Figure 2-11. 1992-1994 Refractory Particulate Organic Phosphorus Boundary Condition

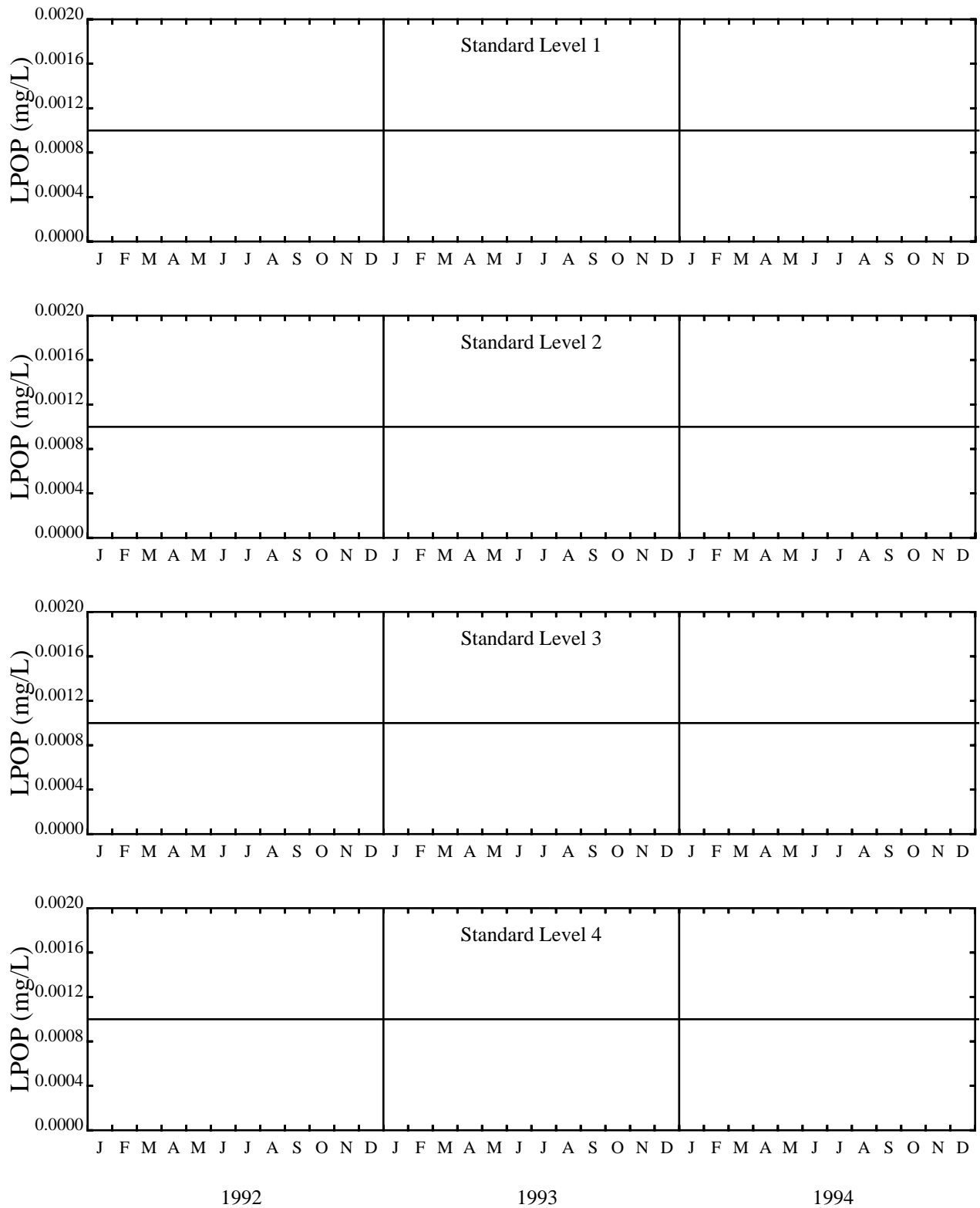


Figure 2-12. 1992-1994 Labile Particulate Organic Phosphorus Boundary Conditions

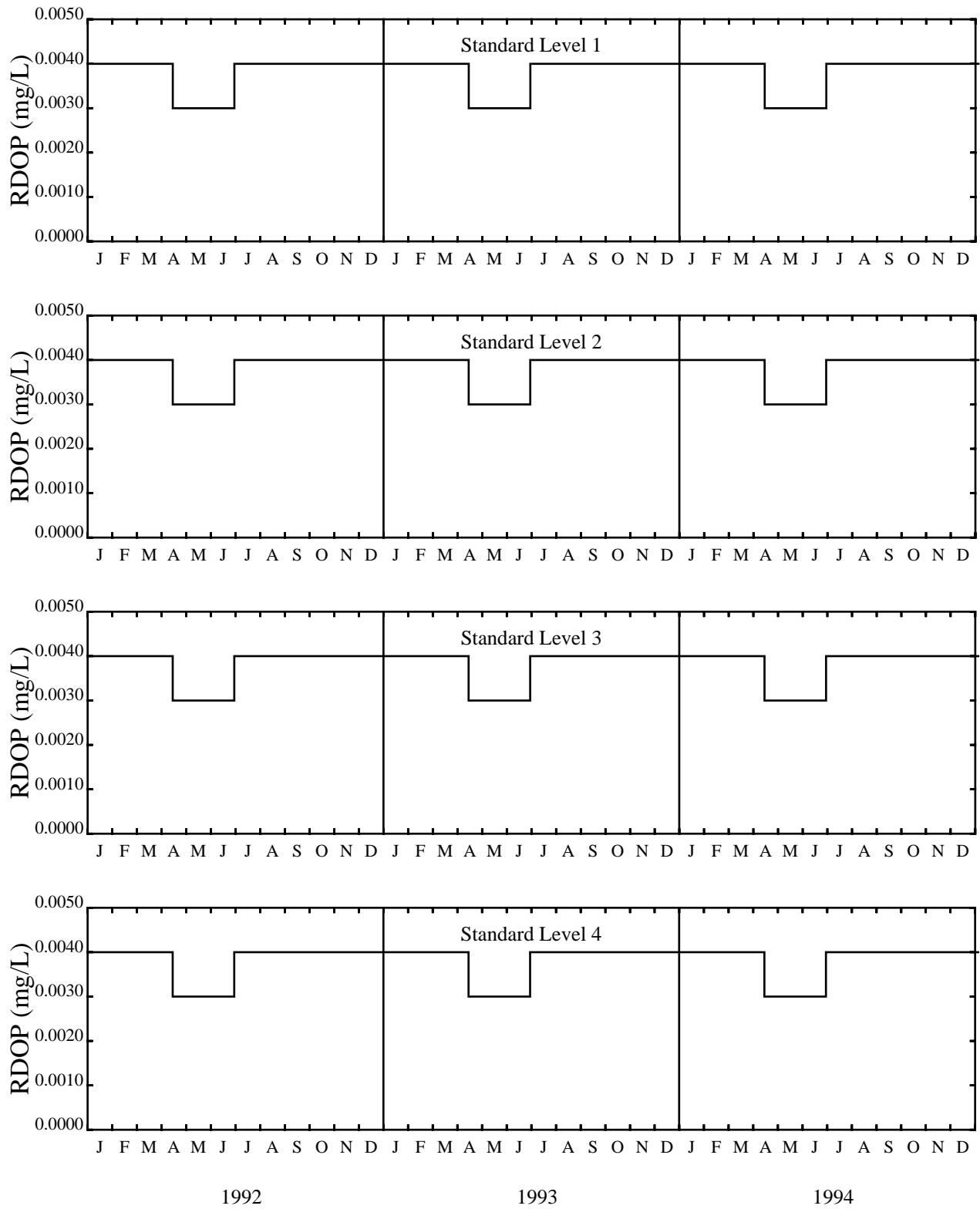


Figure 2-13. 1992-1994 Refractory Dissolved Organic Phosphorus Boundary Conditions

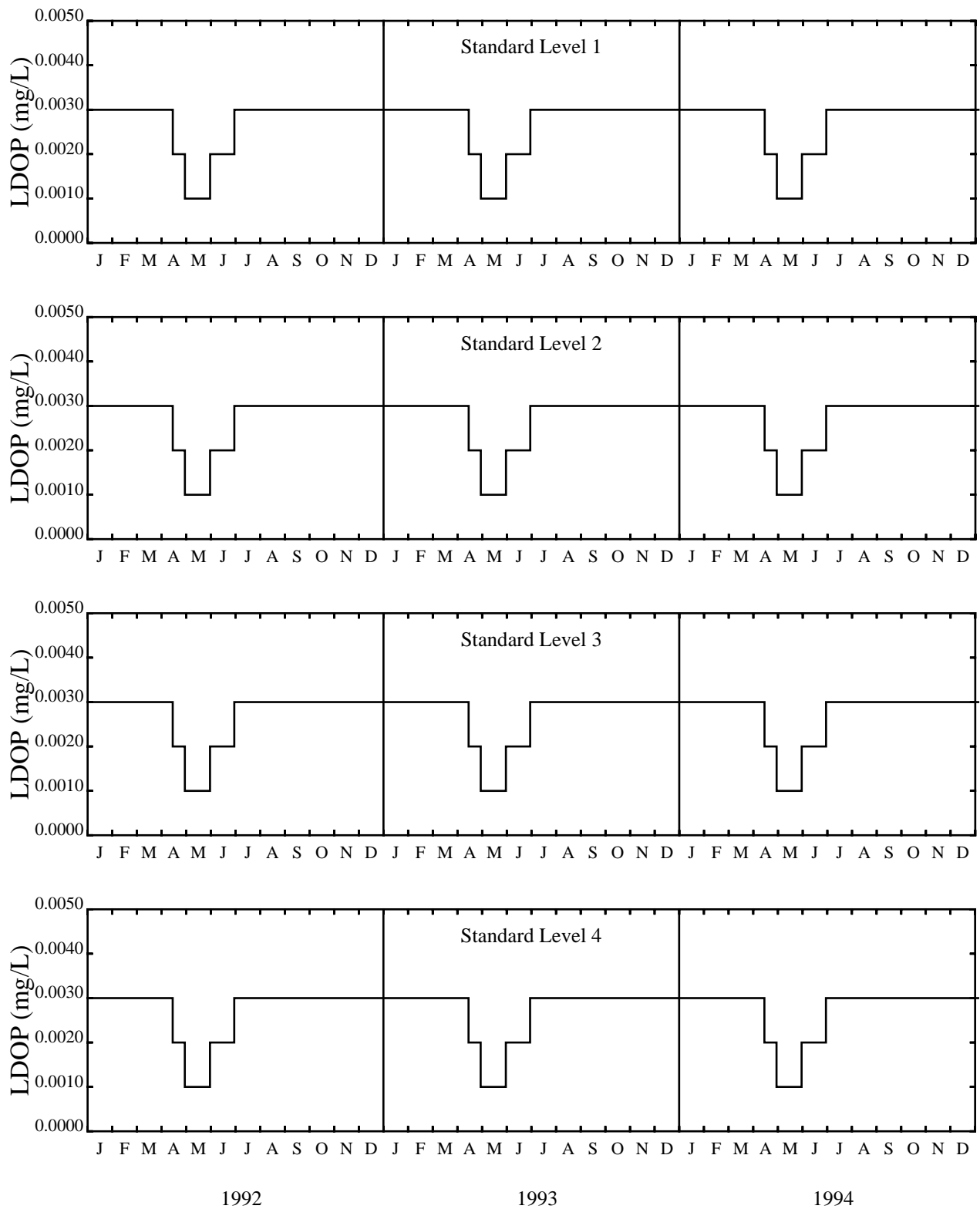


Figure 2-14. 1992-1994 Labile Dissolved Organic Phosphorus Boundary Conditions

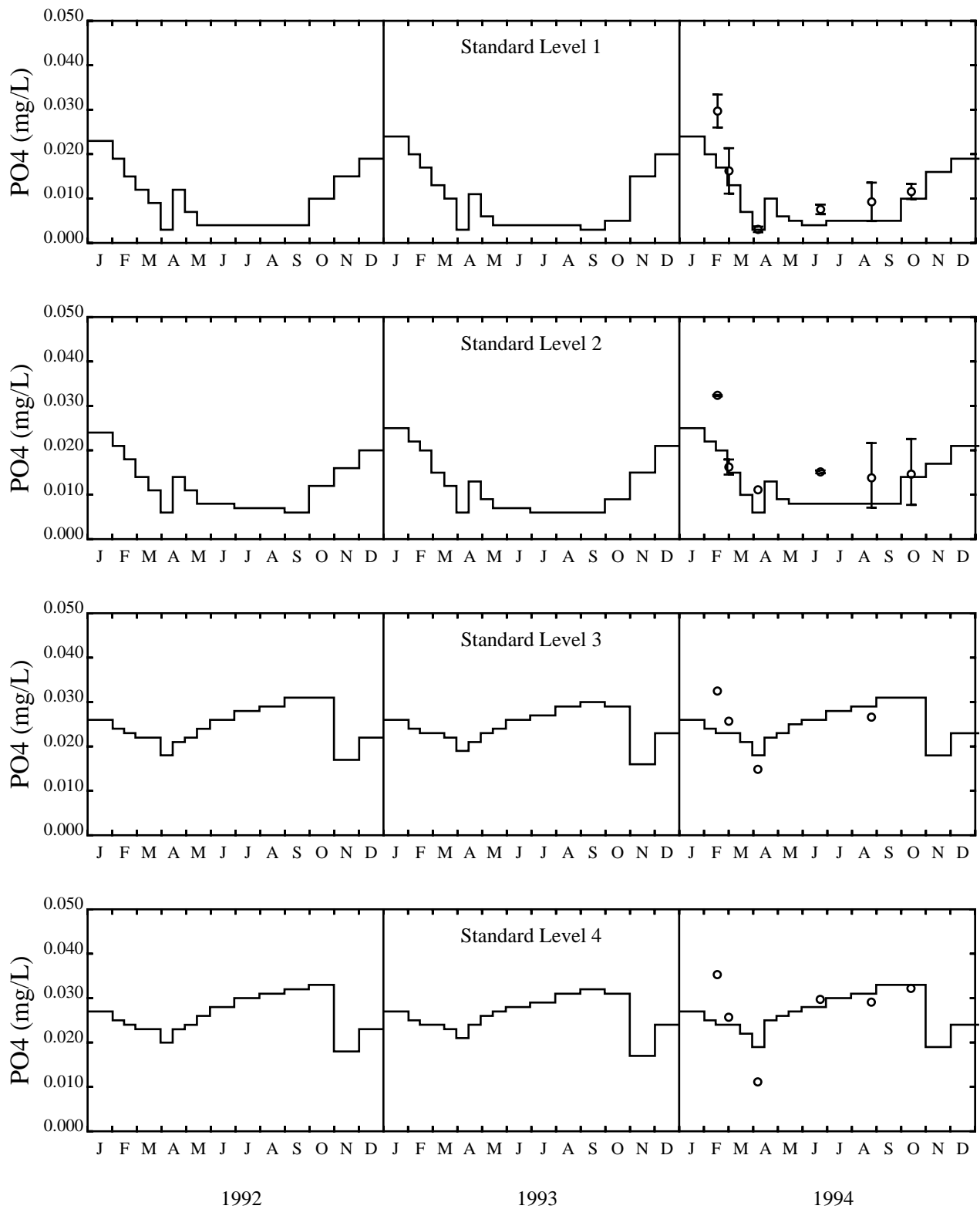


Figure 2-15. 1992-1994 Dissolved Inorganic Phosphorus Boundary Conditions

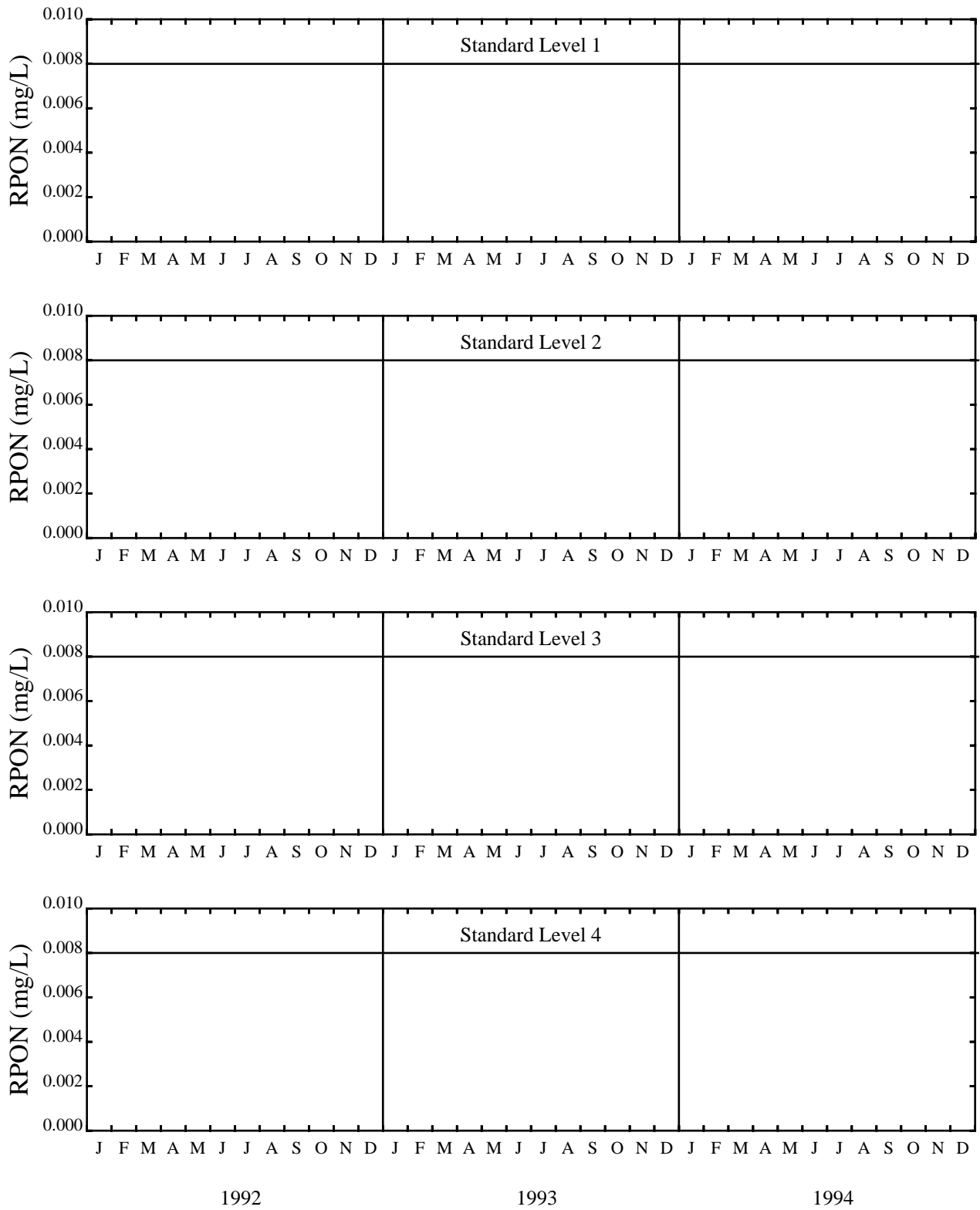


Figure 2-16. 1992-1994 Refractory Particulate Organic Nitrogen Boundary Conditions

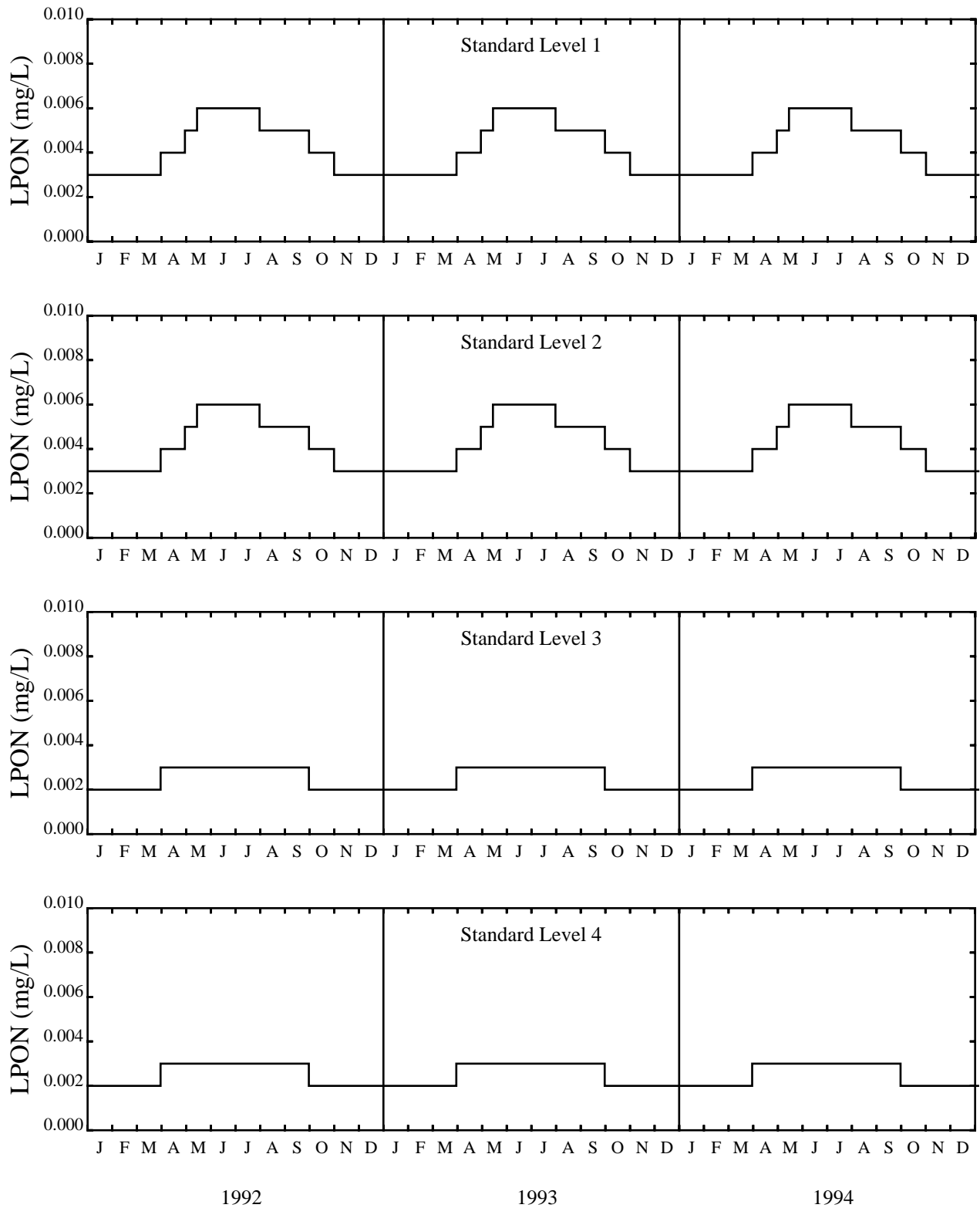


Figure 2-17. 1992-1994 Labile Particulate Organic Nitrogen Boundary Conditions

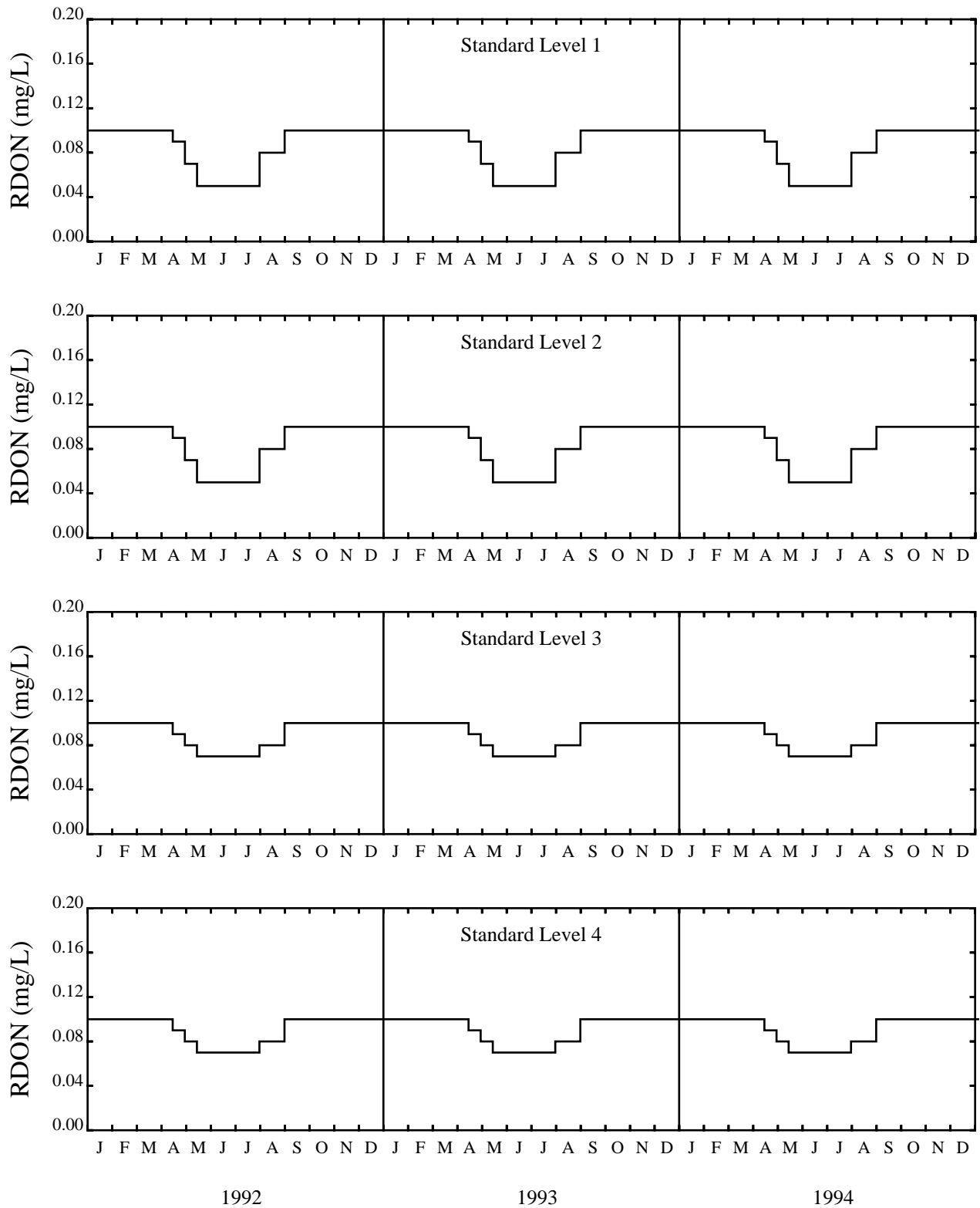


Figure 2-18. 1992-1994 Refractory Dissolved Organic Nitrogen Boundary Conditions

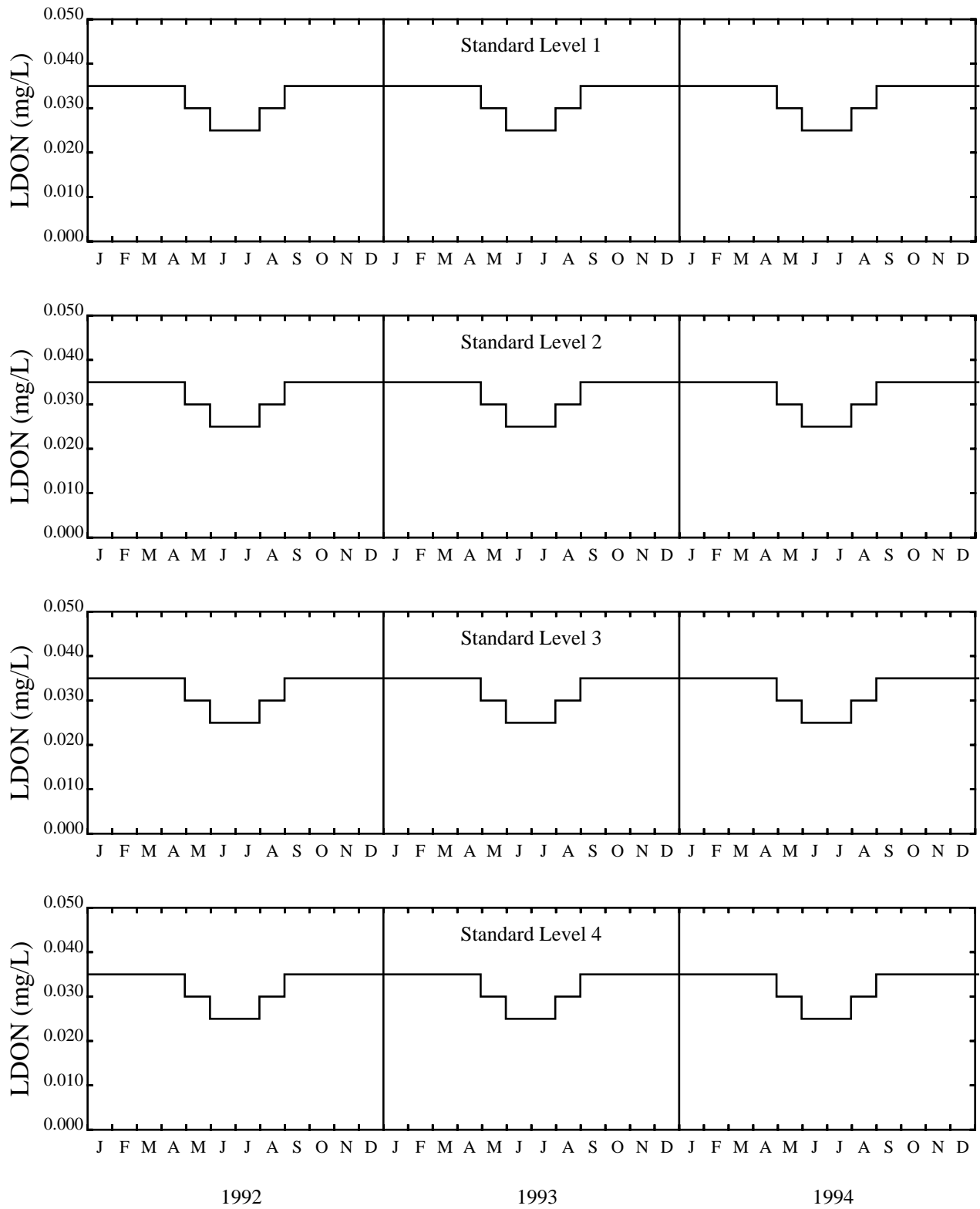


Figure 2-19. 1992-1994 Labile Dissolved Organic Nitrogen Boundary Conditions

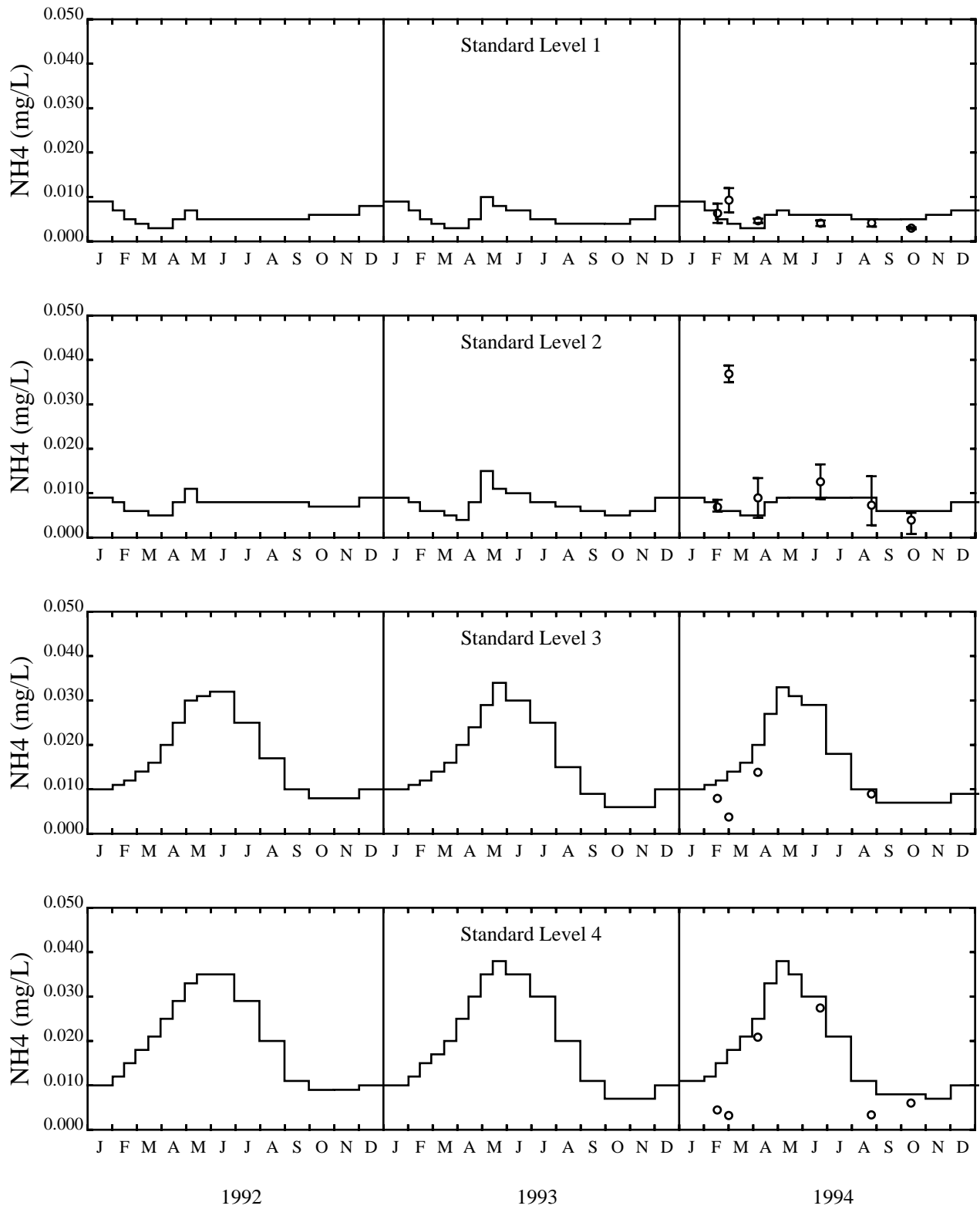


Figure 2-20. 1992-1994 Ammonium - Nitrogen Boundary Conditions

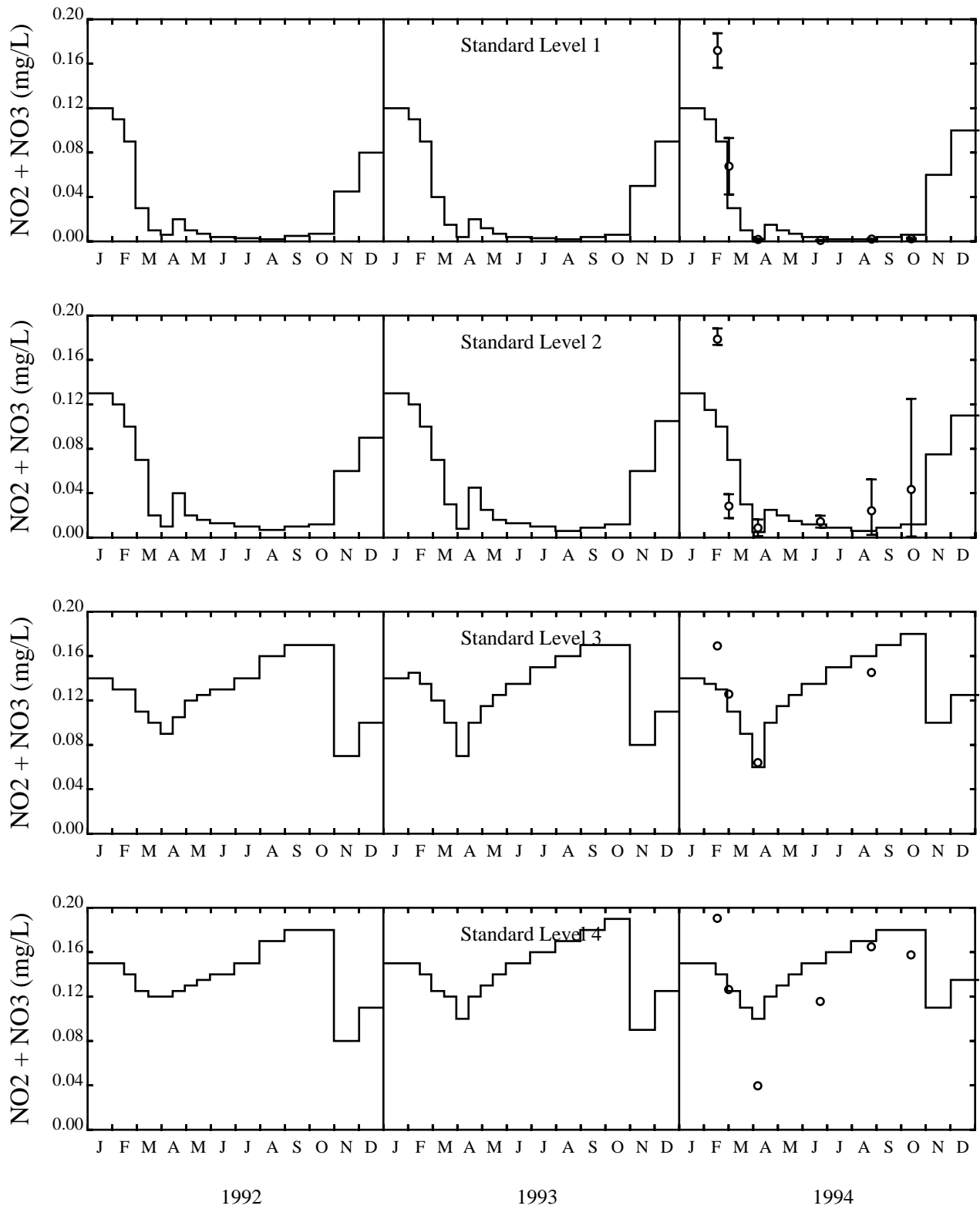


Figure 2-21. 1992-1994 Nitrite + Nitrate-Nitrogen Boundary Conditions

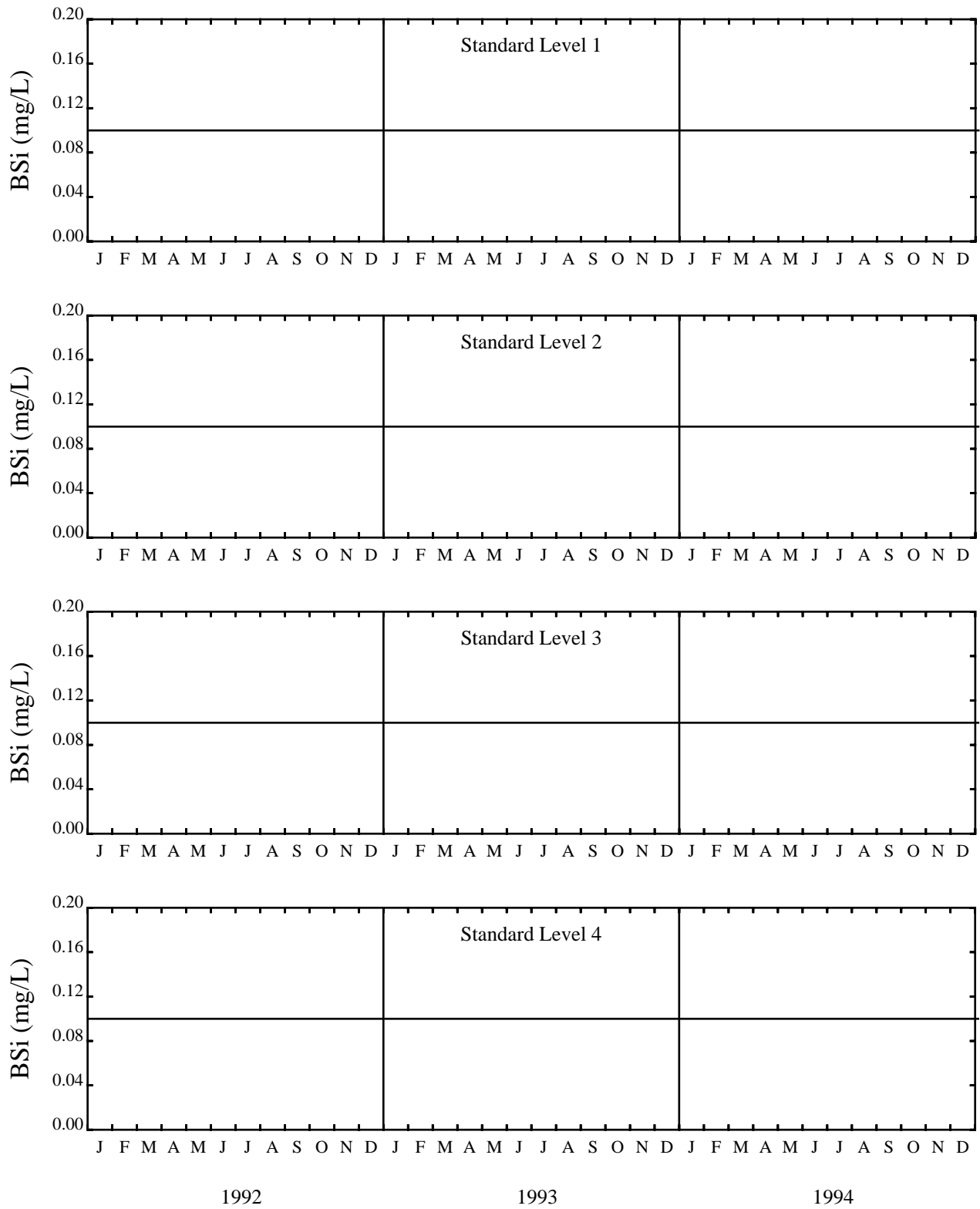


Figure 2-22. 1992-1994 Biogenic Silica Boundary Conditions

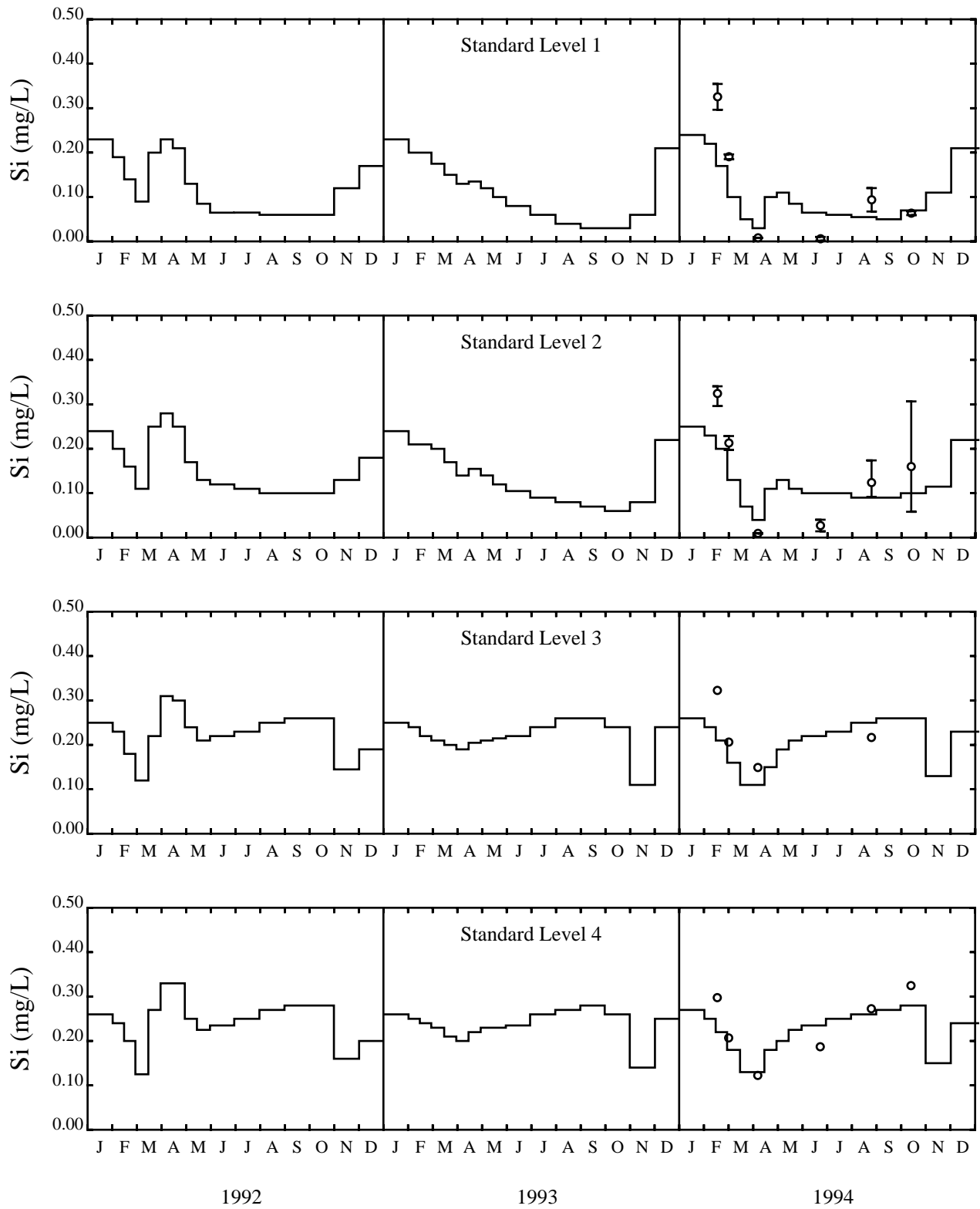


Figure 2-23. 1992-1994 Dissolved Silica Boundary Conditions

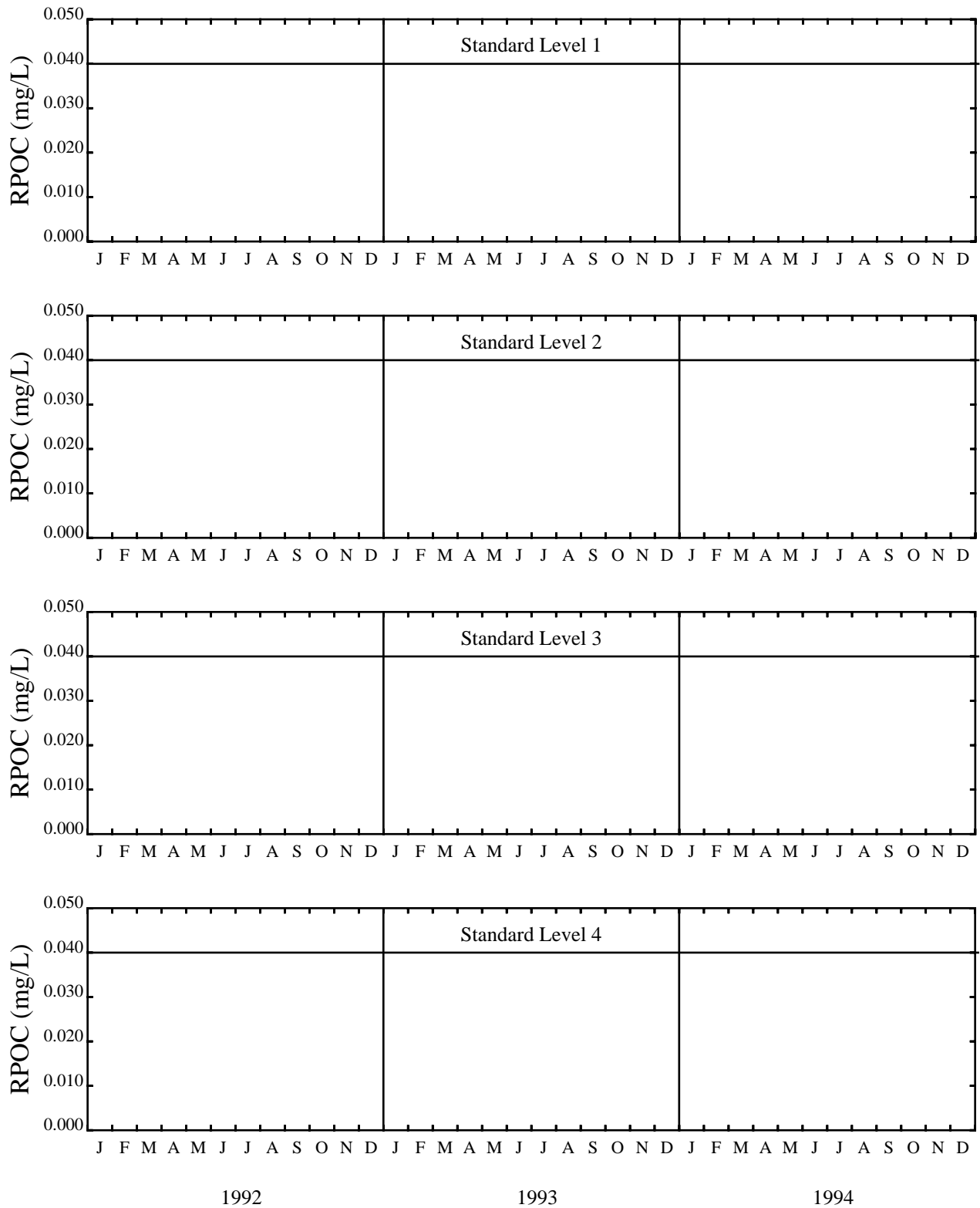


Figure 2-24. 1992-1994 Refractory Particulate Organic Carbon Boundary Conditions

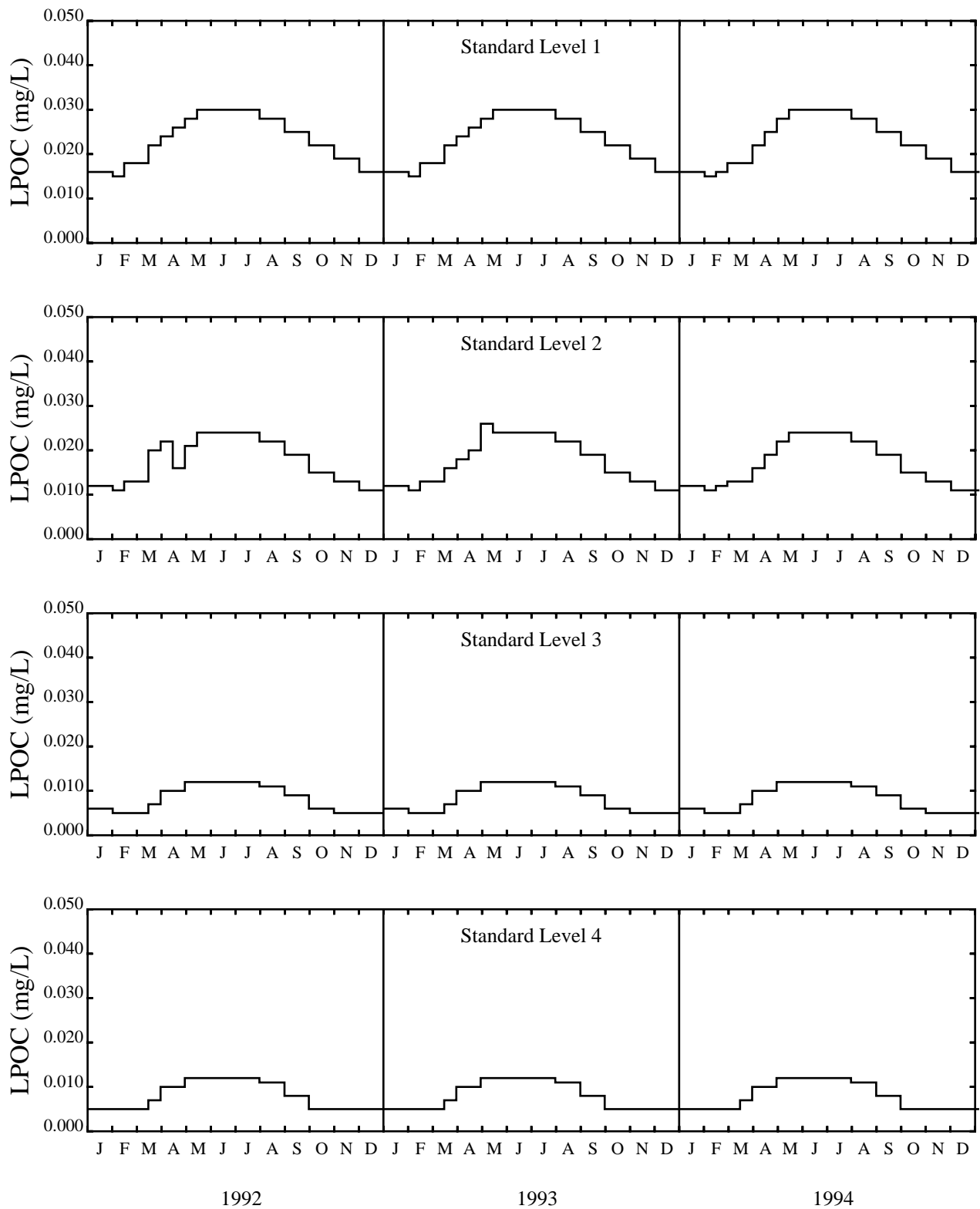


Figure 2-25. 1992-1994 Labile Particulate Organic Carbon Boundary Conditions

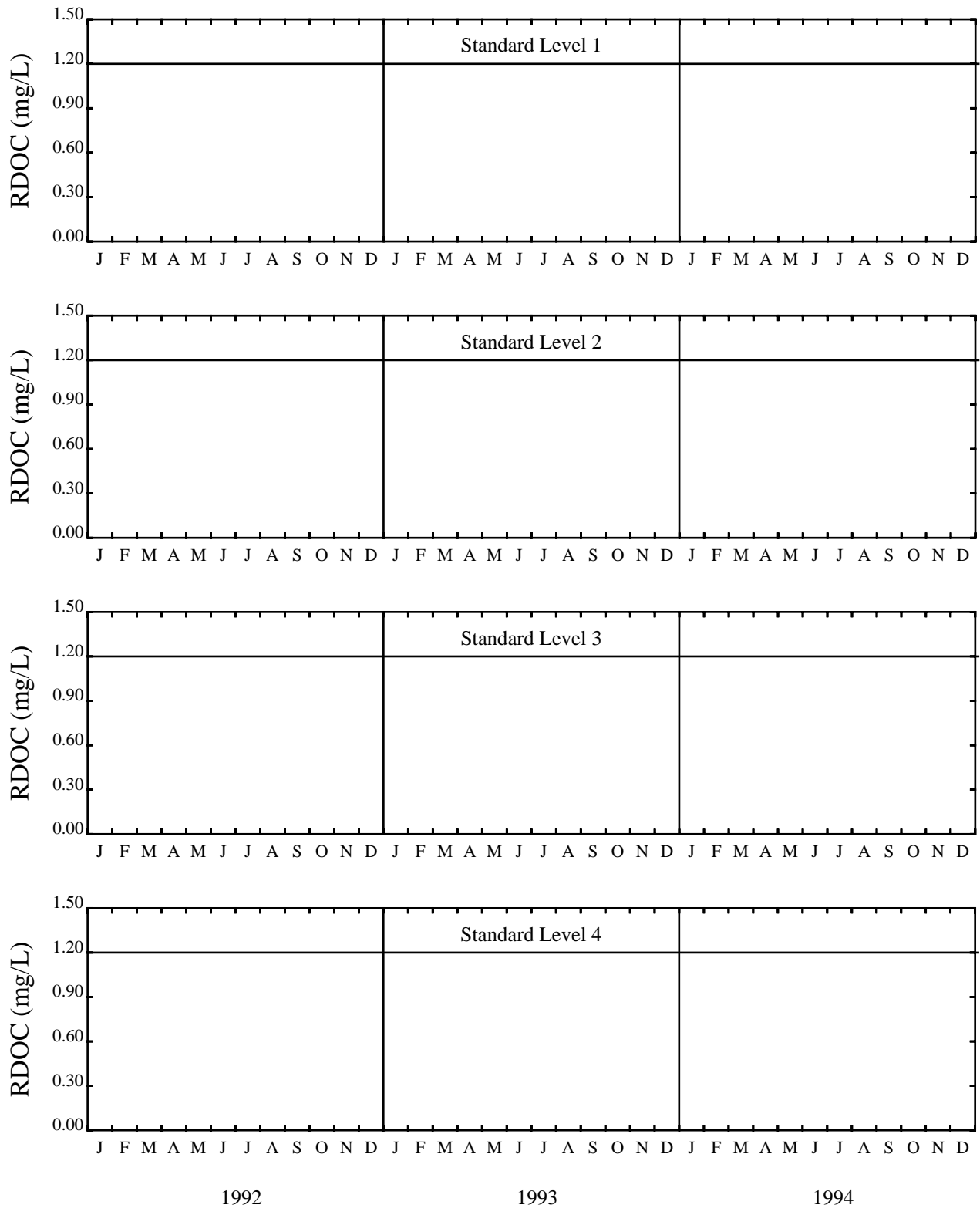


Figure 2-26. 1992-1994 Refractory Dissolved Organic Carbon Boundary Conditions

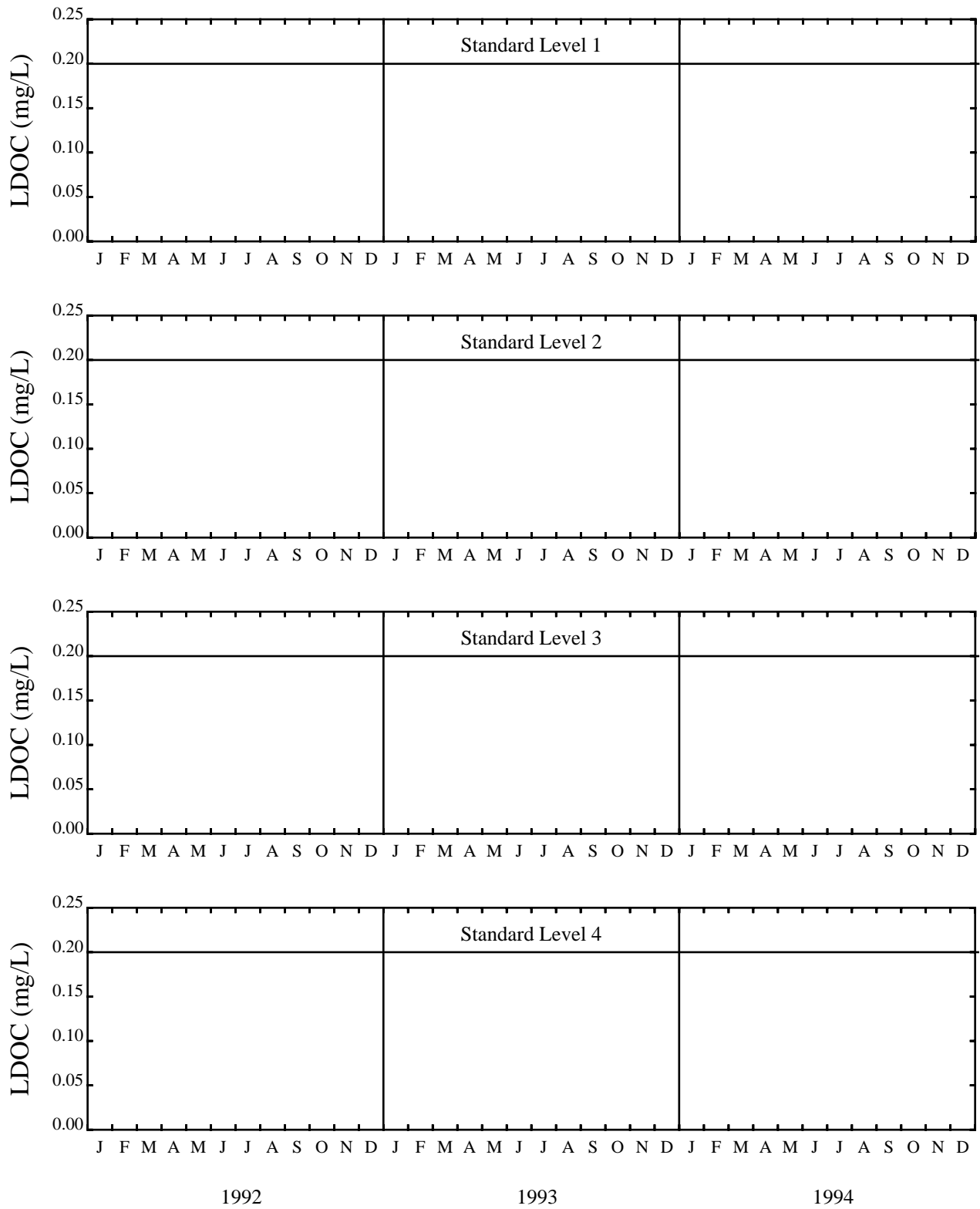


Figure 2-27. 1992-1994 Labile Dissolved Organic Carbon Boundary Conditions

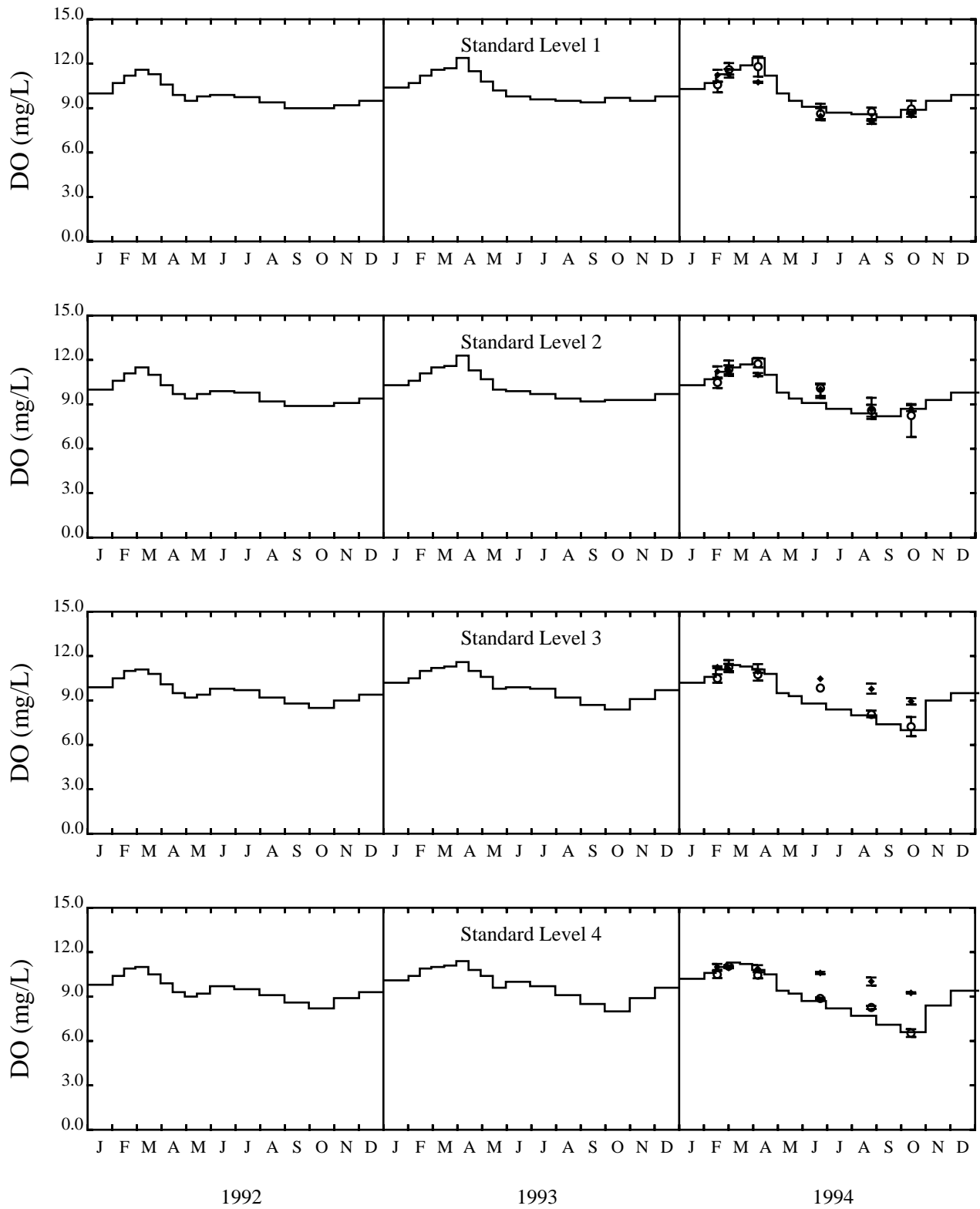


Figure 2-28. 1992-1994 Dissolved Oxygen Boundary Conditions

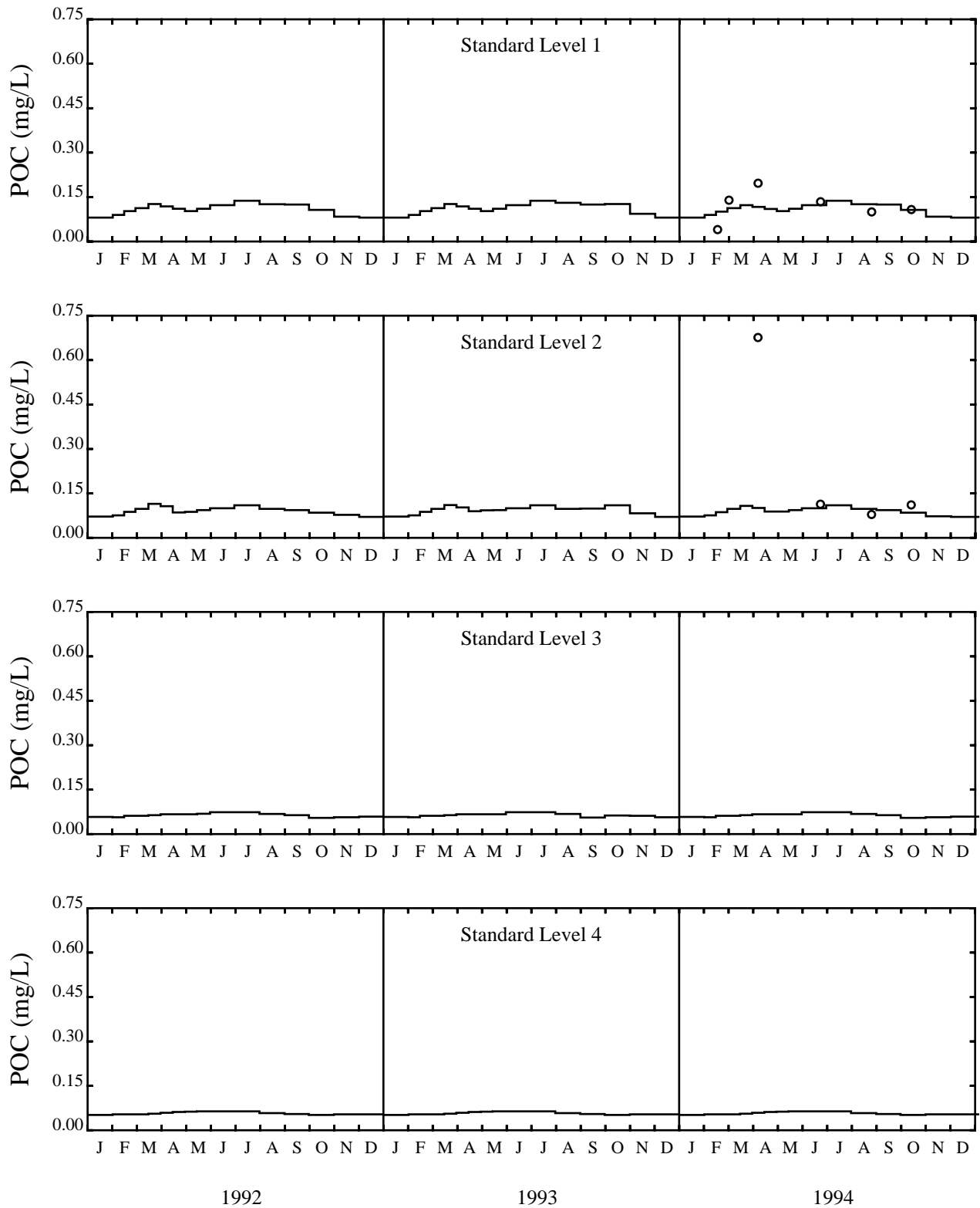


Figure 2-29. 1992-1994 Particulate Organic Carbon Boundary Conditions

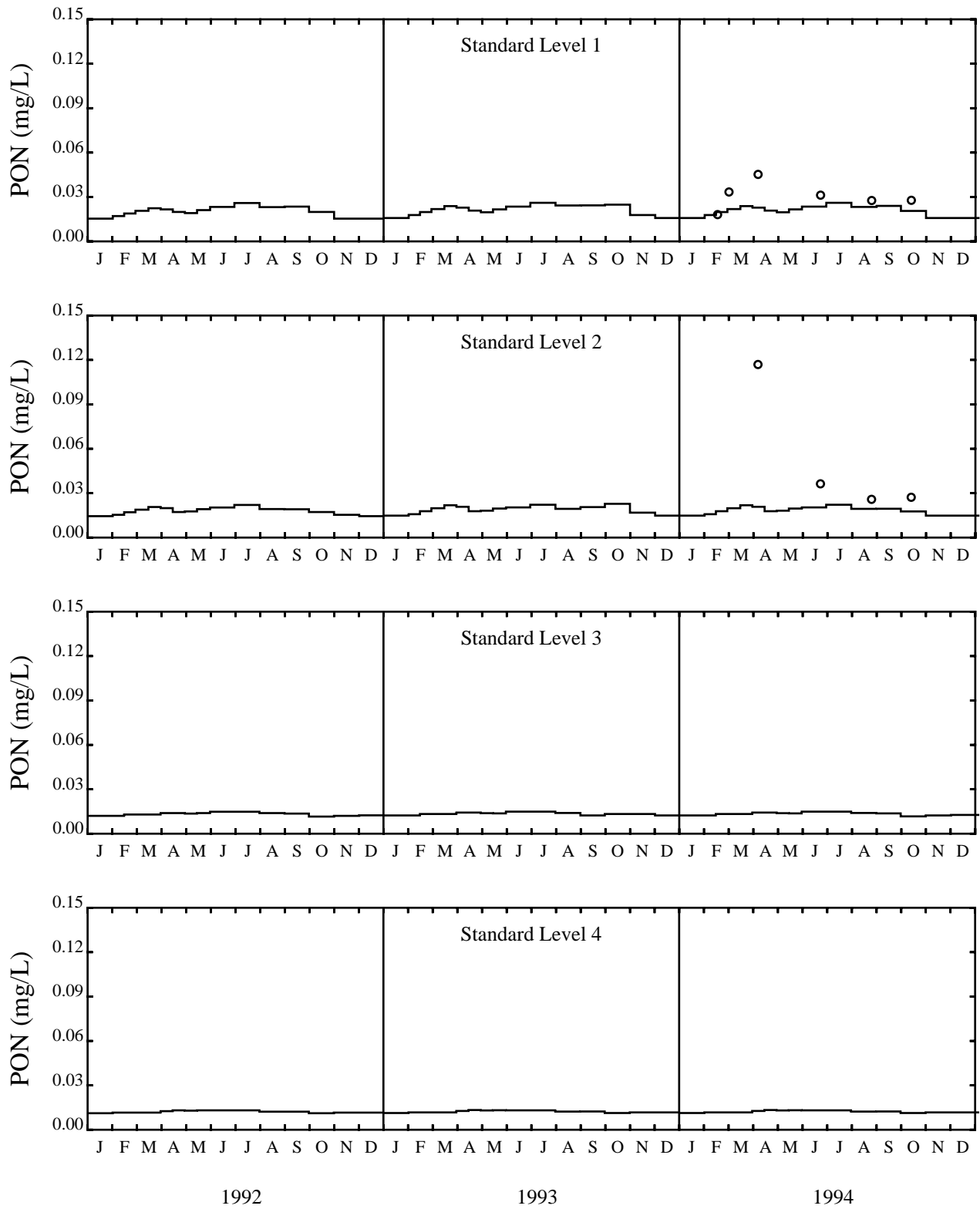


Figure 2-30. 1992-1994 Dissolved Organic Nitrogen Boundary Conditions

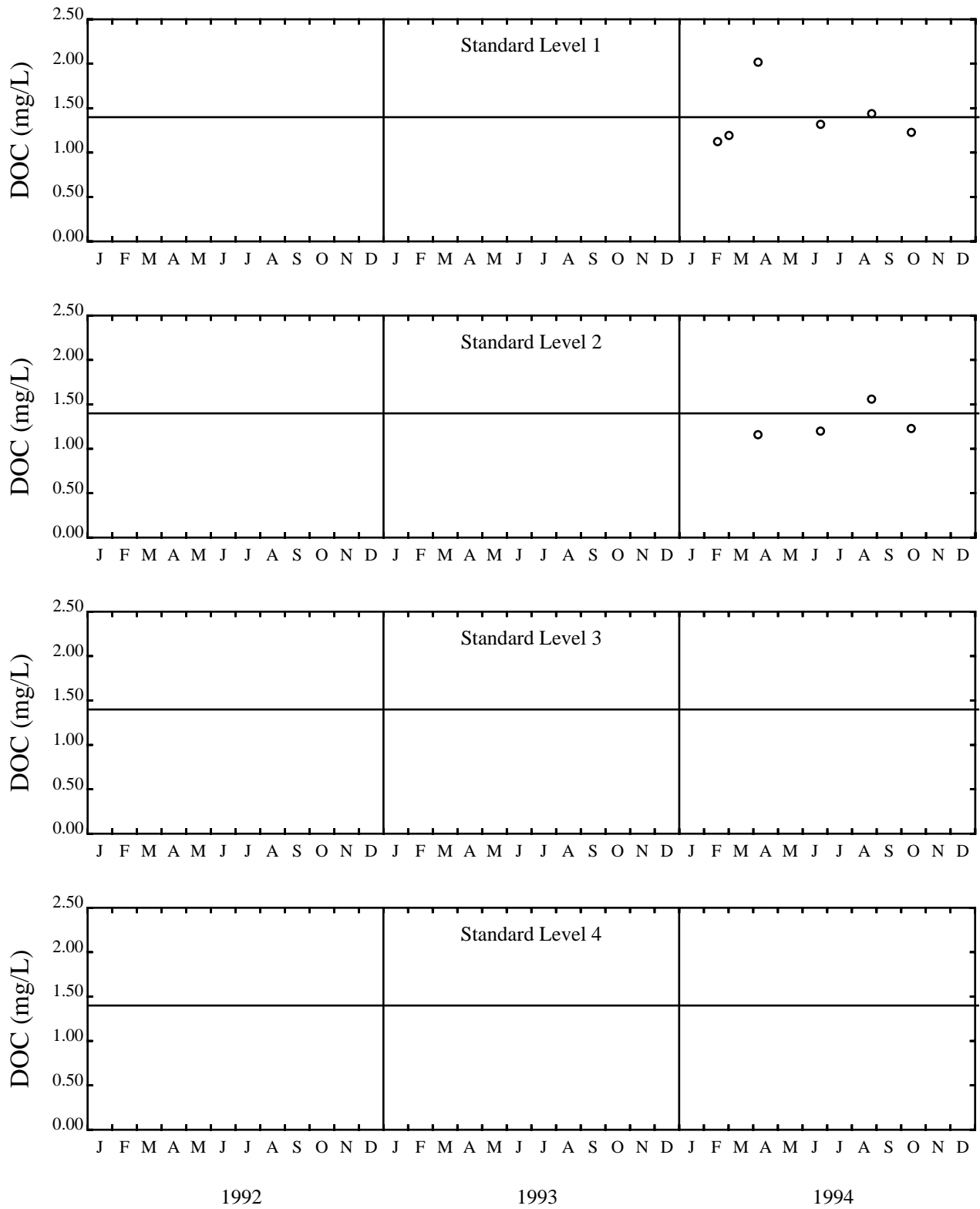


Figure 2-31. Dissolved Organic Carbon Boundary Conditions

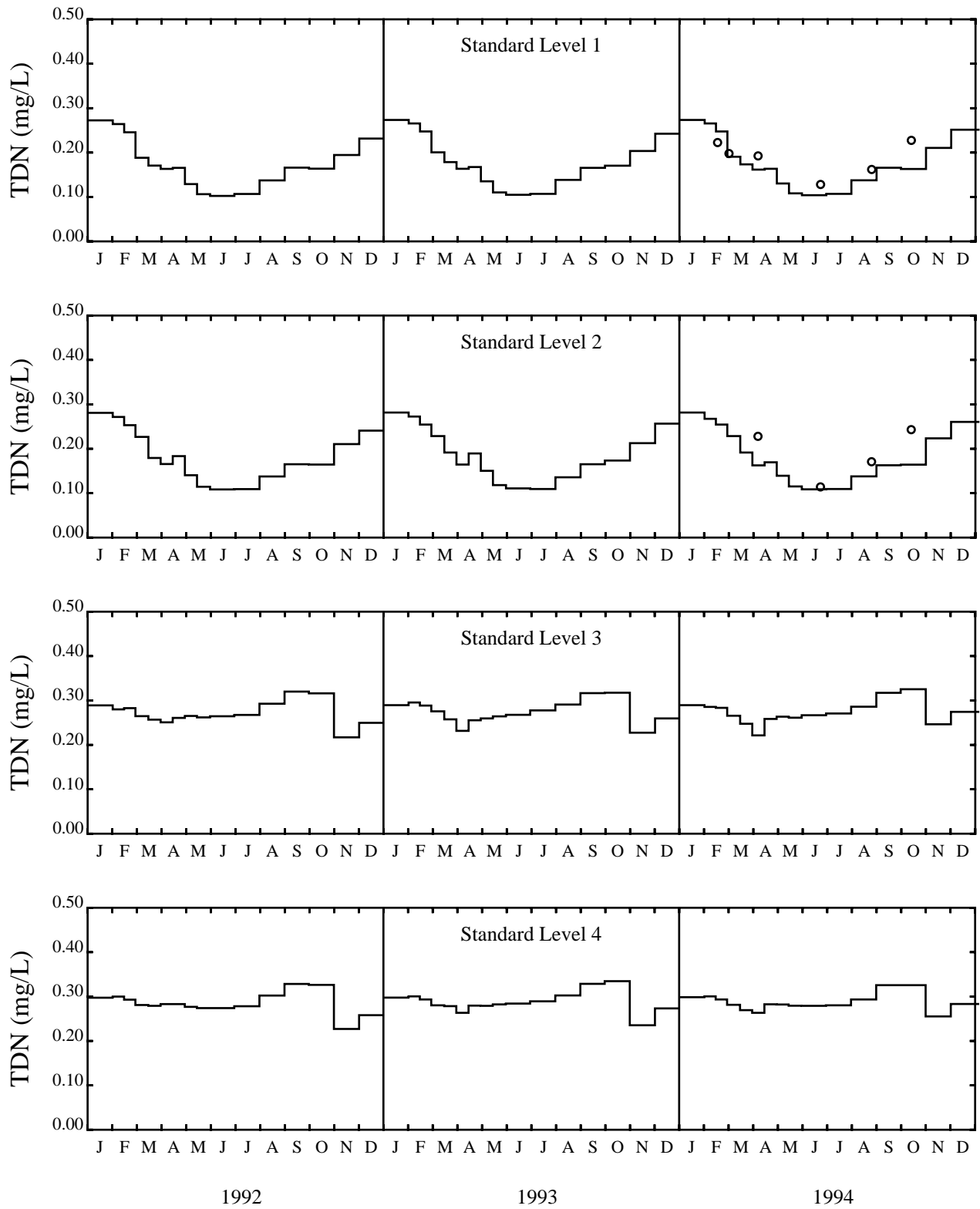


Figure 2-32. 1992-1994 Total Dissolved Nitrogen Boundary Conditions

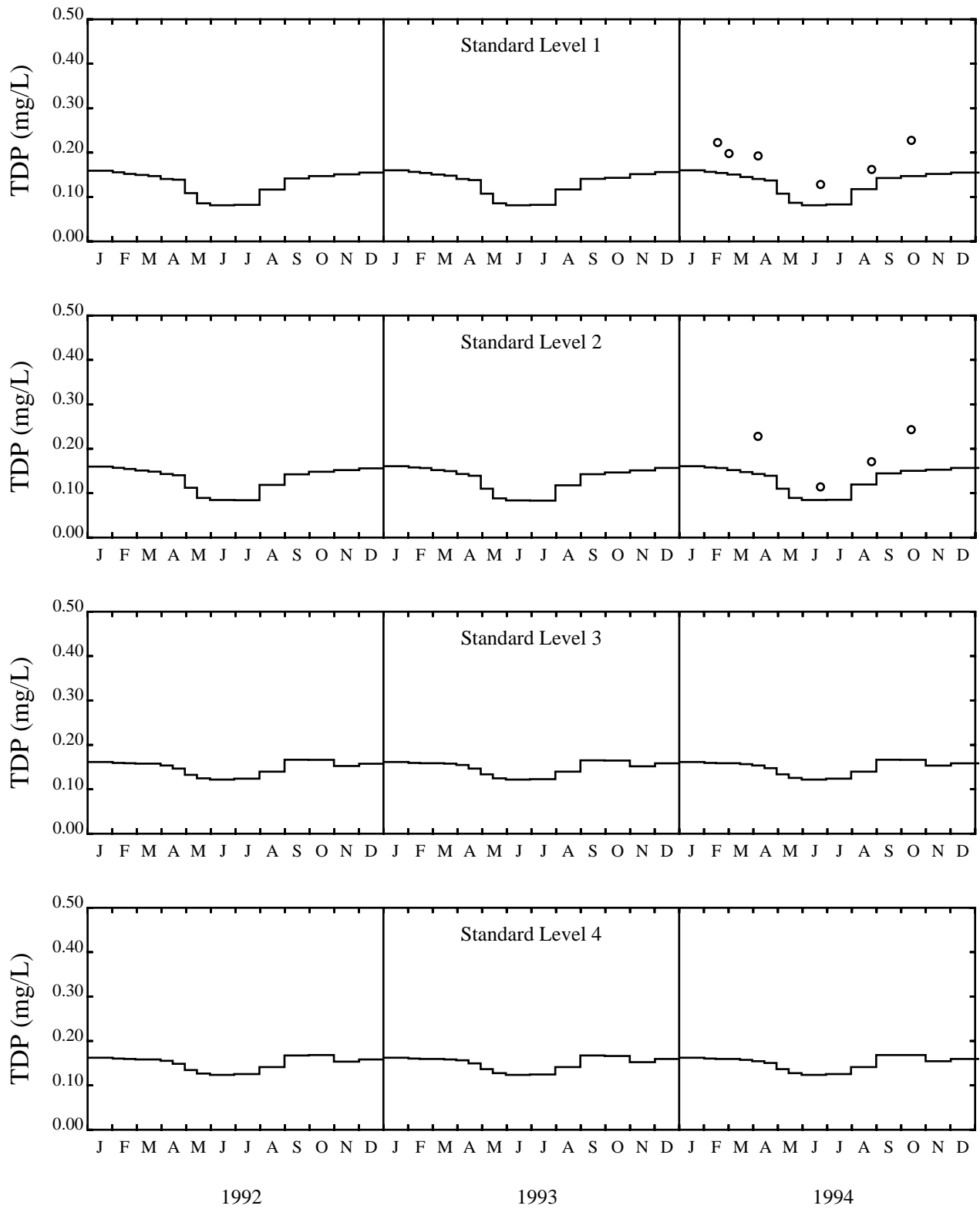


Figure 2-33. 1992-1994 Total Dissolved Phosphorus Boundary Conditions

SECTION 3

MODEL COEFFICIENTS

3.1 WATER QUALITY MODEL COEFFICIENTS

3.1.1 Rationale for Modifying Model Coefficients

The modeling analysis for the years 1993 and 1994 was meant to be a verification of the earlier model calibration. However, the earlier calibration (October, 1989-May, 1991; 1992) was based on data from numerous sources: Bigelow Laboratory, Woods Hole Oceanographic Institution, the University of Massachusetts at Boston, the University of New Hampshire, the U.S. Geological Survey, and MWRA. With the exception of the MWRA data, none of the sampling programs provided temporal or spatial detail necessary for a rigorous calibration. With the addition of the 1993 and 1994 data sets, a more consistent long term data set was available for the water quality model calibration. This data set also included data near the model boundary. The availability of the additional data prompted efforts to improve the original model calibration by modifying the boundary conditions as discussed earlier and by modifying a few of the model coefficients.

A second reason for modifying the model coefficients was because the hydrodynamic model had been adjusted for the 1992 calibration period between the original water quality model calibration for the year 1992 and the start up of the 1993-1994 verification analysis. The modifications to the hydrodynamic input to the water quality model slightly altered the original water quality model results for 1992.

Finally, through the work of the HOM program, additional insight to the regional behavior of the Gulf of Maine and the Massachusetts and Cape Cod Bays system had been obtained in the years since the original calibration. The improved understanding pointed to the importance of the boundary for the bays. This led to modification of the boundary conditions of the model. The modification of the boundary conditions, in turn, required modification of some of the model parameters to improve the model's fit to the data. It was necessary to modify some of the model parameters because changing the boundary conditions changed the distribution of mass within the model domain. In order to balance the effects of the new boundary conditions, mass had to be redistributed by either changing model parameters, model loads, or the circulation computed by the hydrodynamic model. Changing model parameters was the most easily implemented and rational choice.

3.1.2 Final Model Coefficients

This section presents the biological and chemical reaction rate equations used in the water quality model of Massachusetts and Cape Cod Bays first listed as Appendix A of HydroQual and Normandeau (1995). The section will provide the mathematical realization of the model framework for the variables contained in Table 3-1.

Table 3-1 presents the state system variables utilized by the kinetic framework. Table 3-2 presents the phytoplankton net growth equations as influenced by temperature, light and nutrients. Table 3-3 presents the biological and chemical source/sink terms for the phosphorus state-variables including the effects of algal uptake, cell lysing and grazing, and hydrolysis and mineralization. Table 3-4 presents the biological and chemical source/sink terms for the nitrogen state-variables including the effects of algal uptake, cell lysing and grazing, hydrolysis and mineralization. Table 3-5 presents the biological and chemical source/sink terms for biogenic and dissolved silica including the effects of algal uptake, cell lysing and grazing and mineralization. Table 3-6 presents the biological and chemical source/sink terms for the various organic carbon state-variables. Finally, Table 3-7 presents the biological and chemical source/sink terms for dissolved oxygen and oxygen equivalents (i.e., hydrogen sulfide released from the sediment under anaerobic conditions). These effects include atmospheric reaeration, algal photosynthesis and respiration, oxidation of organic carbon, nitrification and oxidation of oxygen equivalents (hydrogen sulfide). Changes in model coefficients made for the revised 1992-1994 calibration are highlighted in each of the tables, as appropriate.

**Table 3-1. State System Variables
Utilized by the Kinetic Framework**

1. - salinity (Sal)
2. - phytoplankton carbon - winter diatoms (P_{C1})
3. - phytoplankton carbon - summer assemblage (P_{C2})
4. - refractory particulate organic phosphorus (RPOP)
5. - labile particulate organic phosphorus (LPOP)
6. - refractory dissolved organic phosphorus (RDOP)
7. - labile dissolved organic phosphorus (LDOP)
8. - dissolved inorganic phosphorus (PO_4)
9. - refractory particulate organic nitrogen (RPON)
10. - labile particulate organic nitrogen (LPON)
11. - refractory dissolved organic nitrogen (RDON)
12. - labile dissolved organic nitrogen (LDON)
13. - ammonia nitrogen (NH_4)
14. - nitrite + nitrate nitrogen ($NO_2 + NO_3$)
15. - biogenic silica (BSi)
16. - available silica (Si)
17. - refractory particulate organic carbon (RPOC)
18. - labile particulate organic carbon (LPOC)
19. - refractory dissolved organic carbon (RDOC)
20. - labile dissolved organic carbon (LDOC)
21. - reactive dissolved organic carbon (ReDOC)
22. - algal exudate dissolved organic carbon (ExDOC)
23. - aqueous sediment oxygen demand (O_2^*)
24. - dissolved oxygen (DO)

Table 3-2. Phytoplankton Net Growth Equations

Net Growth Rate

$$G_{\text{net}} = (\mu_{\text{Pmax}}(T) \cdot G_N(N) - k_{\text{RB}} - k_{\text{sp}}(T) - k_{\text{grz}}(T)) \cdot P_c$$

Specific Growth Rate

$$G_p = \mu_{\text{Pmax}}(T) \cdot G_N(N)$$

Nutrient Saturated Growth Rate

$$\mu_{\text{Pmax}}(T_{\text{opt}}) = \frac{G_{\text{prd}} \cdot (1 - k_{\text{RG}}) \cdot (1 - S/C) \cdot I}{G_{\text{prd}} / G_{\text{prlo}} + I(1 + G_{\text{prd}} / I_s G_{\text{prlo}})} - k_{\text{RB}}$$

Temperature Correction

$$\mu_{\text{Pmax}}(T) = \mu_{\text{Pmax}}(T_{\text{opt}}) \cdot e^{-\beta_1(T - T_{\text{opt}})^2} \quad T \leq T_{\text{opt}}$$

$$\mu_{\text{Pmax}}(T) = \mu_{\text{Pmax}}(T_{\text{opt}}) \cdot e^{-\beta_2(T - T_{\text{opt}})^2} \quad T > T_{\text{opt}}$$

Light Attenuation

$$I(z, t) = I_{\text{surf}}(t) e^{-k_e z}$$

Average Light

$$I_{\text{ave}} = \frac{I_{\text{surf}}(t)}{k_e H} (1 - e^{-k_e H})$$

$$k_e = k_{e_{\text{max}}} + k_c \cdot a_{\text{chl}c} \cdot P_c$$

$$I_{\text{surf}}(t) = \frac{I_{\text{tot}}}{0.635 \cdot f} \sin\left(\frac{\pi(t_d - t_{\text{sunrise}})}{f}\right)$$

$$I_s = (I_{\text{tot}_{n-3}} + I_{\text{tot}_{n-2}} + I_{\text{tot}_{n-1}}) / 3$$

Table 3-2. Phytoplankton Net Growth Equations
(Continued)

Chlorophyll to Carbon Ratio (a_{ChlC})

$$a_{\text{ChlC}} = \frac{1 - (1 - QF) (1 - \mu / \mu_{\text{Pmax}}) - S / C - (\mu + k_{\text{RB}} / C) / [(1 - k_{\text{RG}}) G_{\text{prd}}]}{W_{\text{Chl}}}$$

Nutrient Uptake

$$G_{\text{N}}(\text{N}) = \text{Min} \left(\frac{\text{DIN}}{K_{\text{mN}} + \text{DIN}}, \frac{\text{DIP}}{K_{\text{mP}} + \text{DIP}}, \frac{\text{Si}}{K_{\text{mSi}} + \text{Si}} \right)$$

DIN = dissolved inorganic nitrogen = $\text{NH}_3 + \text{NO}_2 + \text{NO}_3$
 DIP = dissolved inorganic phosphorus
 Si = available silica

Endogenous Respiration

$$k_{\text{PR}} = \frac{k_{\text{RB}} + k_{\text{RG}} \cdot \mu}{1 - k_{\text{RG}}}$$

$$\mu = G_{\text{N}}(\text{N}) \cdot \mu_{\text{Pmax}}$$

Algal Settling

$$k_{\text{sP}}(\text{T}) = \left(\frac{v_{\text{sPb}}}{H} + \frac{v_{\text{sPn}}}{H} \cdot (1 - G_{\text{N}}(\text{N})) \right) \cdot \theta_{\text{sP}}^{(\text{T}-20)}$$

Zooplankton Grazing

$$k_{\text{grz}}(\text{T}) = k_{\text{grz}}(20^\circ \text{C}) \cdot \theta_{\text{grz}}^{(\text{T}-20)}$$

**Table 3-2. Phytoplankton Net Growth Equations
(Continued)**

<u>Exogenous Variables</u>			
<u>Description</u>	<u>Notation</u>	<u>Units</u>	
Total Extinction Coefficient	k_e	m^{-1}	
Base Extinction Coefficient	k_{ebase}	m^{-1}	
Total Daily Surface Solar Radiation	I_{tot}	langleys/day	
Temperature	T	$^{\circ}C$	
Segment Depth	H	m	
Fraction of Daylight	f	day	
Time of Day	t_d	day	
Time of Sunrise	$t_{sunrise}$	day	
Growth Rate	μ	day^{-1}	
Structural Carbon	S	g/cell	
Reservoir Carbon	R	g/cell	
Carbon Associated with the Light Reactions of Photosynthesis	L	g/cell	
Carbon Associated with the Dark Reactions of Photosynthesis	D	g/cell	
Total Cell Carbon	C	g/cell	
Irradiance	I	$mol\ quanta/m^2-d$	
Value of I when $G_{prls} = G_{prlo}/2$	I_s	$mol\ quanta/m^2-d$	
Value of G_{prl} under Nutrient-saturated Conditions	G_{prls}	$m^2/mol\ quanta$	
Gross Rate of Photosynthesis per unit L per unit Light Intensity	G_{prl}	$m^2/mol\ quanta$	
Phytoplankton Biomass	P_c	$mg\ C/L$	
Total Algal Respiration Rate	k_{PR}	day^{-1}	
Net Growth Rate	G_{net}	$mg\ C/day$	
Specific Growth Rate	G_p	day^{-1}	

**Table 3-2. Phytoplankton Net Growth Equations
(Continued)**

<u>Rate Constants</u>				
<u>Description</u>	<u>Notation</u>	Winter Diatoms	Summer Assemblage	<u>Units</u>
Gross photosynthetic rate per unit D	G_{prd}	2.5	3.0	day ⁻¹
Gross photosynthetic rate per unit L per unit light intensity in the limit of zero irradiance	G_{prlo}	0.28	0.28	m ² /mol quanta
Quotient of nutrient to carbon ratios at relative growth rates of 0 and 1	QF	0.85	0.85	
Effect of Temperature below T _{opt} on growth	β_1	0.004	0.004	
Effect of Temperature above T _{opt}	β_2	0.006	0.006	
Temperature Optimum	T _{opt}	8.	18.	°C
Phytoplankton Self-Shading Attenuation	k _c	0.017	0.017	m ² /mg chl-a
Half-Saturation Constant for Nitrogen	K _{mN}	0.010	0.010	mg N/L
Half-Saturation Constant for Phosphorus	K _{mP}	0.001	0.001	mg P/L
Half-Saturation Constant for Silica	K _{mSi}	0.020	0.005	mg Si/L
Growth Related Respiration Coefficient	k _{RG}	0.28	0.28	
Basal Respiration Rate	k _{RB}	0.03	0.036	day ⁻¹
Base Algal Settling Rate	v _{sPb}	0.5	0.3	m/day
Nutrient Dependent Algal Settling Rate	v _{sPn}	1.0	0.7	m/day
Temperature Coefficient	θ_{sp}	1.027	1.027	@ 20°C
Loss Due to Zooplankton Grazing	k _{grz}	0.1	0.1	day ⁻¹
Temperature Coefficient	θ_{grz}	1.10	1.10	@ 20°C
Nutrient Saturated Carbon/Chlorophyll Ratio in L	W _{CChl}	40.	65.	mg C/mg chl-a
Ratio of Structural to Total Carbon	S/C	0.1	0.1	

Table 3-3. Phosphorus Reaction Equations

Labile Particulate Organic Phosphorus (LPOP)

$$\begin{aligned}
 S_5 = & a_{PC} \cdot f_{LPOP} \cdot [k_{PR} + k_{grz}(T)] \cdot P_c \\
 & - k_{5,7} \theta_{5,7}^{(T-20)} \cdot LPOP \cdot \frac{P_c}{K_{mP_c} + P_c} \\
 & - \frac{V_{sPOM}}{H} (T) \cdot LPOP
 \end{aligned}$$

Refractory Particulate Organic Phosphorus (RPOP)

$$\begin{aligned}
 S_4 = & a_{PC} \cdot f_{RPOP} \cdot [k_{PR} + k_{grz}(T)] \cdot P_c - \frac{V_{sPOM}}{H} (T) \cdot RPOP \\
 & - k_{4,6} \theta_{4,6}^{(T-20)} \cdot RPOP \cdot \frac{P_c}{K_{mP_c} + P_c}
 \end{aligned}$$

Labile Dissolved Organic Phosphorus (LDOP)

$$\begin{aligned}
 S_7 = & a_{PC} \cdot f_{LDOP} \cdot [k_{PR} + k_{grz}(T)] \cdot P_c \\
 & + k_{5,7} \theta_{5,7}^{(T-20)} \cdot LPOP \cdot \frac{P_c}{K_{mP_c} + P_c} \\
 & - k_{7,8} \theta_{7,8}^{(T-20)} \cdot LDOP \cdot \frac{P_c}{K_{mP_c} + P_c}
 \end{aligned}$$

Table 3-3. Phosphorus Reaction Equations
(Continued)

Refractory Dissolved Organic Phosphorus (RDOP)

$$\begin{aligned}
 S_6 = & a_{PC} \cdot f_{RDOP} \cdot [k_{PR} + k_{grz}(T)] \cdot P_c \\
 & + k_{4,6} \theta_{4,6}^{(T-20)} \cdot RPOP \cdot \frac{P_c}{K_{mP_c} + P_c} \\
 & - k_{6,8} \theta_{6,8}^{(T-20)} \cdot RDOP \cdot \frac{P_c}{K_{mP_c} + P_c}
 \end{aligned}$$

Dissolved Inorganic Phosphorus (PO₄)

$$\begin{aligned}
 S_8 = & (k_{7,8} \theta_{7,8}^{(T-20)} \cdot LDOP \\
 & + k_{1,8} \theta_{1,8}^{(T-20)} \cdot RDOP) \cdot \frac{P_c}{K_{mP_c} + P_c} \\
 & - a_{pc} \cdot (1 - f_{EDOC}) \cdot G_p \cdot P_c
 \end{aligned}$$

Phosphorus to Carbon Ratio (a_{PC})

$$\begin{aligned}
 a_{PC} = & (QF + (1 - QF) (\mu / \mu_{Pmax})) / W_{CP} \\
 = & 1 / W_{CP} \quad \text{when } \mu = \mu_{Pmax}
 \end{aligned}$$

**Table 3-3. Phosphorus Reaction Equations
(Continued)**

<u>Description</u>	<u>Notation</u>	<u>Value</u>	<u>Units</u>
Phytoplankton Biomass	P_c	-	mg C/L
Algal Respiration Rate	k_{PR}		day ⁻¹
Temperature Corrected Grazing Rate	$k_{grz}(T)$		day ⁻¹
Specific Phytoplankton Growth Rate	G_p		day ⁻¹
Nutrient-Saturated Carbon to Phosphorus Ratio:	W_{CN}	40	mg C/mg P
Fraction of Primary Productivity Going to the Algal Exudate DOC pool	f_{ExDOC}	0.1	
Fraction of Respired and Grazed Algal Phosphorus Recycled to			
the LPOP pool	f_{LPOP}	0.30	
the RPOP pool	f_{RPOP}	0.15	
the LDOP pool	f_{LDOP}	0.15	
the RDOP pool	f_{RDOP}	0.10	
the PO ₄ pool	f_{PO_4}	0.30	
LPOP Hydrolysis Rate at 20°C	$k_{5,7}$	0.05	day ⁻¹
Temperature Coefficient	$\theta_{5,7}$	1.08	
Base Settling Rate of POM (LPOP, RPOP)	v_{sPOM}	1.00	m/day
RPOP Hydrolysis Rate at 20°C	$k_{4,6}$	0.01	day ⁻¹
Temperature Coefficient	$\theta_{4,6}$	1.08	
LDOP Mineralization Rate at 20°C	$k_{7,8}$	0.10	day ⁻¹
Temperature Coefficient	$\theta_{7,8}$	1.08	
RDOP Mineralization Rate at 20°C	$k_{6,8}$	0.01	day ⁻¹
Temperature Coefficient	$\theta_{6,8}$	1.08	

Table 3-4. Nitrogen Reaction Equations

Labile Particulate Organic Nitrogen (LPON)

$$\begin{aligned}
 S_{10} &= a_{\text{NC}} \cdot f_{\text{LPON}} \cdot [k_{\text{PR}} + k_{\text{grz}}(T)] \cdot P_c \\
 &- k_{10,12} \theta_{10,12}^{(T-20)} \cdot \text{LPON} \cdot \frac{P_c}{K_{\text{mP}_c} + P_c} \\
 &- \frac{V_{\text{sPOM}}}{H} (T) \cdot \text{LPON}
 \end{aligned}$$

Refractory Particulate Organic Nitrogen (RPON)

$$\begin{aligned}
 S_9 &= a_{\text{NC}} \cdot f_{\text{RPON}} \cdot [k_{\text{PR}} + k_{\text{grz}}(T)] \cdot P_c \\
 &- k_{9,11} \theta_{9,11}^{(T-20)} \cdot \text{RPON} \cdot \frac{P_c}{K_{\text{mP}_c} + P_c} \\
 &- \frac{V_{\text{sPOM}}}{H} (T) \cdot \text{RPON}
 \end{aligned}$$

Labile Dissolved Organic Nitrogen (LDON)

$$\begin{aligned}
 S_{12} &= a_{\text{NC}} \cdot f_{\text{LDON}} \cdot [k_{\text{PR}} + k_{\text{grz}}(T)] \cdot P_c \\
 &+ k_{10,12} \theta_{10,12}^{(T-20)} \cdot \text{LPON} \cdot \frac{P_c}{K_{\text{mP}_c} + P_c} \\
 &- k_{12,13} \theta_{12,13}^{(T-20)} \cdot \text{LDON} \cdot \frac{P_c}{K_{\text{mP}_c} + P_c}
 \end{aligned}$$

Table 3-4. Nitrogen Reaction Equations
(Continued)

Refractory Dissolved Organic Nitrogen (RDON)

$$\begin{aligned}
 S_{11} = & a_{\text{NC}} \cdot f_{\text{RDON}} \cdot [k_{\text{PR}} + k_{\text{grz}}(T)] \cdot P_c \\
 & + k_{9,11} \theta_{9,11}^{(T-20)} \cdot \text{RPN} \cdot \frac{P_c}{K_{\text{mP}_c} + P_c} \\
 & - k_{11,13} \theta_{11,13}^{(T-20)} \cdot \text{RDON} \cdot \frac{P_c}{K_{\text{mP}_c} + P_c}
 \end{aligned}$$

Ammonia Nitrogen (NH₃ - N)

$$\begin{aligned}
 S_{13} = & a_{\text{NC}} \cdot f_{\text{NH}_3} \cdot [k_{\text{PR}} + k_{\text{grz}}(T)] \times P_c \\
 & + k_{12,13} \theta_{12,13}^{(T-20)} \cdot \text{LDON} \\
 & + k_{11,13} \theta_{11,13}^{(T-20)} \cdot \text{RDON} \cdot \frac{P_c}{K_{\text{mP}_c} + P_c} \\
 & - a_{\text{NC}} \cdot \alpha_{\text{NH}_3} \cdot (1 - f_{\text{ExDOC}}) \cdot G_P \cdot P_c \\
 & - k_{13,14} \theta_{13,14}^{(T-20)} \cdot \text{NH}_3 \cdot \frac{\text{DO}}{K_{\text{nitr}} + \text{DO}}
 \end{aligned}$$

Table 3-4. Nitrogen Reaction Equations
(Continued)

Nitrite + Nitrate Nitrogen ($\text{NO}_2 + \text{NO}_3$)

$$\begin{aligned}
 S_{14} &= k_{13,14} \theta_{13,14}^{(T-20)} \cdot \text{NH}_3 \cdot \frac{\text{DO}}{K_{\text{nitr}} + \text{DO}} \\
 &\quad - a_{\text{NC}} \cdot (1 - \alpha_{\text{NH}_3}) \cdot (1 - f_{\text{ExDOC}}) \cdot G_P \cdot P_c \\
 &\quad - k_{14,0} \theta_{14,0}^{(T-20)} \cdot (\text{NO}_2 + \text{NO}_3) \cdot \frac{\text{DO}}{K_{\text{NO}_3} + \text{DO}}
 \end{aligned}$$

Nitrogen to Carbon Ratio (a_{NC})

$$\begin{aligned}
 a_{\text{NC}} &= (QF + (1 - QF)(\mu / \mu_{\text{Pmax}})) / W_{\text{CN}} \\
 &= 1 / W_{\text{CN}} \quad \text{when } \mu = \mu_{\text{Pmax}}
 \end{aligned}$$

**Table 3-4. Nitrogen Reaction Equations
(Continued)**

<u>Description</u>	<u>Notation</u>	<u>Value</u>	<u>Units</u>
Phytoplankton Biomass	P_c	-	mg C/L
Algal Respiration Rate	k_{PR}		day ⁻¹
Temperature Corrected Grazing Rate	$k_{grz}(T)$		day ⁻¹
Specific Phytoplankton Growth Rate	G_p		day ⁻¹
Nutrient Saturated Carbon to Nitrogen Ratio	W_{CN}		mg C/mg N
Winter		5.00	
Summer		5.67	
Fraction of Respired and Grazed Algal Nitrogen Recycled to			
the LPON pool	f_{LPON}	0.325	
the RPON pool	f_{RPON}	0.15	
the LDON pool	f_{LDON}	0.175	
the RDON pool	f_{RDON}	0.15	
the NH ₃ pool	f_{NH_3}	0.20	
LPON Hydrolysis Rate at 20°C	$k_{10,12}$	0.05	day ⁻¹
Temperature Coefficient	$\theta_{10,12}$	1.08	
Base Settling Rate of POM (LPON, RPON)	v_{sPOM}	1.0	m/day
RPON Hydrolysis Rate at 20°C	$k_{9,11}$	0.008	day ⁻¹
Temperature Coefficient	$\theta_{9,11}$	1.08	
LDON Mineralization Rate at 20°C	$k_{12,13}$	0.05	day ⁻¹
Temperature Coefficient	$\theta_{12,13}$	1.08	
RDON Mineralization Rate at 20°C	$k_{11,13}$	0.008	day ⁻¹
Temperature Coefficient	$\theta_{11,13}$	1.08	
Nitrification Rate at 20°C	$k_{13,14}$	0.10	day ⁻¹
Temperature Coefficient	$\theta_{13,14}$	1.08	
Half Saturation Constant for Nitrification Oxygen Limitation	K_{nitr}	1.0	mg O ₂ /L
Denitrification Rate at 20°C	$k_{14,0}$	0.05	day ⁻¹
Temperature Coefficient	$\theta_{14,0}$	1.045	
Michaelis Constant for Denitrification	K_{NO_3}	0.10	mg O ₂ /L

Table 3-5. Silica Reaction Equations

Biogenic Silica (BSi)

$$\begin{aligned}
 S_{15} &= [k_{PR} + k_{grz}(T)] \cdot P_c \\
 &- k_{15,16} \theta_{15,16}^{(T-20)} \cdot BSi \cdot \frac{P_c}{K_{mP_c} + P_c} \\
 &- \frac{V_{sPOM}}{H} \cdot BSi
 \end{aligned}$$

Available Silica (Si)

$$\begin{aligned}
 S_{16} &= k_{15,16} \theta_{15,16}^{(T-20)} \cdot BSi \cdot \frac{P_c}{K_{mP_c} + P_c} \\
 &- (1 - f_{ExDOC}) \cdot G_P \cdot P_c
 \end{aligned}$$

Silica to Carbon Ratio (a_{SC})

$$\begin{aligned}
 a_{SC} &= (QF + (1 - QF) (m / m_{Pmax})) / W_{CS} \\
 &= 1 / W_{CS} \quad \text{when } m = m_{Pmax}
 \end{aligned}$$

**Table 3-5. Silica Reaction Equations
(Continued)**

<u>Description</u>	<u>Notation</u>	<u>Value</u>	<u>Units</u>
Phytoplankton Biomass	P_c	-	mg C/L
Algal Respiration Rate	k_{PR}		day ⁻¹
Temperature Corrected Grazing Rate	$k_{grz}(T)$		day ⁻¹
Specific Phytoplankton Growth Rate	G_p		day ⁻¹
Nutrient Saturated Carbon to Silica Ratio	W_{CS}		mg C/mg Si
Winter		2.5	
Summer		7.0	
Mineralization Rate of Biogenic Silica	$k_{15,16}$	0.08	day ⁻¹
Temperature Coefficient	$\theta_{15,16}$	1.08	
Base Settling Rate for POM (BSi)	v_{sPOM}	1.0	m/day

Table 3-6. Organic Carbon Reaction Equations

Labile Particulate Organic Carbon (LPOC)

$$\begin{aligned}
 S_{18} &= f_{\text{LPOC}} \times k_{\text{grz}}(T) \times P_c \\
 &- k_{18,20} \theta_{18,20}^{(T-20)} \cdot \text{LPOC} \cdot \frac{P_c}{K_{mP_c} + P_c} \\
 &- \frac{V_{\text{sPOM}}}{H} (T) \cdot \text{LPOC}
 \end{aligned}$$

Refractory Particulate Organic Carbon (RPOC)

$$\begin{aligned}
 S_{17} &= f_{\text{RPOC}} \cdot k_{\text{grz}}(T) \cdot P_c \\
 &- k_{17,19} \theta_{17,19}^{(T-20)} \times \text{RPOC} \times \frac{P_c}{K_{mP_c} + P_c} \\
 &- \frac{V_{\text{sPOM}}}{H} (T) \cdot \text{RPOC}
 \end{aligned}$$

Labile Dissolved Organic Carbon (LDOC)

$$\begin{aligned}
 S_{20} &= f_{\text{LDOC}} \cdot k_{\text{grz}}(T) \cdot P_c \\
 &+ k_{18,20} \theta_{18,20}^{(T-20)} \cdot \text{LPOC} \cdot \frac{P_c}{K_{mP_c} + P_c} \\
 &- k_{20,0} \theta_{20,0}^{(T-20)} \cdot \text{LDOC} \cdot \frac{P_c}{K_{mP_c} + P_c} \cdot \frac{\text{DO}}{K_{\text{DO}} + \text{DO}}
 \end{aligned}$$

Table 3-6. Organic Carbon Reaction Equations
 (Numbering scheme refers to the variable list in Table 3-1)
 (Continued)

Refractory Dissolved Organic Carbon (RDOC)

$$\begin{aligned}
 S_{19} = & f_{\text{RDOC}} \cdot k_{\text{grz}}(T) \cdot P_c \\
 & + k_{17,19} \theta_{17,19}^{(T-20)} \cdot \text{RPOC} \cdot \frac{P_c}{K_{mP_c} + P_c} \\
 & - k_{19,0} \theta_{19,0}^{(T-20)} \cdot \text{RDOC} \cdot \frac{P_c}{K_{mP_c} + P_c} \cdot \frac{\text{DO}}{K_{\text{DO}} + \text{DO}}
 \end{aligned}$$

Reactive Dissolved Organic Carbon (ReDOC)

$$S_{21} = - k_{21,0} \theta_{21,0}^{(T-20)} \cdot \text{ReDOC} \cdot \frac{P_c}{K_{mP_c} + P_c} \cdot \frac{\text{DO}}{K_{\text{DO}} + \text{DO}}$$

Algal Exudate Dissolved Organic Carbon (ExDOC)

$$\begin{aligned}
 S_{22} = & f_{\text{ExDOC}} \cdot G_P \cdot P_c \\
 & - k_{22,0} \theta_{22,0}^{(T-20)} \cdot \text{ExDOC} \cdot \frac{P_c}{K_{mP_c} + P_c} \cdot \frac{\text{DO}}{K_{\text{DO}} + \text{DO}}
 \end{aligned}$$

Table 3-6. Organic Carbon Reaction Equations
(Numbering scheme refers to the variable list in Table 3-1)
(Continued)

<u>Description</u>	<u>Notation</u>	<u>Value</u>	<u>Units</u>
Phytoplankton Biomass	P_c	-	mg C/L
Specific Phytoplankton Growth Rate	G_p		day ⁻¹
Half Saturation Constant for Phytoplankton Limitation	K_{mPc}	0.05	mg C/L
Fraction of Grazed Organic Carbon Recycled to:			
the LPOC pool	f_{LPOC}	0.35	
the RPOC pool	f_{RPOC}	0.15	
the LDOC pool	f_{LDOC}	0.40	
the RDOC pool	f_{RDOC}	0.10	
Fraction of Primary Productivity Going to the Algal Exudate DOC pool	f_{ExDOC}	0.10	
Hydrolysis Rate for LPOC	$k_{18,20}$	0.07	day ⁻¹
Temperature Coefficient	$\theta_{18,20}$	1.08	
Base Settling Rate of POM (LPOC, RPOC)	v_{sPOM}	1.00	m/day
Hydrolysis Rate for RPOC	$k_{17,19}$	0.01	day ⁻¹
Temperature Coefficient	$\theta_{17,19}$	1.08	
Segment depth	H	-	m
Oxidation Rate of LDOC	$k_{20,0}$	0.100	day ⁻¹
Temperature Coefficient	$\theta_{20,0}$	1.08	
Oxidation Rate RDOC	$k_{19,0}$	0.008	day ⁻¹
Temperature Coefficient	$\theta_{19,0}$	1.08	
Oxidation Rate of ReDOC	$k_{21,0}$	0.30	day ⁻¹
Temperature Coefficient	$\theta_{21,0}$	1.047	
Oxidation Rate of ExDOC	$k_{22,0}$	0.15	day ⁻¹
Temperature Coefficient	$\theta_{22,0}$	1.080	
Half Saturation for Oxygen Limitation	K_{DO}	0.20	mg O ₂ /L
Dissolved Oxygen	DO	-	mg O ₂ /L

Table 3-7. Dissolved Oxygen and Oxygen Reaction Rates

Dissolved Oxygen (DO)

$$\begin{aligned}
S_{24} = & a_{OC} \cdot \alpha_{NH_3} \cdot G_P \cdot P_C + a_{NO_3C} \cdot (1 - \alpha_{NH_3}) \cdot G_P \cdot P_C \\
& + k_4 \theta_4^{(T-20)} \cdot (DO_{sat} - DO) - a_{OC} \cdot k_{PR}(T) \cdot P_C \\
& - 2 \cdot a_{ON} \cdot k_{13,14} \theta_{13,14}^{(T-20)} \cdot NH_3 \cdot \frac{DO}{K_{nitr} + DO} \\
& - (k_{20,\rho} \theta_{20,\rho}^{(T-20)} \cdot LDOC + k_{19,\rho} \theta_{19,\rho}^{(T-20)} \cdot RDOC + k_{21,\rho} \theta_{21,\rho}^{(T-20)} \cdot ReDOC) \\
& + (k_{22,\rho} \theta_{22,\rho}^{(T-20)} \cdot ExDOC) \cdot \frac{P_C}{K_{mp_e} + P_C} \cdot \frac{DO}{K_{DO} + DO} \\
& - k_{O_2'} \theta_{O_2'}^{(T-20)} \cdot O_2^* \cdot \frac{DO}{K_{DO} + DO}
\end{aligned}$$

Oxygen Equivalents (O_2^*)

$$S_{23} = - k_{O_2^*} \theta_{O_2^*}^{(T-20)} \cdot O_2^* \cdot \frac{DO}{K_{DO} + DO}$$

**Table 3-7. Dissolved Oxygen and Oxygen Reaction Rates
(Continued)**

<u>Description</u>	<u>Rate Constants</u>		
	<u>Notation</u>	<u>Value</u>	<u>Units</u>
Phytoplankton Biomass	P_c	-	mg C/L
Specific Phytoplankton Growth Rate	G_p	-	day ⁻¹
Oxygen to Carbon Ratio	a_{OC}	32/12	mg O ₂ /mg C
Oxygen to Nitrogen Ratio	a_{ON}	32/14	mg O ₂ /mg N
Oxygen to Carbon Ratio for Nitrate Uptake	a_{NO_3C}	$\frac{48a_{NC}}{14}$	mg O ₂ /mg C
Ammonia Preference Term for Nitrogen Uptake	α_{NH_3}	-	
Nitrogen to Carbon Ratio	a_{NC}	-	mg N/mg C
Temperature Corrected Algal Respiration Rate	$k_{PR}(T)$	-	day ⁻¹
Half Saturation Constant for Oxygen Limitation	K_{nitr}	1.0	mg O ₂ /L
Reaeration Rate at 20°C	k_a	-	day ⁻¹
Temperature Coefficient	θ_a	1.024	
Oxygen Transfer Coefficient	k_L	0.75-1.8	m ⁻¹
Dissolved Oxygen Saturation	DO_{sat}		mg O ₂ /L
Oxidation Rates and Temperature Coefficients			
for LDOC	$k_{20,0}$ $\theta_{20,0}$	0.100 1.080	day ⁻¹
for RDOC	$k_{19,0}$ $\theta_{19,0}$.008 1.080	day ⁻¹
for ExDOC	$k_{22,0}$ $\theta_{22,0}$	0.150 1.080	day ⁻¹
for NH ₃	$k_{13,14}$ $\theta_{13,14}$	0.100 1.08	day ⁻¹
Oxidation Rate of Oxygen Equivalents	$k_{O_2^*}$	0.15	day ⁻¹
Temperature Coefficient	$\theta_{O_2^*}$	1.080	
Half Saturation for Oxygen Limitation	K_{DO}	0.10	mg O ₂
Dissolved Oxygen	DO	-	mg O ₂ /L

Table 3-8 presents the model parameters that were modified between the original 1992 model calibration and the revised 1992 model calibration. Only four constants were modified. The carbon to nitrogen ratio for the winter group (Table 3-4) was modified in an attempt to increase the amount of inorganic nitrogen that was taken up by the phytoplankton during the winter and spring. The Michaelis term for the winter group (Table 3-2) was modified so that silica would not be as limiting to the diatom group during the spring. In effect, this was also changed to induce more uptake of nitrogen by the diatoms. The basal respiration rate for the summer group (Table 3-2) was increased to reduce the net growth rate of the summer algae. Finally, the nitrification rate (Table 3-4) was increased to reduce the amount of ammonia in the water column. All of these changes are small and biologically reasonable. These parameter modifications improved the overall model calibration.

Table 3-8. Constants Varied Between 1989-1992 Calibration and 1992-1994 Calibration

	1989-1992	1992-1994
Diatom C:N Ratio	5.67	5.00
Diatom Silica Michaelis Concentration (mg/L)	0.025	0.020
Summer Assemblage Basal Respiration Rate (day ⁻¹)	0.030	0.036
Nitrification Rate (day ⁻¹)	0.080	0.100

3.2 SEDIMENT MODEL COEFFICIENTS

Table 3-9 lists the constants used for the sediment model calibration. None of the model coefficients listed in Table 3-9 were modified from the original calibration effort.

Table 3-9. Sediment Model Coefficients

DESCRIPTION	NOTATION	VALUE	UNITS
Aerobic layer solids concentration	m_1	0.500	kg/L
Anaerobic layer solids concentration	m_2	0.500	kg/L
Particle mixing diffusion coefficient	D_p	0.00012	m ² /d
Sedimentation velocity	w_2	0.25	cm/yr
Pore water diffusion coefficient	D_d	0.002	m ² /d

**Table 3-9 Sediment Model Coefficients
(Continued)**

DESCRIPTION	NOTATION	VALUE	UNITS
Temperature coefficient	θ_{Dp}	1.15	
Temperature coefficient	θ_{Dd}	1.15	
Water-sediment diffusion coefficient	D_{d0}	0.001	m ² /d
Temperature coefficient	θ_{Dd0}	1.08	
Reaction velocity for nitrification	κ_{nh4}	0.1313	m/d
Ammonia partition coefficient	π_{nh4}	1.0	L/kg
Temperature coefficient	θ_{nh4}	1.123	
Nitrification half saturation constant for ammonia	k_{mnh4}	728.	mg N/L
Temperature coefficient	θ_{k_mnh4}	1.125	
Nitrification half saturation constant for oxygen	k_{mnh4o2}	0.74	mg O ₂ /L
Aerobic denitrification velocity	κ_{1no3}	0.100	m/d
Anaerobic layer reaction velocity	k_{2no3}	0.23	m/d
Temperature coefficient	θ_{no3}	1.08	
Reaction velocity for dissolved sulfide oxidation in the aerobic layer	κ_{d1}	0.2	m/d
Reaction velocity for particulate sulfide oxidation in the aerobic layer	κ_{p1}	0.4	m/d
Partition coefficient for sulfide in the aerobic layer	π_{1s}	100.	L/kg
Partition coefficient for sulfide in the anaerobic layer	π_{2s}	100.	L/kg
Temperature coefficient	θ_{dp1}	1.08	
Sulfide oxidation normalization constant for oxygen	k_{mhso2}	4.	mg O ₂ /L
First order reaction rate	k_{si}	0.5	/day
Silica saturation concentration	c_{sisat}	40000.	µg Si/L
Incremental partition coefficient for silica in the aerobic layer	$\Delta\pi_{1si}$	10.	L/kg

**Table 3-9 Sediment Model Coefficients
(Continued)**

DESCRIPTION	NOTATION	VALUE	UNITS
Partition coefficient for silica in the anaerobic layer	π_{2si}	100.	L/kg
Temperature coefficient	θ_{si}	1.10	
Particulate biogenic silica half saturation constant for dissolution	k_{mpsi}	5.0E+07	mg Si/m ³
Overlying water oxygen concentration at which aerobic layer incremental partitioning starts to decrease	$O_{2critsi}$	2.0	mg O ₂ /L
Flux of detrital silica	$j_{si_{detr}}$	10.	mg Si/m ² -d
Incremental partition coefficient for phosphate in the aerobic layer	$\Delta\pi_{1po4}$	20.	L/kg
Partition coefficient for phosphate in the anaerobic layer	π_{2po4}	20.	L/kg
Overlying water oxygen concentration at which aerobic layer incremental partitioning starts to decrease	O_{2crit}	2.0	mg O ₂ /L
Particle mixing half saturation constant for oxygen	k_{mo2Dp}	4.0	mg O ₂ /L
Temperature which benthic community begins to recover after an anoxic event	$tempbnth$	10.0	°C
Rate at which benthic stress is dissipated	$k_{bnthstr}$	0.03	/d
Scale factor for enhancement of dissolved phase mixing due to benthic activity	k_{lbnth}	0.0	
Minimum particle mixing coefficient	D_{pmin}	0.0	m ² /d
Reaction velocity for methane oxidation in the aerobic layer	κ_{ch4}	0.2	m/d
Temperature coefficient	θ_{ch4}	1.08	
Fraction PON in G_1	fr_{pon1}	0.65	
Reaction rate constant for G_{PON1}	k_{pon1}	0.035	/day
Temperature coefficient	θ_{pon1}	1.10	
Fraction PON in G_2	fr_{pon2}	0.25	
Reaction rate constant for G_{PON2}	k_{pon2}	0.0018	/day

**Table 3-9 Sediment Model Coefficients
(Continued)**

DESCRIPTION	NOTATION	VALUE	UNITS
Temperature coefficient	θ_{pon2}	1.10	
Fraction PON in G_3	fr_{pon3}	0.10	
Reaction rate constant for G_{PON3}	k_{pon3}	0.000001	/day
Temperature coefficient	θ_{pon3}	1.17	
Fraction POC in G_1	fr_{poc1}	0.65	
Reaction rate constant for G_{POC1}	k_{poc1}	0.035	/day
Temperature coefficient	θ_{poc1}	1.10	
Fraction POC in G_2	fr_{poc2}	0.20	
Reaction rate constant for G_{POC2}	k_{poc2}	0.0018	/day
Temperature coefficient	θ_{poc2}	1.15	
Fraction POC in G_3	fr_{poc3}	0.15	
Reaction rate constant for G_{POC3}	k_{poc3}	0.000001	/day
Temperature coefficient	θ_{poc3}	1.17	
Fraction POP in G_1	fr_{pop1}	0.65	
Reaction rate constant for G_{POP1}	k_{pop1}	0.035	/day
Temperature coefficient	θ_{pop1}	1.10	
Fraction POP in G_2	fr_{pop2}	0.20	
Reaction rate constant for G_{POP2}	k_{pop2}	0.0018	/day
Temperature coefficient	θ_{pop2}	1.15	
Fraction POP in G_3	fr_{pop3}	0.15	
Reaction rate constant for G_{POP3}	k_{pop3}	0.000001	/day
Temperature coefficient	θ_{pop3}	1.17	

SECTION 4

GRID AGGREGATION

4.1 INTRODUCTION

In order to provide reasonable computer execution or turnaround times during the initial development and calibration of the water quality portion of the Bays Eutrophication Model (BEM), it was necessary to utilize a procedure known as grid-aggregation. Grid-aggregation was used to reduce the number of computational elements or segments in the water quality model (as compared to the hydrodynamic model) and, thus, reduce the computational burden or “clock-time” associated with performing model runs. This was necessary for a number of reasons, including:

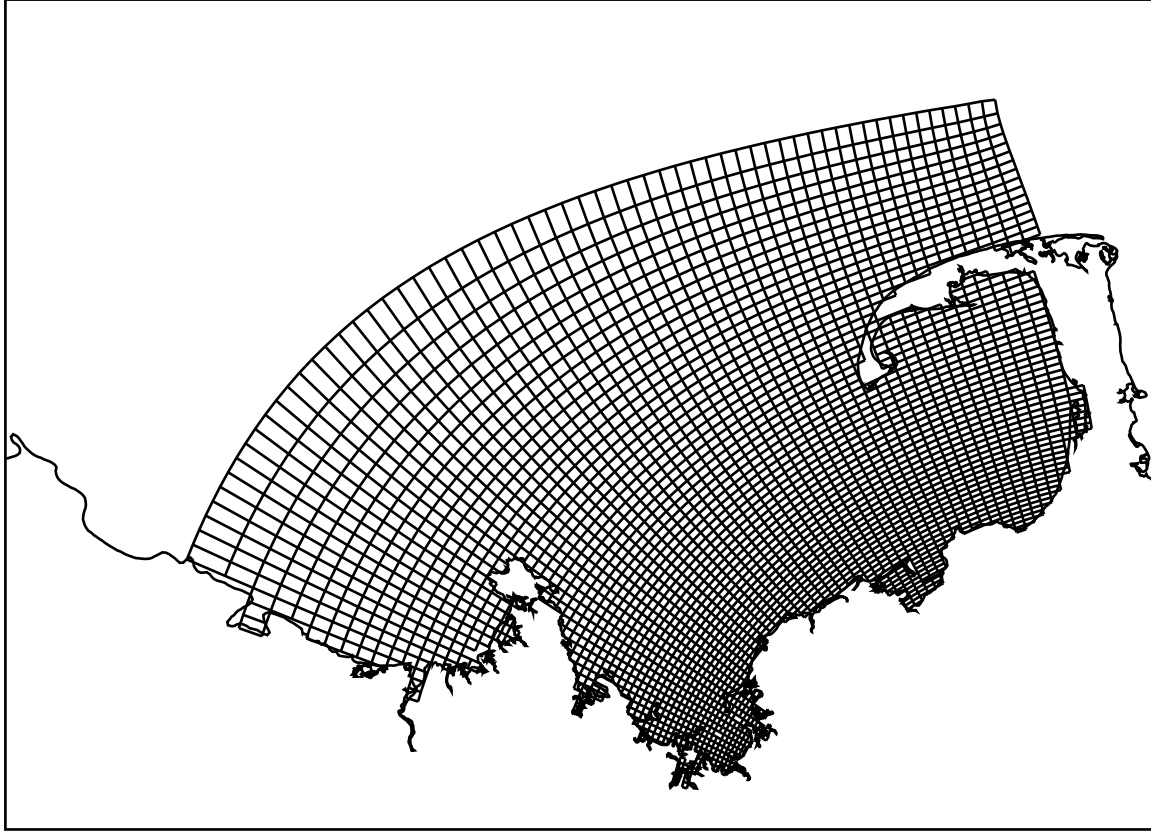
- the number of state-variables in the water quality model was significantly greater than that of the hydrodynamic model (twenty-four versus eight (flow (x, y, z), dispersion (x, y, z), temperature and salinity)),
- the water quality model also includes a sediment bed flux sub-model, which includes sixteen variables and two vertical layers,
- the need to cycle the water quality model for 3-5 years, in order to bring the sediment bed into equilibrium to the overlying water column inputs.

Figure 4-1, illustrates the fine-grid (which extends into the Gulf of Maine) used for the BEM hydrodynamic model (a.k.a. ECOM) versus the aggregated or coarse-grid model used for the water quality portion of the BEM.

The initial development of the BEM focused on the year 1992, the first year with extensive water quality and sediment nutrient flux data collected as part of the HOM program. In order to ensure that the grid aggregation scheme was functioning properly, i.e., that the spatial (and temporal) averaging did not result in an inability of the spatially aggregated model to properly account for the transport of particulate and dissolved constituents within the model domain, comparisons were made between computations of salinity using both grids. Salinity was chosen to perform this check because it was felt that, as a conservative material, potential errors introduced by the spatial and temporal averaging would not be offset by local source/sinks terms, as would be the case for the other water quality state-variables. The results (Figure 4-2) from the initial calibration effort (HydroQual and Normandeau, 1995) suggested that no significant differences could be discerned between salinities computed on the fine and the coarse-grids.



Water Quality Model Grid for Massachusetts Bay



Hydrodynamic Model Grid for Massachusetts Bay

Figure 4-1. Hydrodynamic Model Grid an Aggregated Water Quality Model Grid

However, since the early 1990's, when the BEM was developed, computer architecture and the speed of computer CPUs have increased significantly. Therefore, one of the recommendations of the Model Evaluation Group was to evaluate the feasibility of running the water quality model portion of the BEM on the same computational grid as used by the hydrodynamic model within the Massachusetts Bay and Cape Cod Bay system (Figure 4-3). The purpose of this section is to report on the findings of that evaluation.

4.2 METHODOLOGY

While the analysis of the effect of grid aggregation could have been evaluated using the 1992 calibration period, it was decided to use the 1994 model validation period instead. The year 1994 was chosen because of the unusually low dissolved oxygen levels that were observed in the fall of that year. While the aggregated version of the water quality model was able to partially reproduce the observed levels of low dissolved oxygen that occurred during the fall of 1994, it was not fully able to reproduce the actual minima. The MEG questioned whether grid aggregation may have contributed to this inability and, therefore, using 1994 to evaluate the effects of grid aggregation on water quality model computations would provide some useful insights as to the cause(s) of BEM's failure to reproduce the observed dissolved oxygen minima.

The first step in the process of dis-aggregating the water quality model was to assign all of the 1994 coarse-grid model inputs (water column and sediment initial conditions, boundary conditions, pollutant loadings, model parameters, etc.) to the fine-grid model (which had the same spatial extent as the coarse-grid model, i.e. not as far as the hydrodynamic model boundary). Once this task was performed, the fine-grid version of the model was run and the model computations were compared to the coarse-grid results for a number of the key water quality state-variables or constituents. This was accomplished by computing the volume-weighted concentrations for the nine fine-grid model segments that lay within the corresponding single coarse-grid model segment (Figure 4-4). It was decided to select a coarse-grid model segment, (11,18) in the vicinity of the new outfall in northwest Massachusetts Bay as designated by the "x" in Figure 4-3, to use for comparison.

Figure 4-5 presents comparisons of the volume-weighted concentration of salinity from the fine-grid versus the coarse-grid concentration of salinity for the surface and bottom waters. As can be seen there is little difference between the two sets of profiles, with the exception of bottom water salinity in mid-May and early June, which corresponds to the period of the spring freshet. The maximum differences are on the order of 0.3 ppt. Figure 4-6 presents a similar set of comparisons for surface and bottom chlorophyll-a.

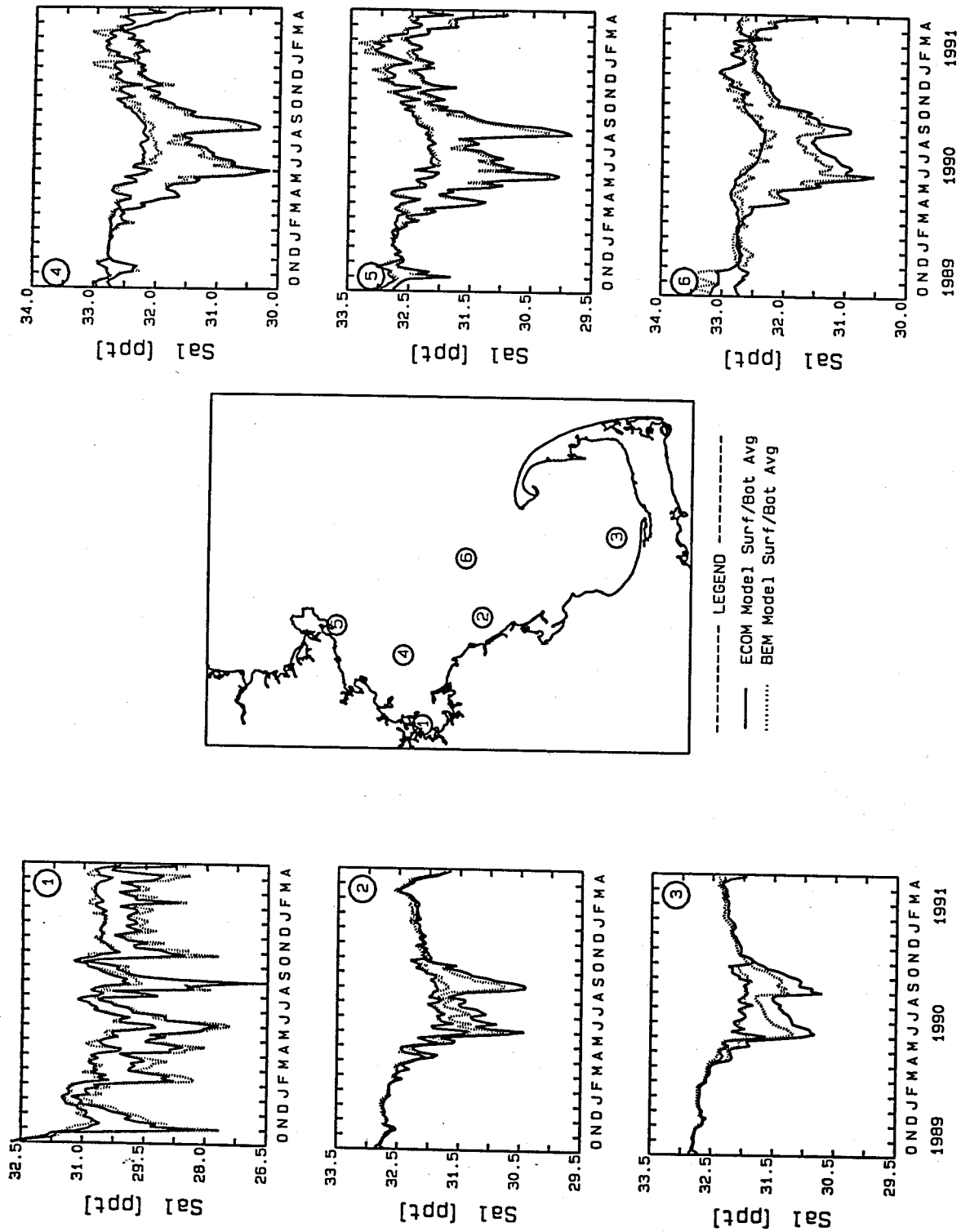


Figure 4-2. Comparison of Salinity Results from the Hydrodynamic Model and the Aggregated Water Quality Model

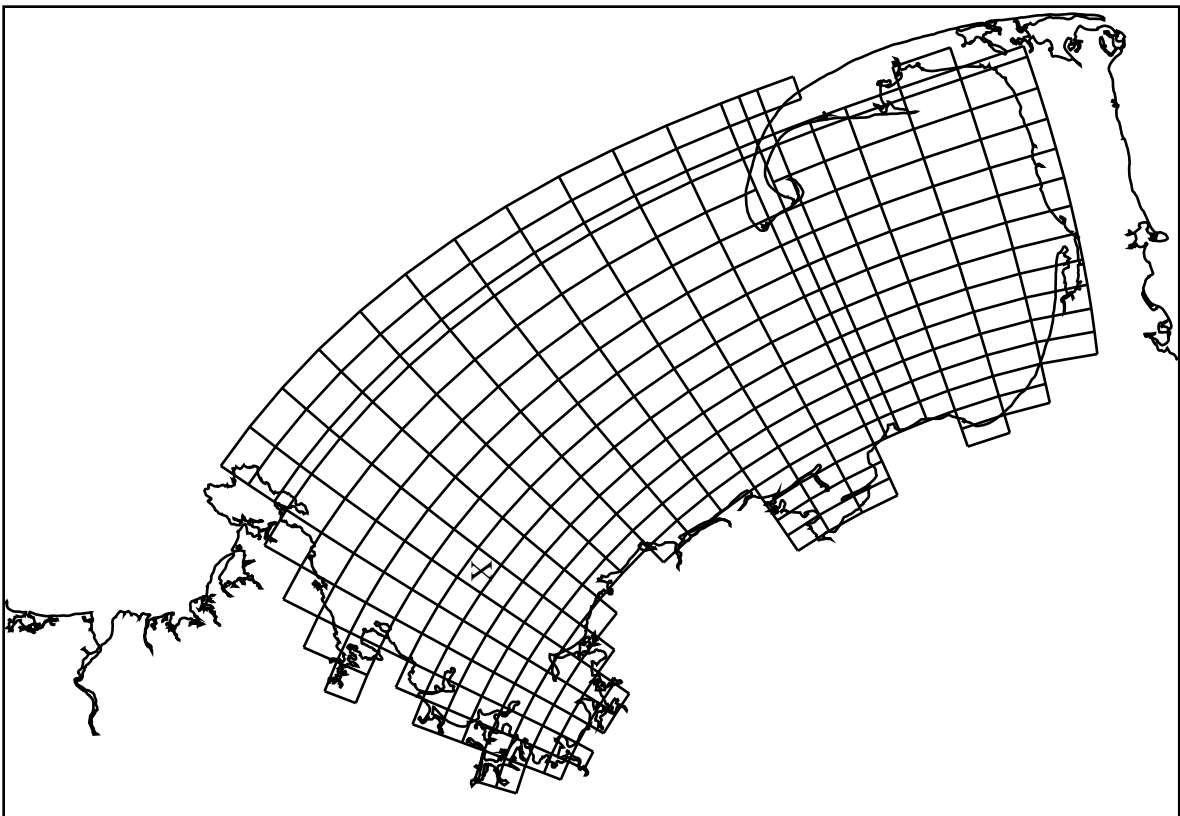
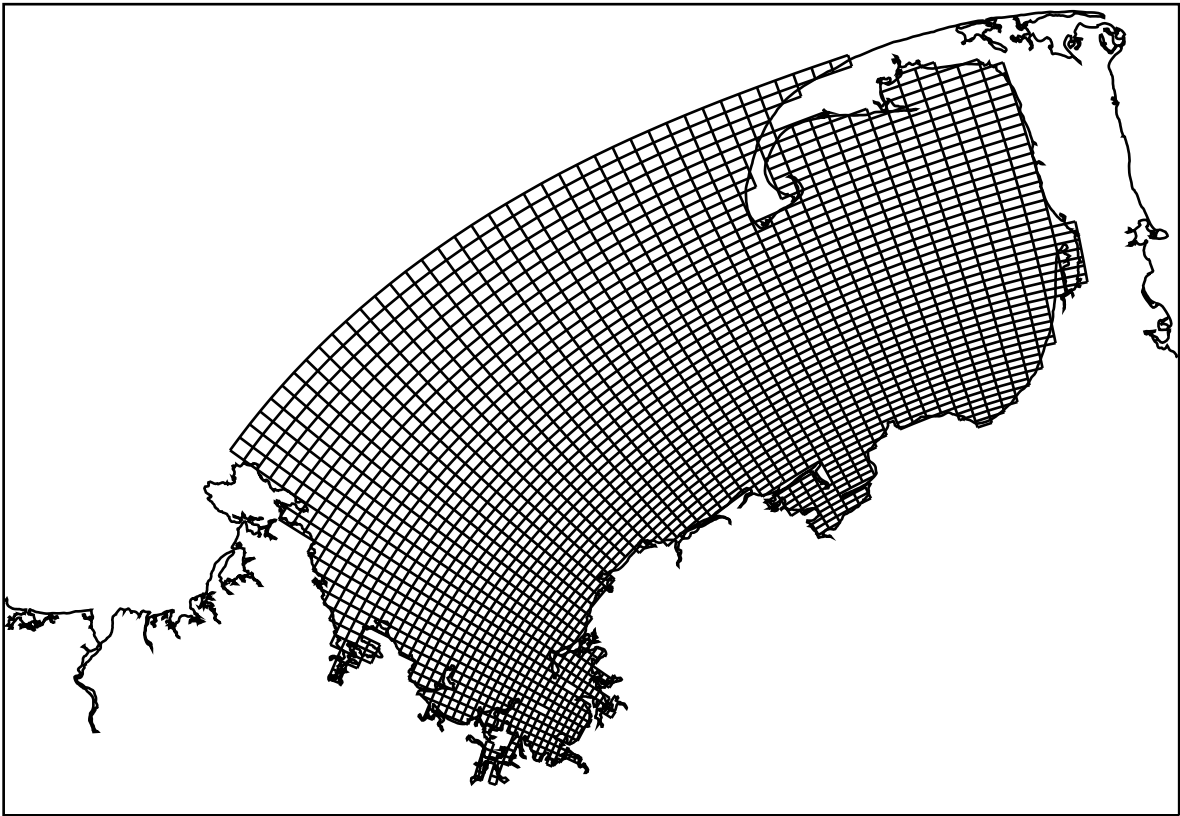
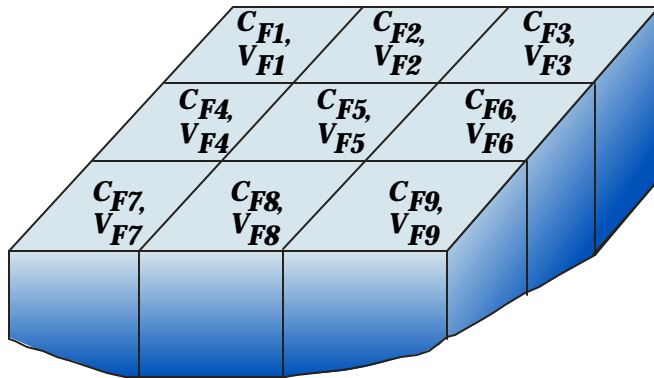
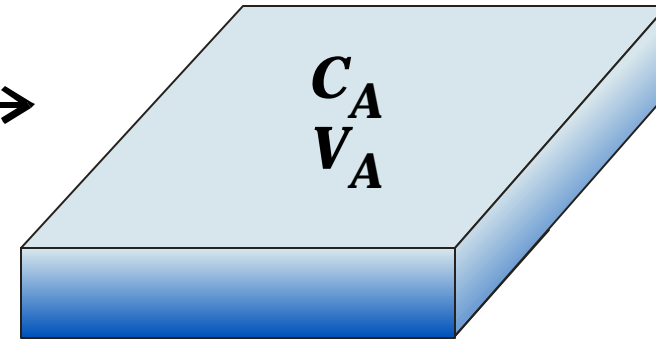


Figure 4-3. Aggregated and Unaggregated Water Quality Model Grids

Fine Grid



Aggregated Grid



$$\frac{\sum_{i=1}^{n=9} C_{Fi} V_{Fi}}{\sum_{i=1}^{n=9} V_{Fi}} = C_F$$

Compare C_F to C_A

C_{Fi} - fine segment i concentration

V_{Fi} - fine segment i volume

C_A - aggregated segment concentration

V_A - aggregated segment volume

Figure 4-4. Volume Weighted Averaged

Again, the differences between the fine-grid and coarse-grid computations tend to be relatively small. Fine-grid concentrations of surface chlorophyll are slightly higher (~ 0.2 - 0.5 ug Chl-a/L) than the coarse-grid computations for some short periods between late-April and the end of September and are slightly lower (~ 0.1 - 0.5 ug Chl-a/L) for some periods in October and November. Differences in chlorophyll between the two model grids show the opposite temporal patterns compared to salinity (i.e., when fine-grid salinity is lower than the coarse-grid salinity, fine-grid chlorophyll is greater than coarse-grid chlorophyll and vice-versa) and the differences are usually smaller in magnitude. Overall, however, there is not a significant difference between the concentrations computed by the two model grids. Differences in the computations of particulate organic carbon (POC) between the two model grids (Figure 4-7) are similar to those observed for chlorophyll.

The differences between the fine-grid and coarse-grid computations of dissolved oxygen in the surface layer are virtually indistinguishable (Figure 4-8). However, in the bottom layer, the differences are more discernable. Dissolved oxygen concentrations computed by the fine-grid model are slightly higher (~ 0.1 - 0.5 mg/L) than those computed by the coarse-grid model. These differences are larger than might be anticipated given the relatively small differences between the fine-grid and coarse-grid computations of chlorophyll and POC. An interesting pattern is also observed for the computation of nitrate+nitrite ($\text{NO}_2 + \text{NO}_3$) between the two model grids (Figure 4-9). There is virtually no difference between the surface computations of $\text{NO}_2 + \text{NO}_3$ between the two grids. There is, however, a notable difference for the bottom water computations. The fine-grid $\text{NO}_2 + \text{NO}_3$ concentration is noticeably lower for the fine-grid when compared to the coarse-grid. This was surprising, since with the possible exception of a small denitrification flux from the water column into the sediment it was anticipated that $\text{NO}_2 + \text{NO}_3$ would be approximately conservative in the bottom layers of the water column and in the model computations. It would have been expected, then, that the computations of $\text{NO}_2 + \text{NO}_3$ between the two model grids would have been quite similar, as was the case with salinity. Since, this was not the case and since bottom water dissolved oxygen differed more than expected it was decided to investigate what was the cause of the observed concentration discrepancies.

The initial list of potential causes of the observed discrepancies in bottom water dissolved oxygen and $\text{NO}_2 + \text{NO}_3$ focused on the following list: errors in remapping water column or sediment initial conditions or loads from the coarse-grid model onto the fine-grid model, errors in remapping model parameters required by the sediment model, or errors associated with remapping the boundary conditions.

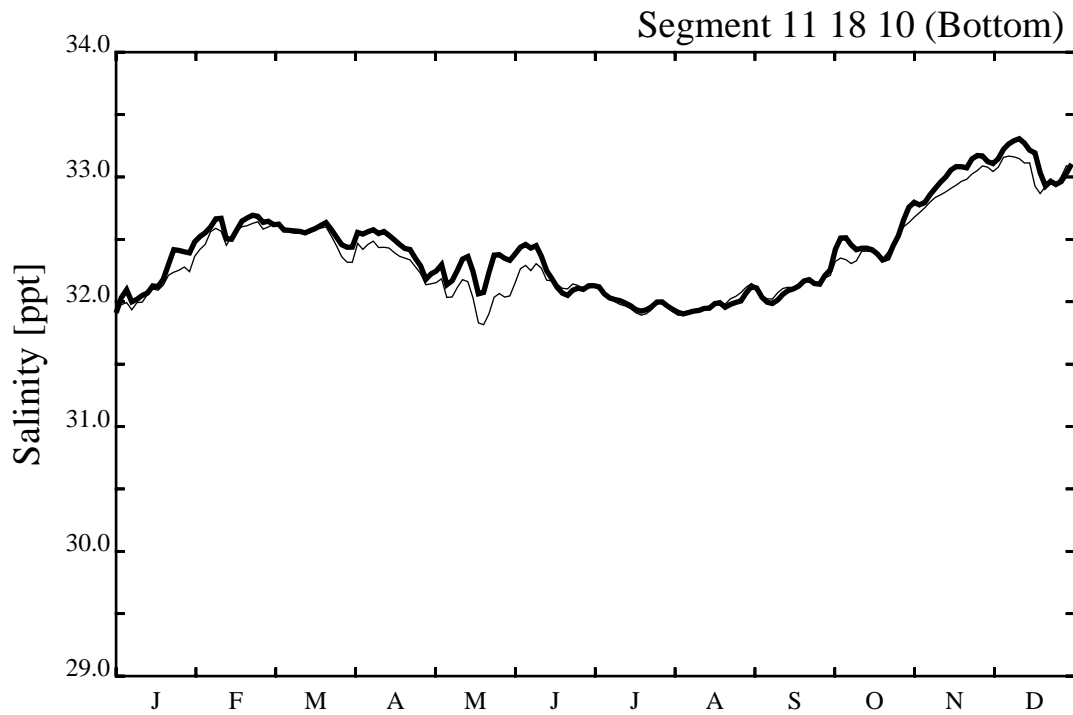
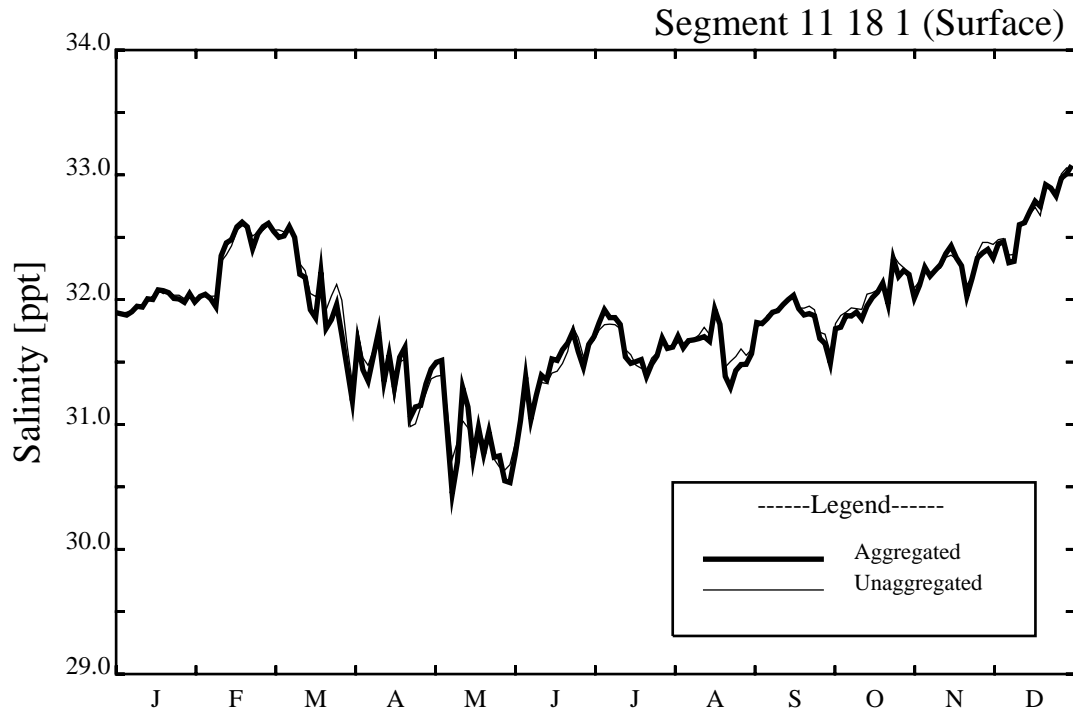


Figure 4-5. Comparison of Surface and Bottom Salinity Results Between the Aggregated and Unaggregated Water Quality Model Grids

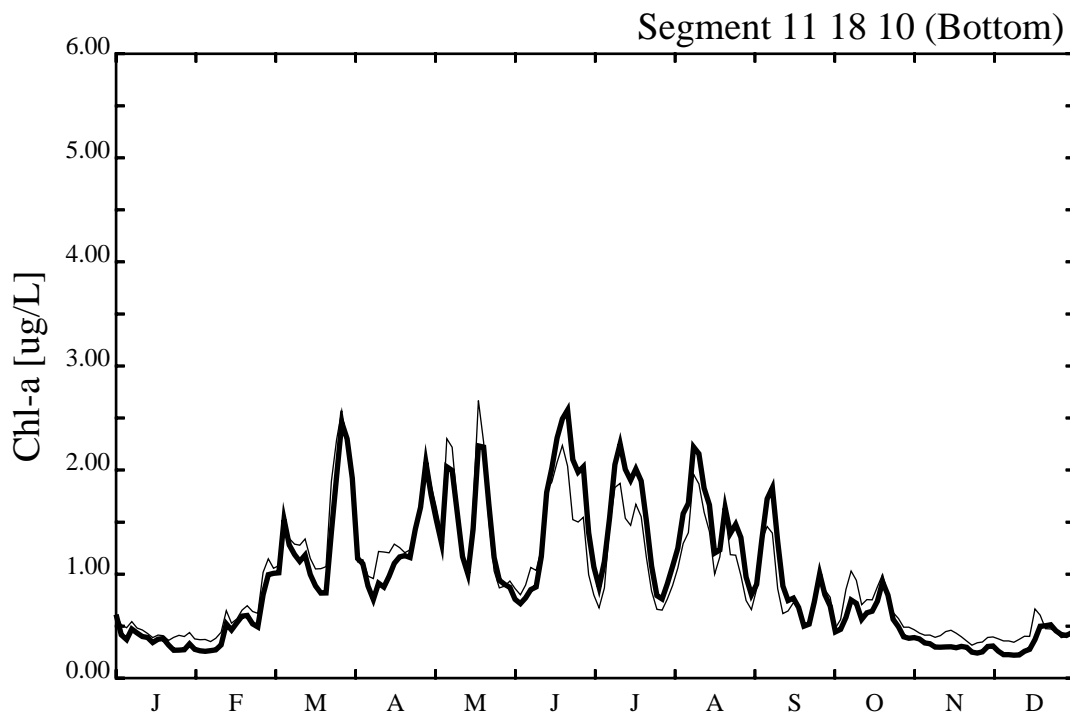
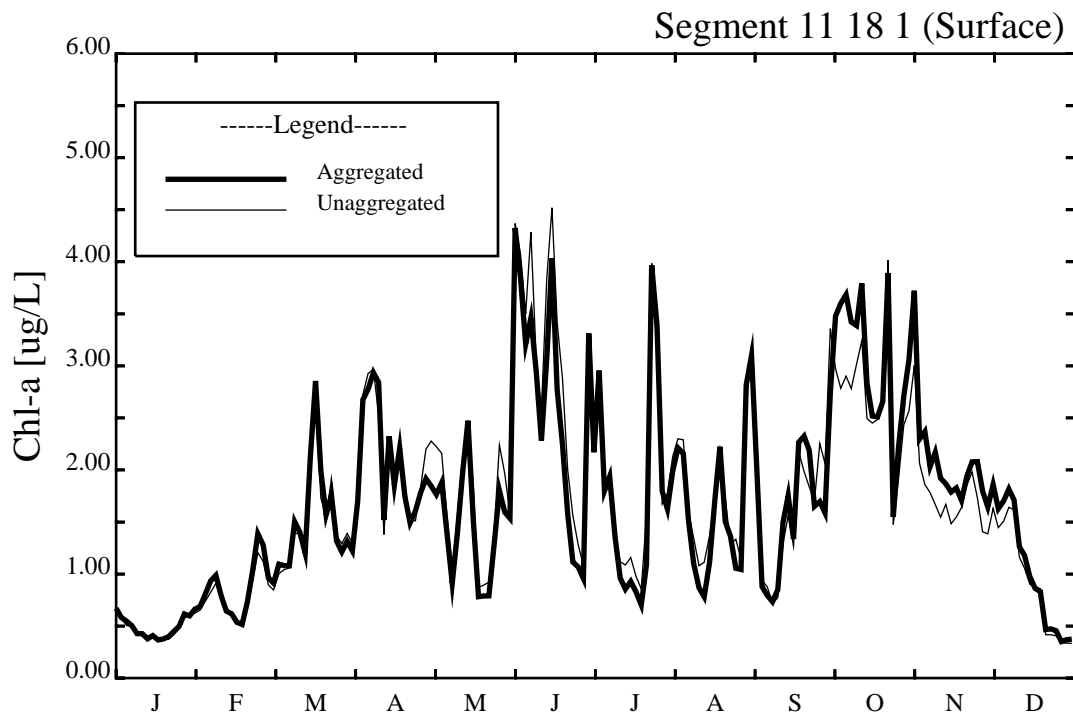


Figure 4-6. Comparison of Surface and Bottom Chlorophyll-a Results Between the Aggregated and Unaggregated Water Quality Model Grids

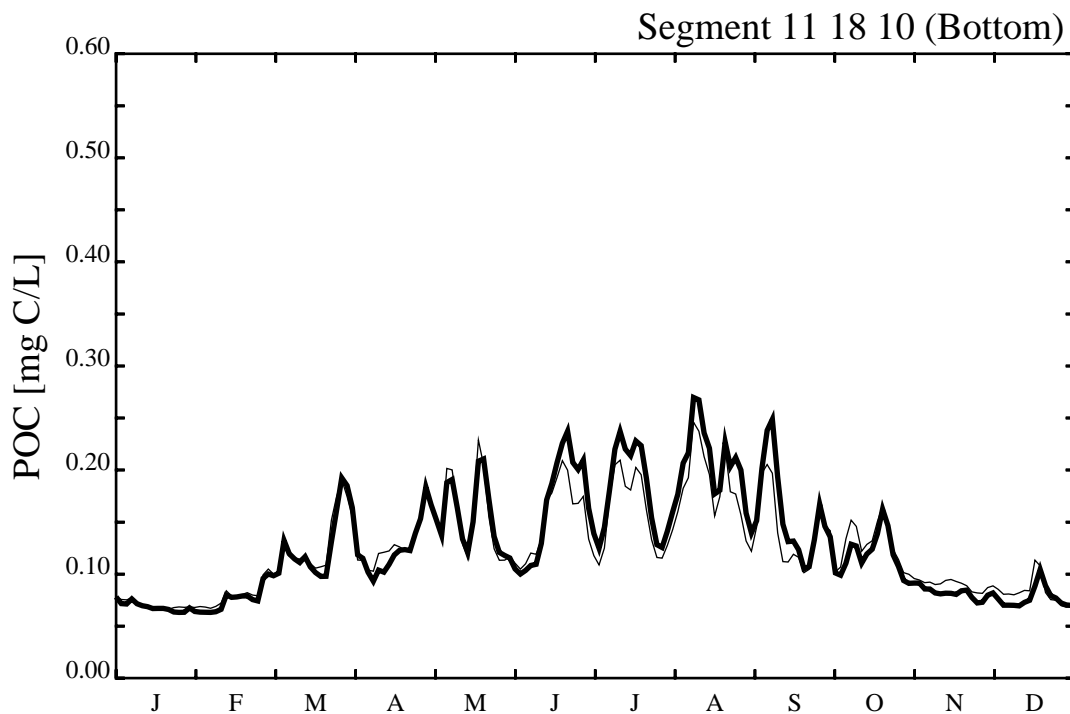
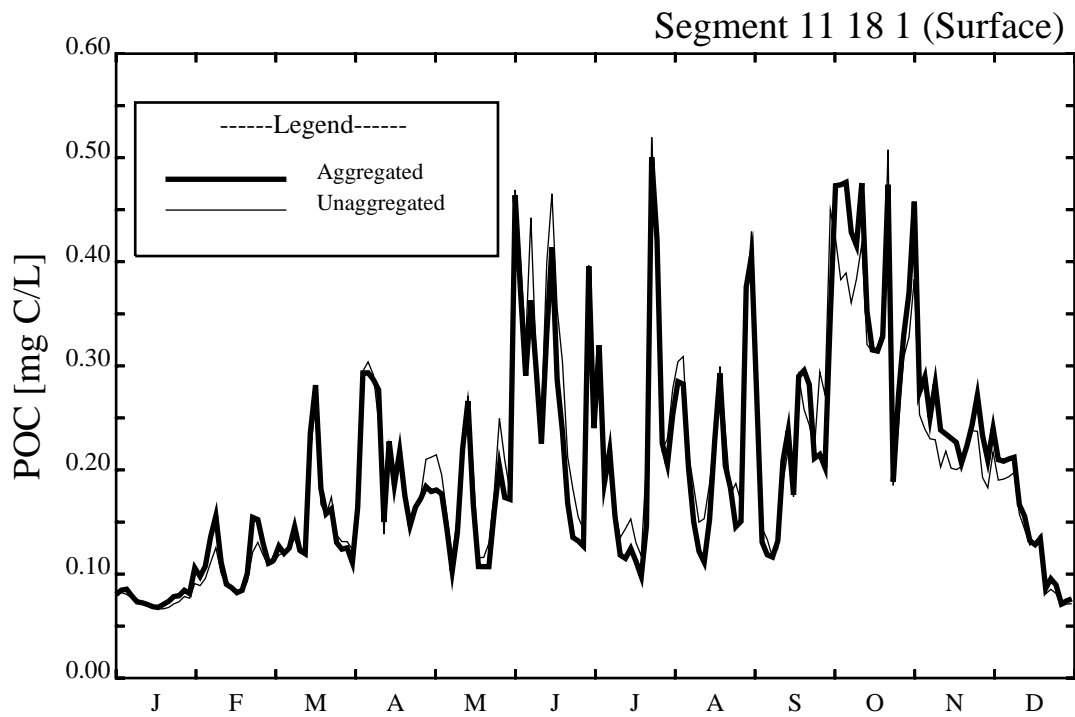


Figure 4-7. Comparison of Surface and Bottom Particulate Organic Carbon Results Between the Aggregated and Unaggregated Water Quality Model Grids

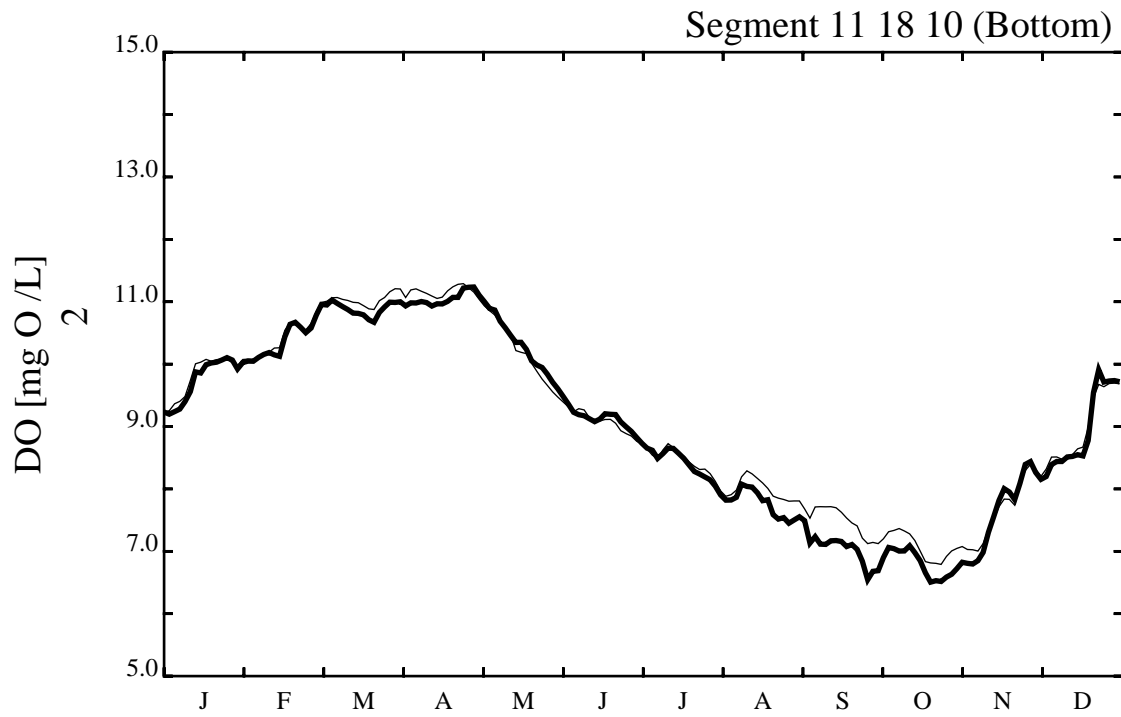
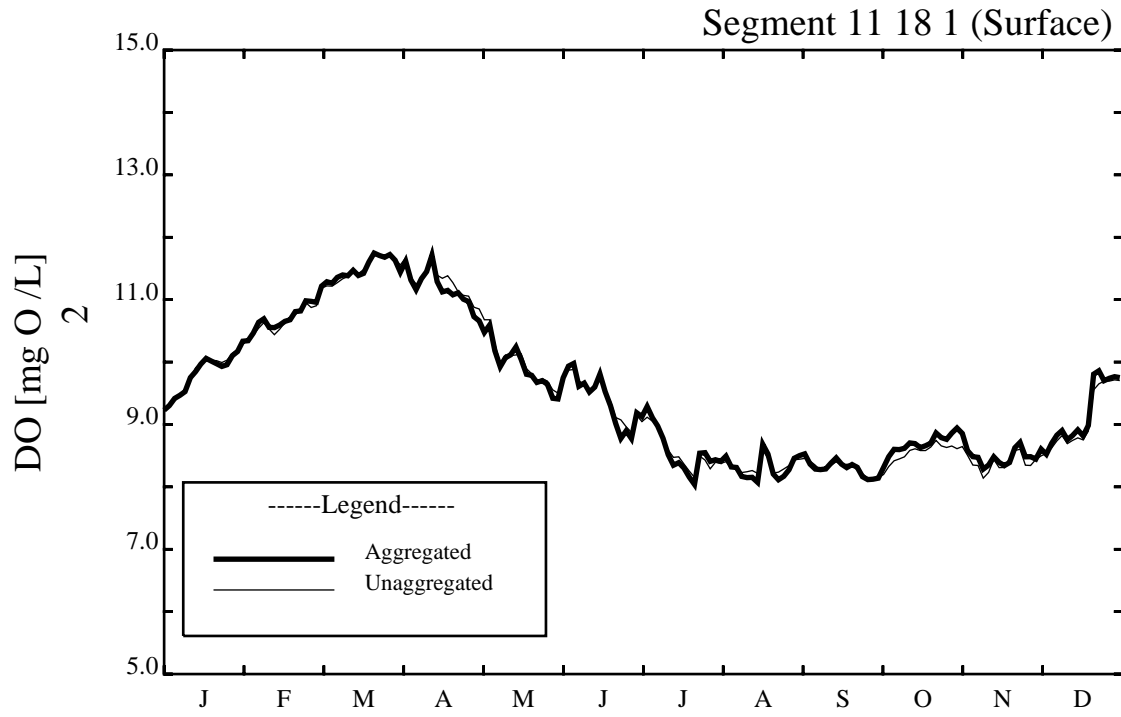


Figure 4-8. Comparison of Surface and Bottom Dissolved Oxygen Results Between the Aggregated and Unaggregated Water Quality Model Grids

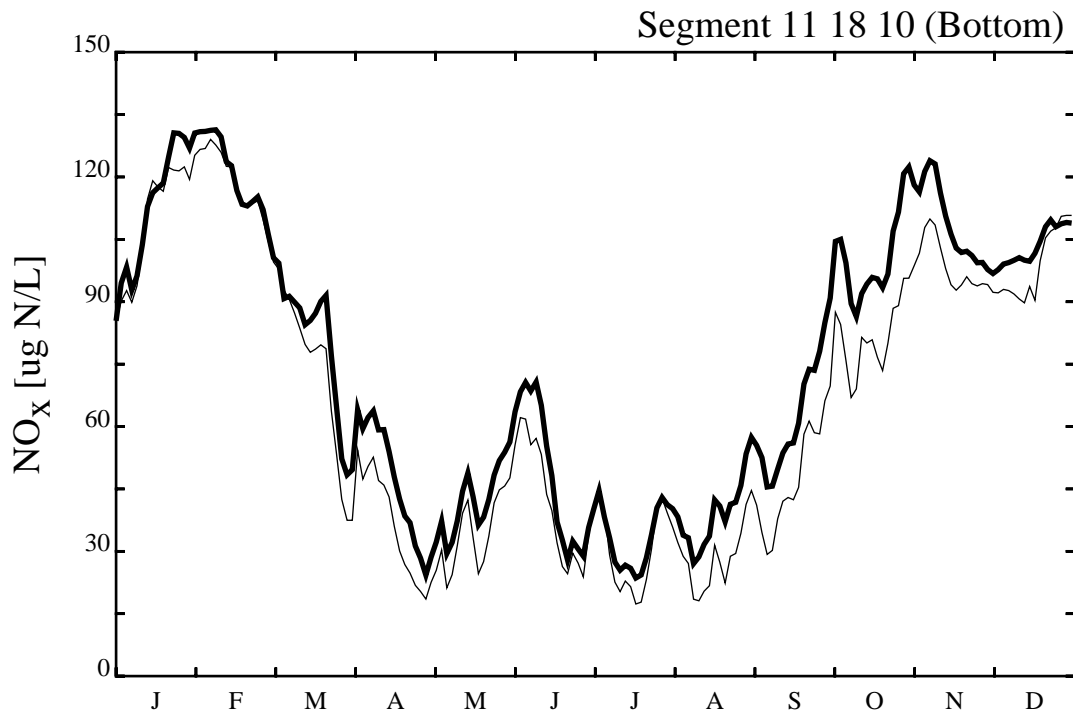
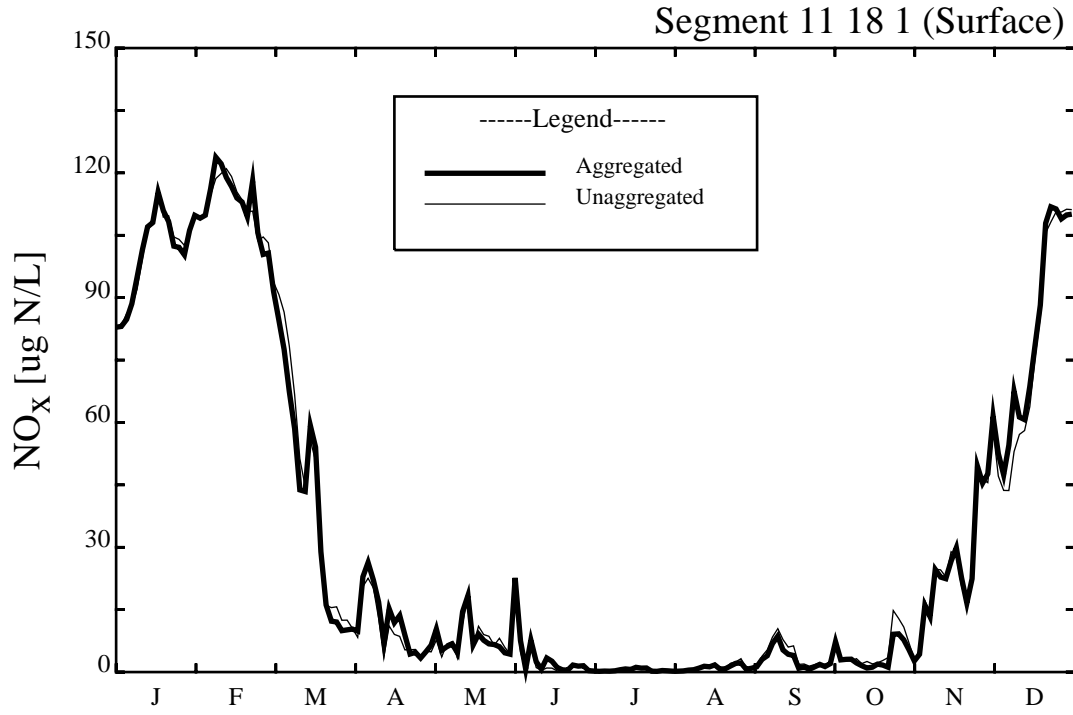


Figure 4-9. Comparison of Surface and Bottom NO₂ + NO₃ Results Between the Aggregated and Unaggregated Water Quality Model Grids

A check of model inputs was performed and indicated that all initial conditions, loads, and model parameters were mapped correctly onto the fine-grid from the coarse-grid model. Since bottom layer dissolved oxygen and $\text{NO}_2 + \text{NO}_3$ showed the greatest differences and since these variables are strongly influenced by sediment fluxes, the first diagnosis involved an examination of model computations resulting from the sediment flux submodel. A comparison between model computations of pore water NO_3 , sediment organic matter (POC and PON), sediment oxygen demand (SOD), and the flux of NO_3 to and from the water column were quite similar and, thus, indicated that the sediment portion of BEM was not responsible for the observed differences in the water column.

Next it was decided to investigate the boundary conditions. Figure 4-10 presents a comparison between the surface and bottom concentrations of $\text{NO}_2 + \text{NO}_3$ for the two northernmost coarse-grid model segments (in the vicinity of Cape Ann) versus the associated fine-grid model. This figure shows that the surface boundary concentrations for both model grids are the same (4-10a and 4-10b) but that the bottom layer boundary concentrations are slightly different with the boundary cells closest to Cape Ann (4-10c) differing most. It was determined that the cause of this problem was associated with the fact that the bottom depths increase significantly with distance for the first 30 km along the Cape Ann-Cape Cod model boundary. Since the model boundary concentrations are interpolated onto the ten sigma-level depths from four values specified at fixed depths, this would explain the difference in the boundary concentrations. However, further analysis of the models indicated that only a small portion of the total inflow into the Massachusetts Bays system from the Gulf of Maine was associated with the northern most boundary cell and the effect of this difference was considered to be small. To further investigate the potential reason for the differences in computed $\text{NO}_2 + \text{NO}_3$ concentrations between the two model grids it was decided to run a conservative tracer using the same boundary condition concentrations as $\text{NO}_2 + \text{NO}_3$. Using a conservative tracer removes the influence of the $\text{NO}_2 + \text{NO}_3$ water quality model kinetics and the influence of the sediment nutrient flux model and would point to another reason for the computed differences. Figure 4-11 presents model computations from this tracer run. Once again, the results indicate little difference in model computations in the surface layer between the two model grids. However, differences can be observed in the bottom layer between the two model grids. These results together with visualizations of model outputs from both grids, suggest that the cause of the discrepancies between the two model grids is due to a phenomena known as numerical dispersion. Numerical dispersion is associated with the finite-difference approximations to the exact partial differential equations that represent the conservation of mass for the Massachusetts Bays system. The following equation relates the magnitude of the numerical dispersion to the grid size and advective velocities used in a model:

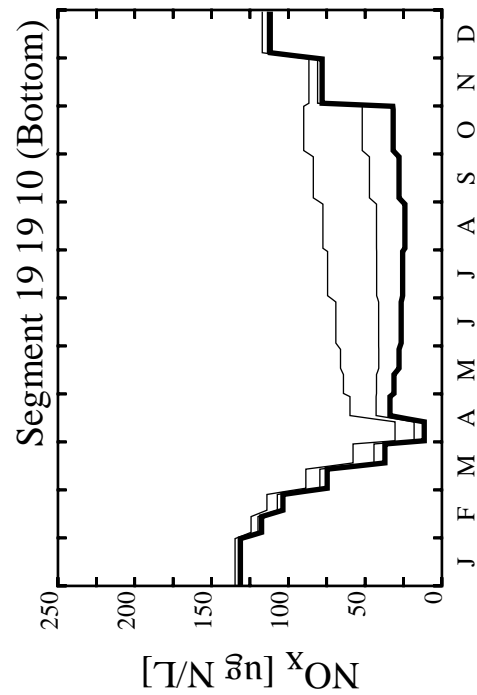
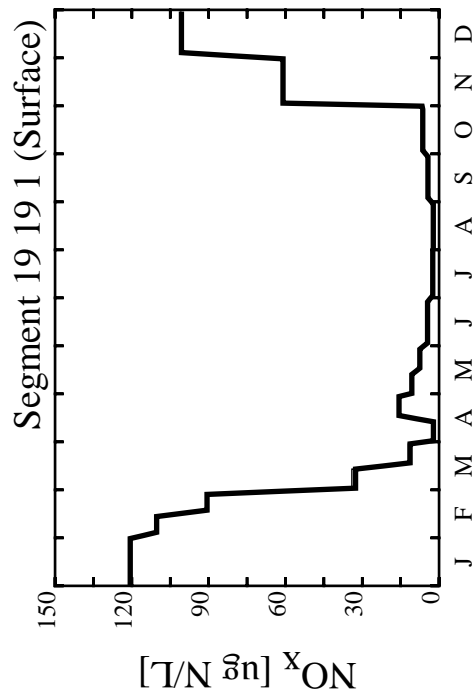
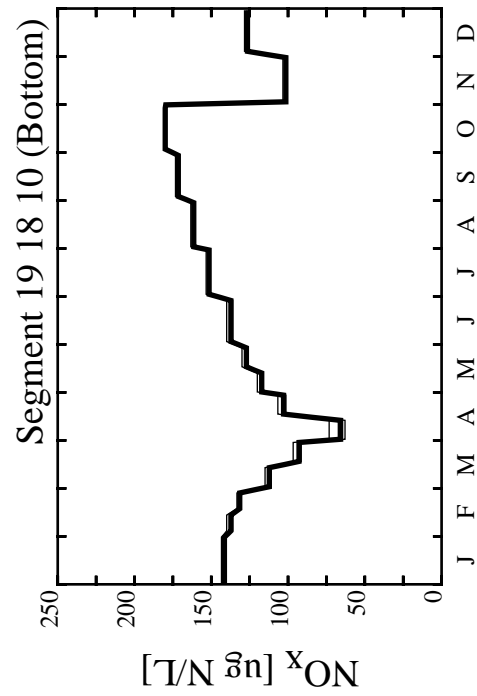
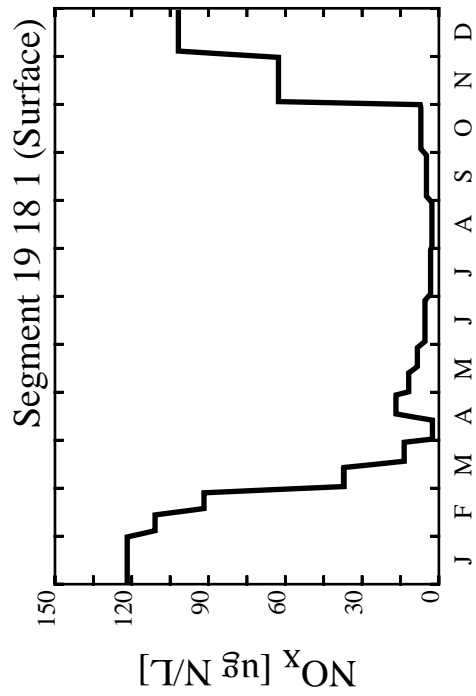


Figure 4-10. NO₂ + NO₃ Concentrations and the Boundary for the Aggregated and Unaggregated Water Quality Model Grids

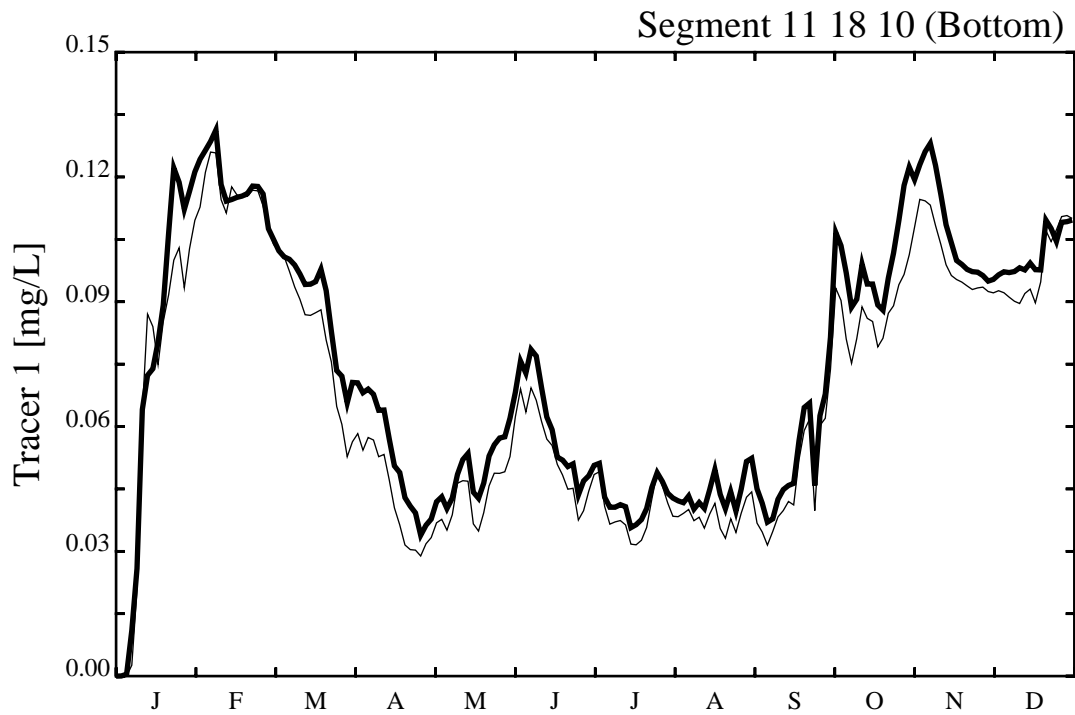
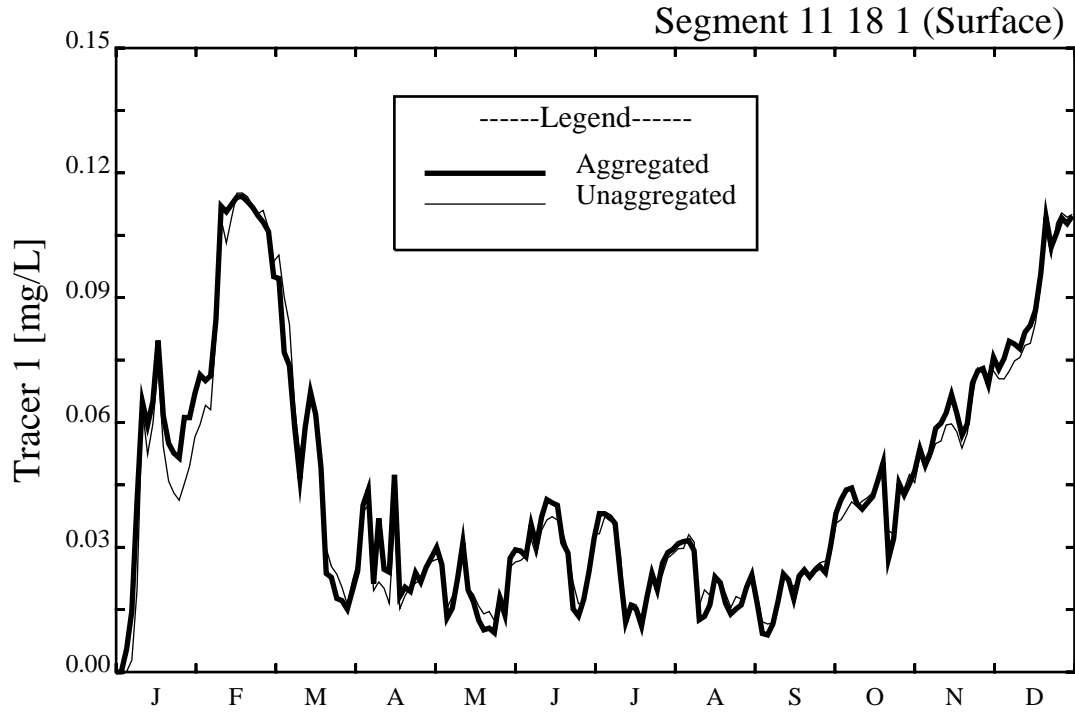


Figure 4-11. Comparison of Surface and Bottom Tracer Concentration Results Between the Aggregated and Unaggregated Water Quality Model Grids

$$E_{\text{num}} = 0.5 U \Delta x$$

where

$$\begin{aligned} E_{\text{num}} &= \text{numerical dispersion, (m}^2\text{/day),} \\ U &= \text{velocity, (m/day)} \\ \Delta x &= \text{length of the model segment, (m).} \end{aligned}$$

This equation indicates, that as one increases the size of the model segment, the numerical dispersion or numerical error increases. Therefore, for the coarse-grid mode the numerical dispersion is approximately three times larger than for the fine-grid model. This problem was not observed in the original modeling effort because the spatial and temporal gradients in salinity were small compared to $\text{NO}_2 + \text{NO}_3$.

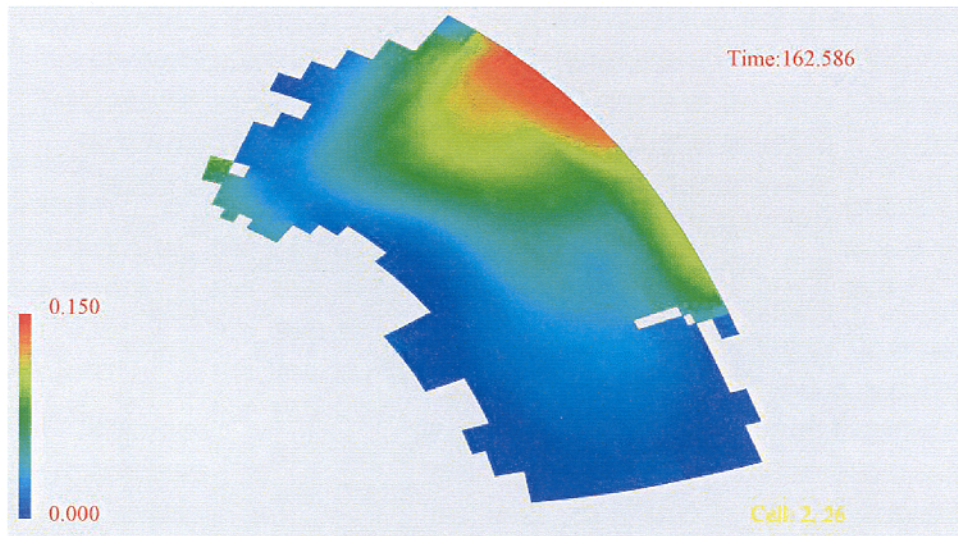
Figures 4-12 through 4-14 present color contour plots for bottom water $\text{NO}_2 + \text{NO}_3$, surface average chlorophyll-a, and bottom minimum dissolved oxygen (The terms average and minimum refer to a five-day interval from which model results were retrieved to create these figures). One can see that the coarse-grid model reproduces the major features observed in the fine-grid model, but does not reproduce some of the fine-grid features. Again this is due to numerical dispersion associated with the coarse-grid model.

4.3 SUMMARY

An analysis of model computations between the coarse-grid and fine-grid versions of the BEM indicates that the coarse-grid model produces the major features of the fine-grid model, but does not fully capture the small scale details of the fine-grid model. Therefore, any model projections made using the coarse-grid model would not differ significantly if the fine-grid version of the model were to be used. However, since computer power has increased since the original coarse-grid model was developed, it is recommended that future model runs be run on the fine-grid model because the fine-grid model provides better resolution. It would still be possible to perform additional model development/calibration, i.e., addition of new phytoplankton groups to BEM or addition of zooplankton kinetics to the model, using the coarse-grid model, but all final production runs should be made using the fine-grid version of the model. The fine-grid model is conceptually more accurate due to less numerical dispersion. While the fine-grid model did not improve the calibration to DO in 1994 (in fact the calibration was worse) with some fine tuning of the boundary conditions and model parameters it would be expected that the fine-grid model would ultimately provide a better fit to the data than the coarse-grid model.

Bottom Nitrate + Nitrite

Aggregated Grid



Unaggregated Grid

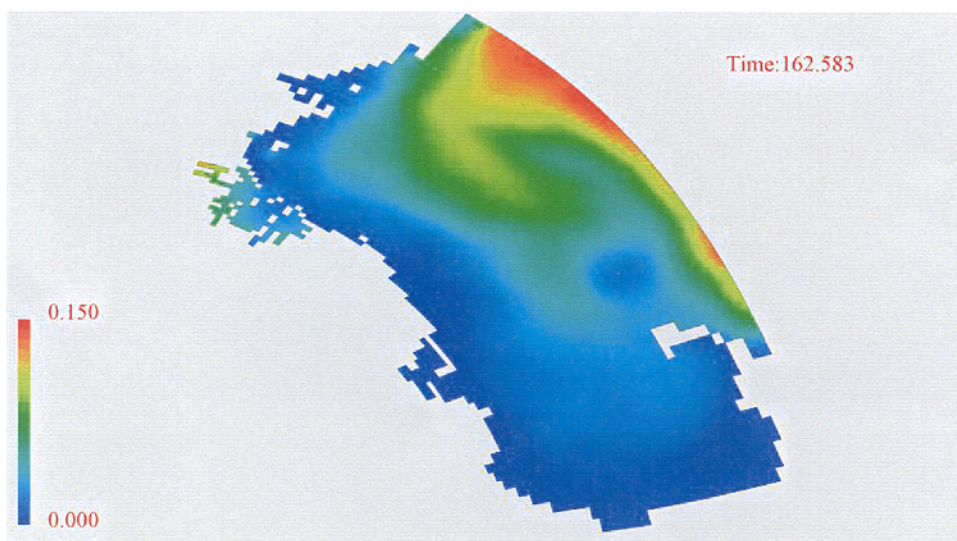
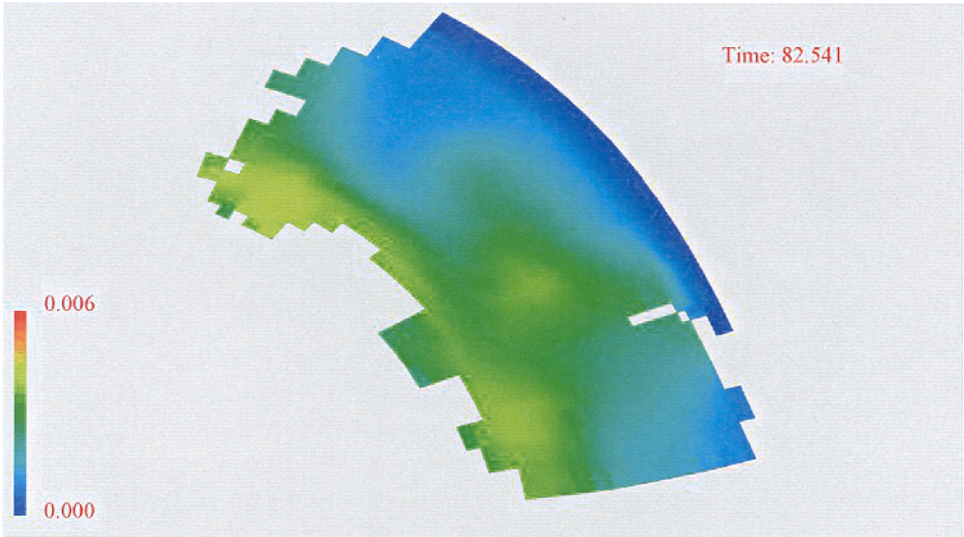


Figure 4-12. Comparison of Bottom $\text{NO}_2 + \text{NO}_3$ Results from the Aggregated and Unaggregated Water Quality Model Grids at Day 162

Surface Average Chlorophyll-a

Aggregated Grid



Unaggregated Grid

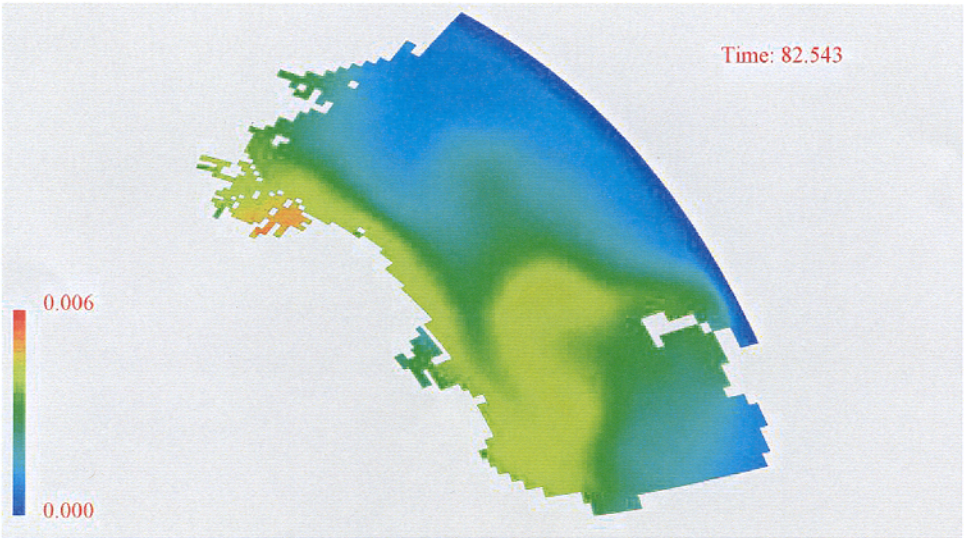
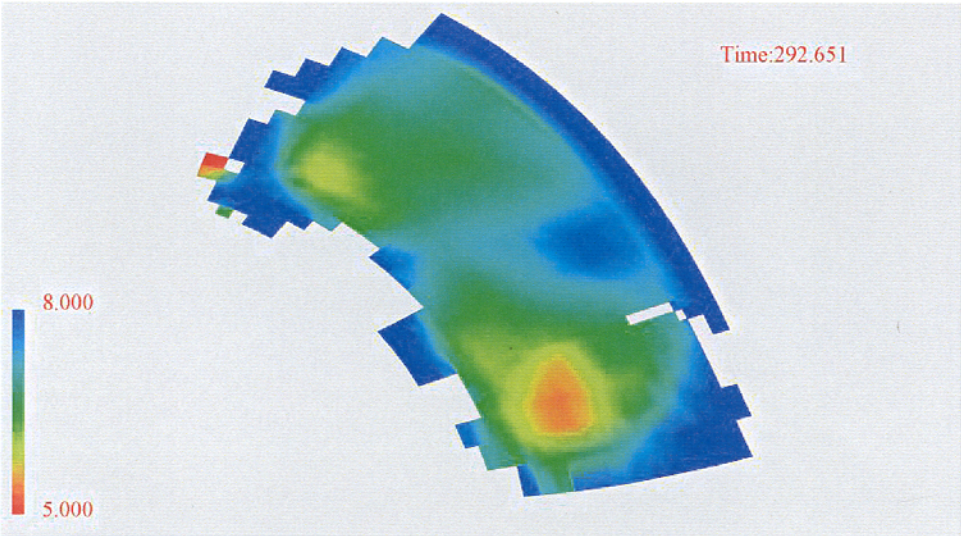


Figure 4-13. Comparison of Surface Average Chl-a Concentration Results from the Aggregated and Unaggregated Water Quality Model Grids at Day 82

Bottom Minimum Dissolved Oxygen

Aggregated Grid



Unaggregated Grid

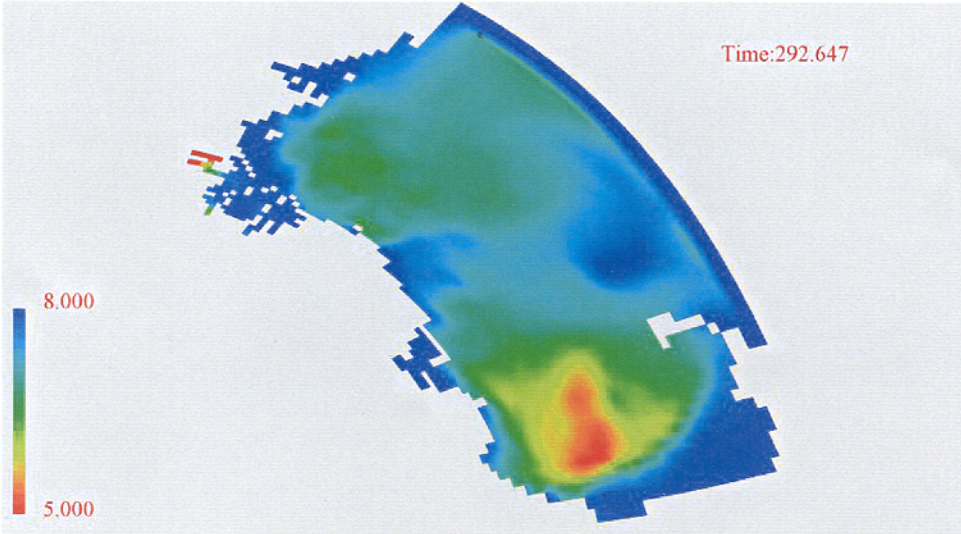


Figure 4-14. Comparison of Bottom Minimum DO Concentration Results from the Aggregated and Unaggregated Water Quality Model Grids at Day 292

SECTION 5

REFERENCES

HydroQual and Normandeau, 1995. A water quality model for Massachusetts and Cape Cod Bays: Calibration of the Bays Eutrophication Model (BEM). Boston: Massachusetts Water Resources Authority. Report ENQUAD 1995-08, 402p.

HydroQual, Inc., 2001a. Boundary sensitivity analysis for the Bays Eutrophication Model (BEM). Boston: Massachusetts Water Resources Authority. Report ENQUAD 2001-13.

HydroQual, Inc., 2001b. Analysis of the addition of a third algal group to the Bays Eutrophication Model (BEM) Kinetics. Boston: Massachusetts Water Resources Authority. Report ENQUAD 2001-14.